

PROTECTIVE EFFECTS OF TIGER MILK MUSHROOM (*Lignosus rhinocerus*) EXTRACTS ON  
OXIDATIVE STRESS-INDUCED NEUROTOXICITY AND AGING IN HT22 CELLS AND *C.*

*elegans*



A Dissertation Submitted in Partial Fulfillment of the Requirements  
for the Degree of Doctor of Philosophy in Clinical Biochemistry and Molecular Medicine

Department of Clinical Chemistry

FACULTY OF ALLIED HEALTH SCIENCES

Chulalongkorn University

Academic Year 2020

Copyright of Chulalongkorn University

ฤทธิ์ของสารสกัดเห็ดนมเสือในการป้องกันพืชต่อเซลล์ประสาทและความชราที่ถูกเหนี่ยวนำโดยภาวะ  
เครียดออกซิเดชันในเซลล์เพาะเลี้ยง HT22 และหนอน *C. elegans*



วิทยานิพนธ์นี้เป็นส่วนหนึ่งของการศึกษาตามหลักสูตรปริญญาวิทยาศาสตรดุษฎีบัณฑิต  
สาขาวิชาชีวเคมีคลินิกและอนุทางการแพทย์ ภาควิชาเคมีคลินิก  
คณะสหเวชศาสตร์ จุฬาลงกรณ์มหาวิทยาลัย  
ปีการศึกษา 2563  
ลิขสิทธิ์ของจุฬาลงกรณ์มหาวิทยาลัย

Thesis Title PROTECTIVE EFFECTS OF TIGER MILK MUSHROOM (*Lignosus rhinocerus*) EXTRACTS ON OXIDATIVE STRESS-INDUCED NEUROTOXICITY AND AGING IN HT22 CELLS AND *C. elegans*

By Miss Parinee Kittimongkolsuk

Field of Study Clinical Biochemistry and Molecular Medicine

Thesis Advisor Assistant Professor TEWIN TENCOMNAO, Ph.D.

Thesis Co Advisor Assistant Professor SIRIPORN CHUCHAWANKUL, Ph.D.

---

Accepted by the FACULTY OF ALLIED HEALTH SCIENCES, Chulalongkorn University  
in Partial Fulfillment of the Requirement for the Doctor of Philosophy

..... Dean of the FACULTY OF ALLIED  
HEALTH SCIENCES  
(Associate Professor PALANEE AMMARANOND, Ph.D.)

DISSERTATION COMMITTEE

..... Chairman  
(Assistant Professor VIROJ BOONYARATANAKORNKIT, Ph.D.)

..... Thesis Advisor  
(Assistant Professor TEWIN TENCOMNAO, Ph.D.)

..... Thesis Co-Advisor  
(Assistant Professor SIRIPORN CHUCHAWANKUL, Ph.D.)

..... Examiner  
(Associate Professor RACHANA SANTIYANONT, Ph.D.)

..... Examiner  
(Assistant Professor TEWARIT SARACHANA, Ph.D.)

..... External Examiner  
(Associate Professor Krai Meemon, Ph.D.)

ภาวิณี กิตติมงคลสุข : ฤทธิ์ของสารสกัดเห็ดนมเสือในการป้องกันพิษต่อเซลล์ประสาทและความชราที่ถูกเหนี่ยวนำโดยภาวะเครียดออกซิเดชันในเซลล์เพาะเลี้ยง HT22 และหนอน *C. elegans*. ( PROTECTIVE EFFECTS OF TIGER MILK MUSHROOM (*Lignosus rhinocerus*) EXTRACTS ON OXIDATIVE STRESS-INDUCED NEUROTOXICITY AND AGING IN HT22 CELLS AND *C. elegans*) อ.ที่ปรึกษาหลัก : ผศ. ดร.เทวิน เทนคำเนาว์, อ.ที่ปรึกษาร่วม : ผศ. ดร.ศิริพร ชื้อชวาลกุล

เห็ดนมเสือ (*Lignosus rhinocerus*) เป็นเห็ดที่มีคุณสมบัติทางการแพทย์มาตั้งแต่สมัยโบราณ มีหลายงานวิจัยพบว่าเห็ดนมเสือมีฤทธิ์ทางเภสัชวิทยาหลายประการ ตัวอย่างเช่น ฤทธิ์ในการรักษาโรคหอบหืด ฤทธิ์ต้านการอักเสบ ฤทธิ์ยับยั้งการเจริญเติบโตของเซลล์มะเร็ง ฤทธิ์ในการปรับเปลี่ยนภูมิคุ้มกัน ช่วยเพิ่มการงอกของเซลล์ประสาทในเซลล์เพาะเลี้ยง PC-12 ด้านการทำงานของเชื้อ HIV-1 และฤทธิ์ต้านสารอนุมูลอิสระ เป็นต้น แต่อย่างไรก็ตามคุณสมบัติต้านสารอนุมูลอิสระเน้นทำการทดลองภายนอกเซลล์เท่านั้นและยังไม่มีการศึกษาฤทธิ์ปกป้องในเซลล์ประสาทส่วนฮิบโปแคมปัสของหนูชนิด HT-22 และ หนอนตัวกลม *Caenorhabditis elegans* ในการวิจัยครั้งนี้มีวัตถุประสงค์เพื่อศึกษาฤทธิ์ในการป้องกันความเสื่อมของเซลล์ประสาทในเซลล์เพาะเลี้ยง HT-22 และ หนอนตัวกลม รวมทั้งศึกษาการมีอายุยืนของหนอนตัวกลม สำหรับเซลล์เพาะเลี้ยง HT-22 ผู้วิจัยได้ทำการทดสอบความเป็นพิษต่อเซลล์ของสารสกัดเห็ดนมเสือที่ได้จากการสกัด 3 วิธี (สารสกัดจากเอทานอล สารสกัดจากน้ำเย็น และสารสกัดจากน้ำร้อน) โดยใช้เทคนิค MTT การตรวจสอบอะพอพโทซิสด้วยการย้อมสี Annexin V-PI ทดสอบศักยภาพเยื่อหุ้มไมโทคอนเดรีย และทดสอบการสะสมของสารอนุมูลอิสระภายในเซลล์ นอกจากนี้ผู้ทำวิจัยยังได้ทำการทดสอบการแสดงออกของยีนที่เกี่ยวข้องกับการต้านอนุมูลอิสระโดยใช้วิธี real-time PCR ส่วนการทดสอบในหนอนตัวกลม *C. elegans* สายพันธุ์ปกติ N2 ได้ทำการทดสอบอัตราการอยู่รอดภายใต้ภาวะเครียดที่เกิดจากออกซิเดชัน และตรวจหาการสะสมของสารอนุมูลอิสระภายในเซลล์ ส่วนสายพันธุ์ที่ได้เปลี่ยนแปลงทางพันธุกรรม ได้แก่ TJ356, TJ375, CF1553, CL2166 และ LD1 ได้นำมาทดสอบดูการแสดงออกของโปรตีน DAF-16, HSP-16.2, SOD-3, GST-4, และ SKN-1 ตามลำดับ และได้ทำการทดสอบเกี่ยวกับอายุขัยและดัชนีชี้วัดทางชีวภาพเกี่ยวกับการชรา ได้แก่ lipofuscin และ อัตราการบีบของส่วนคอหอย นอกจากนี้ฤทธิ์ในการปกป้องเซลล์ประสาทได้ทำการตรวจวัดโดยทดสอบพฤติกรรมทางเคมี และตรวจดูการสะสมของโปรตีน PolyQ40 ผู้ทำวิจัยได้พบว่าสารสกัดที่ได้จากเอทานอลเท่านั้นที่สามารถลดทั้งการตายของเซลล์แบบอะพอพโทซิสและระดับของสารอนุมูลอิสระในเซลล์แต่สามารถเพิ่มการแสดงออกของยีนที่เกี่ยวข้องกับการต้านอนุมูลอิสระอย่างมีนัยสำคัญหลังจากที่เกิดภาวะเครียดที่เกิดจากออกซิเดชันจากการเหนี่ยวนำของกลูตาเมต แต่อย่างไรก็ตามในหนอนตัวกลม *C. elegans* สารสกัดทั้งหมดสามารถลดอนุมูลอิสระภายในเซลล์และปกป้องหนอนจากภาวะเครียดที่เกิดจากออกซิเดชันผ่านทาง DAF-16/FOXO ซึ่งนำไปสู่การเพิ่มขึ้นของ SOD-3 และการลดลงของ HSP-16.2 ในขณะที่ไม่มีการเปลี่ยนแปลงของ SKN-1 และ GST-4 สารสกัดทั้งหมดสามารถเพิ่มอายุขัย และลดจำนวนของ lipofuscin แต่เฉพาะความเข้มข้นสูงเท่านั้นที่สามารถเพิ่มอัตราการบีบของส่วนคอหอยได้ สารสกัดทั้งหมดไม่มีอันตรายต่อความยาวของลำตัว และจำนวนลูกหลานสามารถตัดจากภาวะการถูกควบคุมอาหาร นอกจากนี้ยังมีฤทธิ์ในการปกป้องเซลล์ประสาทโดยการเพิ่มดัชนีทางเคมี (CI) ในหนอนที่มี  $A\beta$  และลดการสะสมของ PolyQ40 เป็นที่น่าสนใจอย่างยิ่งว่าสารสกัดจากเอทานอลเท่านั้นที่มีฤทธิ์ปกป้องเซลล์ประสาททั้งในเซลล์เพาะเลี้ยงและภายในสัตว์ทดลอง ดังนั้นการค้นพบครั้งแรกของงานวิจัยนี้สรุปได้ว่าสารสกัดเห็ดนมเสือ โดยเฉพาะอย่างยิ่งสารสกัดจากเอทานอลสามารถเป็นอีกตัวเลือกหนึ่งในการใช้เป็นอาหารเสริมที่ช่วยป้องกันการเสื่อมของเซลล์

ประสาท

สาขาวิชา

ชีวเคมีคลินิกและอนุทางการแพทย์

ลายมือชื่อนิสิต .....

ปีการศึกษา

2563

ลายมือชื่อ อ.ที่ปรึกษาหลัก .....

ลายมือชื่อ อ.ที่ปรึกษาร่วม .....

# # 5876952137 : MAJOR CLINICAL BIOCHEMISTRY AND MOLECULAR MEDICINE

KEYWORD: *Lignosus rhinocerus*; Tiger Milk Mushroom; *C. elegans*; Aging; Antioxidants; DAF-16; HT-22; Glutamate toxicity; Neuroprotection; Oxidative stress

Parinee Kittimongkolsuk : PROTECTIVE EFFECTS OF TIGER MILK MUSHROOM (*Lignosus rhinocerus*) EXTRACTS ON OXIDATIVE STRESS-INDUCED NEUROTOXICITY AND AGING IN HT22 CELLS AND *C. elegans*. Advisor: Asst. Prof. TEWIN TENCOMNAO, Ph.D. Co-advisor: Asst. Prof. SIRIPORN CHUCHAWANKUL, Ph.D.

*Lignosus rhinocerus* (LR) or Tiger Milk Mushroom, a fork medicinal mushroom, has been reported for several pharmacological effects including asthma treatment, anti-inflammatory, anti-proliferative, immuno-modulating effects, promote neurite outgrowth in PC-12 cells, anti-HIV-1 activity, and antioxidants properties. However, the antioxidant properties have only focus on *in vitro* and no or few studies have reported their protective effects in mouse hippocampal (HT22) cells and *Caenorhabditis elegans* (*C. elegans*). This study aims to investigate the neuroprotective effect of three extracts of LR against oxidative stress in both HT22 cells and *C. elegans* as well as longevity in *C. elegans*. In HT22 cells, we assessed the toxicity of three LR extracts (LRE, LRC, and LRH) and their protective activity by MTT assay, Annexin V-FITC/propidium iodide staining, Mitochondrial Membrane Potential (MMP), and assessment of intracellular ROS accumulation. In addition, we determined the antioxidant gene expression by qRT-PCR. In *C. elegans*, wild-type N2 were determined survival rate under oxidative stress and intracellular ROS. Transgenic strains including TJ356, TJ375, CF1553, CL2166, and LD1 were used to detect DAF-16, HSP-16.2, SOD-3, GST-4, and SKN-1, respectively. Lifespan and aging biomarkers including lipofuscin and pharyngeal pumping rate were also assessed. Furthermore, the neuroprotective effects, such as chemotaxis behavior and PolyQ40 formation were assessed as well. We found that only LRE significantly reduced both apoptotic cells and intracellular ROS level but significantly increased antioxidant genes expression after glutamate-induced oxidative stress in HT-22 cells. However, in *C. elegans*, all LR extracts decreased intracellular ROS and protected the worms from oxidative stress through DAF-16/FOXO pathway leading to increase SOD-3 and decrease HSP-16.2. On the other hand, the SKN-1 and GST-4 were not changed. All the extracts extended lifespan and reduced lipofuscin, whereas only high concentration improved pharyngeal pumping rate. All the extracts did not alter the body length and the progeny of the worms excluding dietary restriction. In addition, they exhibited the neuroprotective effects by enhancing chemotaxis Index (CI) in A $\beta$  containing worms and decreasing PolyQ40 aggregation. Interestingly, only LRE exerted neuroprotection on both *in vitro* and *in vivo*. Therefore, this novel study could suggest that LR extracts, especially LRE, may be an alternative for neuroprotective supplements.

Field of Study: Clinical Biochemistry and Molecular Medicine Student's Signature .....

Academic Year: 2020 Advisor's Signature .....  
Co-advisor's Signature .....

## ACKNOWLEDGEMENTS

First of all, I would like to express my sincere gratitude to my advisor, Asst. Prof. Dr. Tewin Tencomnao, Department of Clinical Chemistry, Faculty of Allied Health Sciences for the continuous support of my research, for his empathy and his considerable guidance that helped me find the solution throughout my research and writing of this dissertation.

I would like to sincerely thank my co-advisor, Asst. Prof. Dr. Siriporn Chuchawankul for her kindness and suggestion.

In addition, I would like to express my special thanks to Prof. Dr. Michael Wink, Institute of Pharmacy and Molecular Biotechnology (IPMB), Department Biology, University of Heidelberg for giving me the great opportunity and experience to do *C. elegans* research internship in Germany, providing facilities and suggestion throughout this research.

My cordially thanks to the examination committee, Asst. Prof. Dr. Viroj Boonyaratanakornkit, Assoc. Prof. Dr. Rachana Santiyanont, Assoc. Prof. Dr. Krai Meemon and Asst. Prof. Dr. Tewart Sarachana for their valuable time, insightful comments, and suggestion.

I wish to thank all the members of TT lab, other members of Clinical Biochemistry and Molecular Medicine (CBMM), as well as all the members at IPMB for their help, encouragement, and friendship.

Thank you to the Clinical Biochemistry and Molecular Medicine Program, Faculty of Allied Health Sciences, for providing facilities and a place for this research study.

I would like to acknowledge the financial support provided by The Royal Golden Jubilee Ph.D. Program Scholarship and The National Research Council of Thailand (NRCT) for graduate dissertation.

Last, but not least I would like to give my whole heart to my dedicated family for their understanding and encouragement throughout my life.

Parinee Kittimongkolsuk

## TABLE OF CONTENTS

	Page
ABSTRACT (THAI).....	iii
ABSTRACT (ENGLISH).....	iv
ACKNOWLEDGEMENTS.....	v
TABLE OF CONTENTS.....	vi
LIST OF TABLES.....	xi
LIST OF FIGURES.....	xii
ABBREVIATIONS.....	xvi
CHAPTER I.....	1
Introduction.....	1
1. Background and rationale.....	1
2. Research questions.....	3
3. Research hypothesis.....	4
4. Research objectives.....	4
5. Research outcomes.....	4
6. Conceptual Framework.....	5
CHAPTER II.....	6
Literature Review.....	6
2.1 Free radicals or reactive oxygen species (ROS) in aging.....	6
2.2 Reactive oxygen species (ROS) in neurodegenerative diseases.....	7
2.3 Role of antioxidant against oxidative stress.....	7
2.4 <i>Lignosus rhinoceros</i> (LR) or Tiger Milk Mushroom.....	8

2.5 Glutamate toxicity.....	13
2.5.1 Receptor-initiated excitotoxicity .....	13
2.5.2 Nonreceptor-mediated oxidative glutamate toxicity .....	14
2.6 <i>Caenorhabditis elegans</i> ( <i>C. elegans</i> ) models.....	15
2.6.1 Anatomy and life cycle.....	15
2.6.2 Stress resistance pathway .....	17
2.6.2.1 DAF-16/FOXO signalling pathway.....	18
2.6.2.2 SKN-1/Nrf2 signalling pathway .....	19
2.6.3 Biomarkers of aging in <i>C. elegans</i> .....	20
2.6.4 Neurotoxic-induced behaviour assessment .....	20
2.6.5 <i>C. elegans</i> -microbiomes interactions.....	21
CHAPTER III.....	23
Materials and Methods.....	23
Chemicals and Reagents.....	23
Equipments and Instruments.....	25
1. Preparation of crude herbal extracts.....	27
2. Gas Chromatograph–Mass Spectrometer (GC-MS) Analysis.....	27
3. Assessment of antioxidant properties of LR <i>in vitro</i> .....	28
3.1 Radical Scavenging Activity Assays: DPPH and ABTS .....	28
3.2 Folin–Ciocalteu Phenol Assay (FCP).....	29
3.3 Total Flavonoid content .....	30
4. <i>In vitro</i> experiments.....	31
4.1 Cell culture and treatments .....	31



4.2 3-(4,5-Dimethylthiazol-2-yl)-2,5-diphenyltetrazolium bromide tetrazolium (MTT) Assay.....	31
4.3 Assessment of apoptosis by Annexin V-FITC/propidium iodide (PI) staining using flow-cytometry.....	32
4.4 Mitochondrial Membrane Potential (MMP) assay .....	33
4.5 Assessment of intracellular ROS accumulation.....	34
4.6 RNA isolation and assessment of antioxidant genes expression by real-time PCR (qPCR).....	35
5. <i>In vivo</i> experiments .....	36
5.1 <i>C. elegans</i> strains and maintenance .....	36
5.2 Synchronization and treatments.....	36
5.3 Microbial susceptibility assays.....	37
5.4 Survival assay under Juglone-induced oxidative stress.....	38
5.5 Measurement of intracellular ROS accumulation.....	38
5.6 Transgenic reporter assays .....	39
5.6.1 Expression of HSP-16.2.....	39
5.6.2 Expression of GST-4.....	39
5.6.3 Expression of SOD-3 .....	40
5.7 Subcellular DAF-16 localization .....	40
5.8 Subcellular SKN-1 localization.....	40
5.9 Lifespan assay.....	41
5.10 Measurement of autofluorescent pigment (Lipofuscin).....	41
5.11 Measurement of pharyngeal pumping rate.....	42
5.12 Measurement of brood size and body length.....	42
5.13 Assessment of neuroprotective effects in <i>C. elegans</i> model.....	43

5.13.1 Chemotaxis assay.....	43
5.13.2 Assessment of PolyQ40 aggregation.....	44
5.14 Statistical Analysis .....	45
CHAPTER IV.....	46
Results.....	46
1. Antioxidant Properties and Total Phenolic and Flavonoid Contents .....	46
2. Phytochemical Constituents of LRE.....	47
3. The biological activities of LR extract in mouse hippocampal HT22 cells ( <i>in vitro</i> ) .....	49
3.1 Effect of LR extracts against glutamate-induced cytotoxicity .....	49
3.2 Anti-apoptotic activity of LR extracts.....	51
3.3 Effect of LR extracts on Mitochondrial Membrane Potential (MMP).....	54
3.4 Effect of LR extracts on intracellular ROS level.....	56
3.5 Effect of LR extracts on antioxidant gene expressions .....	58
4. The biological activities of LR extract in <i>C. elegans</i> ( <i>in vivo</i> ).....	60
4.1 Microbial susceptibility assays.....	60
4.2 Effect of LR extracts against juglone-induced oxidative stress in wild type	61
4.3 Effect of LR extracts on intracellular ROS accumulation in wild type.....	62
4.4 Effect of LR extracts on HSP-16.2 expression .....	64
4.5 Effect of LR extracts on GST-4 expression.....	66
4.6 Effect of LR extracts on SOD-3 expression .....	67
4.7 Effect of LR extracts on DAF-16/FOXO pathway.....	69
4.7.1 Effect of LR extracts against juglone-induced oxidative stress in CF1038 .....	70

4.7.2 Effect of LR extracts on intracellular ROS accumulation in CF1038	72
4.8 Effect of LR extracts on SKN-1/NRF-2 pathway .....	73
4.9 Effect of LR extracts on lifespan extension.....	74
4.10 Effect of LR extracts on Lipofuscin level .....	76
4.11 Effect of LR extracts on pharyngeal pumping rate.....	78
4.12 Effect of LR extracts on body length and Brood size.....	80
4.13 Neuroprotective effect of LR extracts against A $\beta$ -induced deficit in chemotaxis behavior in <i>C. elegans</i> .....	82
4.14 Neuroprotective effect of LR extracts on PolyQ40 aggregation .....	85
CHAPTER V .....	88
Discussion and Conclusion.....	88
REFERENCES .....	94
VITA.....	115

## LIST OF TABLES

	Page
Table 1 Free radical scavenging capacity of three extractions of <i>Lignosus rhinocerus</i> (LR) using DPPH scavenging assay.....	46
Table 2 Free radical scavenging capacity of three extractions of <i>Lignosus rhinocerus</i> (LR) using ABTS scavenging assay.....	47
Table 3 Total phenolic and flavonoid contents of three extractions of <i>Lignosus rhinocerus</i> (LR).....	47
Table 4 Proposed phytochemical constituents in <i>Lignosus rhinocerus</i> (LRE).....	48
Table 5 Microbial susceptibility test .....	60
Table 6 Results and statistical analyses of <i>C. elegans</i> lifespan assay .....	76

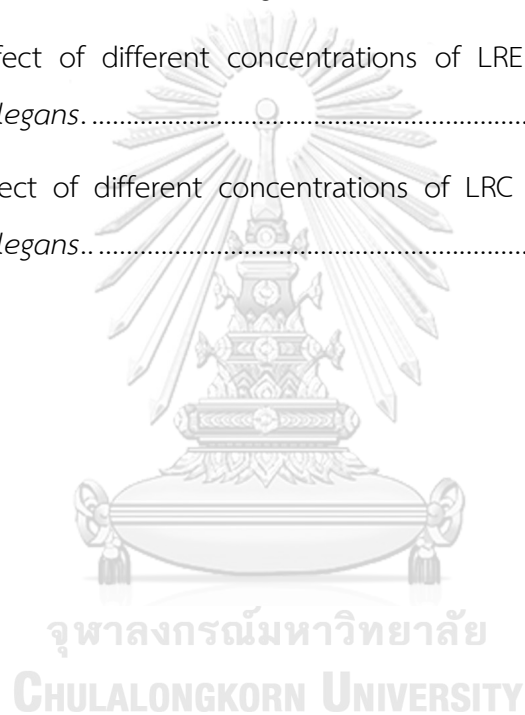
## LIST OF FIGURES

	Page
Figure 1 Model for the neuroprotective effect of LR extracts in HT22 cells and <i>C. elegans</i> .....	5
Figure 2 Intracellular ROS production from mitochondria DNA damage which accelerate aging process.....	6
Figure 3 Enzymatic antioxidant defense system.....	8
Figure 4 The scientific classification of <i>Lignosus rhinocerus</i> .	9
Figure 5 The morphology of Tiger Milk Mushroom ( <i>Lignosus rhinocerus</i> ).....	9
Figure 6 The chemical and nutritional of <i>Lignosus rhinocerus</i> (LR) .....	10
Figure 7 Volatile compounds in <i>Lignosus rhinocerus</i> (LR) .....	11
Figure 8 Glutamate-induced toxicity pathways .....	15
Figure 9 Anatomy of <i>C.elegans</i> .....	16
Figure 10 life cycle of <i>C.elegans</i> .....	17
Figure 11 IIS and DAF-16 pathway.....	19
Figure 12 Schematic of DAF-16 on target gene classes .....	19
Figure 13 Schematic of SKN-1 on target gene classes .....	20
Figure 14 The test for toxicity assessment .....	21
Figure 15 Principle of DPPH radical scavenging capacity assay.....	28
Figure 16 Principle of ABTS radical scavenging capacity assay .....	29
Figure 17 Principle of Folin–Ciocalteu Phenol Assay.....	29
Figure 18 Principle of total flavonoid content .....	30

Figure 19 MTT assay.....	32
Figure 20 Annexin V-FITC/propidium iodide (PI) staining at various stage of apoptosis. .....	33
Figure 21 Mitochondrial Membrane Potential (MMP) assay .....	34
Figure 22 Reactive oxygen species assay.....	35
Figure 23 Synchronization technique .....	37
Figure 24 Chemotaxis assay .....	44
Figure 25 Gas chromatograph–mass spectrometer (GC-MS) chromatogram of ethanol extraction of <i>Lignosus rhinocerus</i> (LRE).....	48
Figure 26 Protective effect of different concentrations of LR extracts against glutamate-induced toxicity in HT22 cells. ....	51
Figure 27 Quantitative flow cytometric analysis of apoptotic cells using annexin V- FITC/PI staining in HT22 cells.....	53
Figure 28 Protective effect of different concentrations of LR extracts on MMP in HT22 cells. ....	55
Figure 29 The effect of different concentration of LR extracts on intracellular ROS accumulation in HT22 cells. ....	57
Figure 30 The effect of different concentrations of LRE extracts on antioxidant gene expressions in HT22 cells. ....	60
Figure 31 Microbial susceptibility test .....	61
Figure 32 Effect of different concentrations of LR extracts on survival rate against juglone-induced oxidative stress in N2 worms. ....	62
Figure 33 Effect of different concentrations of LRE extracts and positive control (EGCG) on intracellular ROS accumulation in N2 worms.. ....	63

Figure 34 Effect of different concentrations of LRC, LRH extracts and positive control (EGCG) on intracellular ROS accumulation in N2 worms. ....	64
Figure 35 Effect of different concentrations of LRE extracts and positive control (EGCG) on HSP-16.2 expression in TJ375 transgenic worms. ....	65
Figure 36 Effect of different concentrations of LRC, LRH extracts and positive control (EGCG) on HSP-16.2 expression in TJ375 transgenic worms. ....	66
Figure 37 Effect of different concentrations of LR extracts on GST-4 expression in CL2166 transgenic worms. ....	67
Figure 38 Effect of different concentrations of LRE extracts and positive control (EGCG) on SOD-3 expression in CF1553 transgenic worms. ....	68
Figure 39 Effect of different concentrations of LRC, LRH extracts and positive control (EGCG) on SOD-3 expression in CF1553 transgenic worms. ....	69
Figure 40 Effect of different concentrations of the extracts on DAF-16 nuclear localization in TJ356 transgenic worms. ....	70
Figure 41 Effect of different concentrations of LR extracts on survival rate against juglone-induced oxidative stress in CE1038 worms. ....	71
Figure 42 Effect of different concentrations of LR extracts on intracellular ROS accumulation in CF1038 worms. ....	72
Figure 43 Effect of different concentrations of the extracts on SKN-1 nuclear localization in LD1 transgenic worms. ....	73
Figure 44 Effect of different concentrations of LR extracts on Longevity. ....	75
Figure 45 Effect of different concentrations of LR extracts on lipofuscin level in BA17 worms. ....	78
Figure 46 Effect of different concentrations of LR extracts on pharyngeal pumping rate in N2 worms. ....	80

Figure 47 Effect of different concentrations of LR extracts on body length in N2 worms.....	81
Figure 48 Effect of different concentrations of LR extracts on brood size in N2 worms. .....	82
Figure 49 The effect of different concentrations of LRE extracts against A $\beta$ -induced deficit in chemotaxis behavior in <i>C. elegans</i> . ....	84
Figure 50 The effect of different concentrations of LRE extracts against PolyQ40 aggregation in <i>C. elegans</i> . ....	86
Figure 51 The effect of different concentrations of LRC and LRH against PolyQ40 aggregation in <i>C. elegans</i> . ....	87





## ABBREVIATIONS

LR	<i>Lignosus rhinocerus</i>
LRE	ethanol extract of <i>Lignosus rhinocerus</i>
LRC	cold water extract of <i>Lignosus rhinocerus</i>
LRH	hot water extract of <i>Lignosus rhinocerus</i>
A $\beta$	amyloid beta
qRT-PCR	real time RT-PCR
MMP	mitochondrial membrane potential
AD	Alzheimer's disease
DCFH2-DA	2',7'- dichlorofluorescein diacetate;
MTT	3-(4,5-dimethylthiazol-2-yl)-2,5- diphenyltetrazolium bromide
Glu	glutamate
CAT	catalase
SOD	superoxide dismutase
GPx	glutathione peroxidase
ROS	reactive oxygen species
CI	chemotaxis index
NAC	N-acetylcysteine
EGCG	Epigallocatechin gallate
ABTS	2,2-Azino-bis(3-ethylbenzothiazoline-6-sulfonic acid)
<i>C. elegans</i>	<i>Caenorhabditis elegans</i>
AD	Alzheimer's disease
DMSO	Dimethyl sulfoxide
DPPH	Diammonium salt, 2,2-Diphenyl-1-picrylhydrazyl
H <sub>2</sub> DCF-DA	2,7-dichlorofluorescein diacetate
PBS	Phosphate buffer saline

## CHAPTER I

### Introduction

#### 1. Background and rationale

Aging is a physiologic state in which a progressive decline of organ functions. This process is the leading cause of age-related diseases such as diabetes [1], cancer [2, 3] and neurodegenerative diseases, including Parkinson's disease (PD), Huntington's diseases (HD), and Alzheimer's diseases (AD) which are one of the major causes of life suffering in worldwide aging population [4-6]. The causes of aging are probably related to a multifactorial process, especially the free radical and mitochondrial dysfunction are the most remarkable theories and show a strong overlap process on aging [7]. Reactive oxygen species (ROS) play complex role in aging by causing oxidative stress to injure cellular. It can be produced not only from extracellular factor including inflammation from pathogen, UV, and radiation but also from intracellular factor including cellular metabolism [8, 9]. ROS accumulation can damage cells by reacting with lipids, proteins, and nucleic acids, particularly in the mitochondrial DNA (mtDNA) [10]. So, the endogenous antioxidants such as superoxide dismutase (SOD), catalase (CAT) and Glutathione Peroxidase (GPx) play an important role to detoxify ROS [11].

In recent years, medicinal mushrooms have become extensive attention as major sources of new therapeutic agents [12, 13].

*Lignosus rhinocerus* (LR) or Tiger Milk Mushroom is an edible mushroom. It has been found in Malaysia, China and Thailand. Its sclerotium (tuber) is commonly used as folk medicinal medicine and first described to treat asthma [14, 15]. Several findings revealed that the sclerotium extracts of LR contain various biologically active

substances such as polysaccharides, polysaccharides-protein complexes,  $\beta$ -glucan and phenolic compounds. Recently, LR have been reported for the anti-inflammatory, antioxidant, anti-proliferative, immuno-modulating effects, promote neurite outgrowth in PC-12 cells [16, 17], and anti-HIV-1 activity [18]. However, antioxidant activities of LR were based upon data from *in vitro* study including 2,2-diphenyl-1-picryl-hydrazyl-hydrate (DPPH) scavenging assay and 2,2'-azino-bis (3-ethylbenzthiazoline-6-sulphonic acid) (ABTS) scavenging assay. Furthermore, no or few studies have reported their effects in mouse hippocampal (HT22) cell and *Caenorhabditis elegans* (*C. elegans*). therefore, in this study, we set out, for the first time, to investigate the neuroprotective effect of three extractions of *Lignosus rhinocerus* (LR); ethanol extract (LRE), cold water extract (LRC), and hot water extract (LRH) against glutamate-induced oxidative stress in HT22 cells as *in vitro* model and investigate antioxidant effects, lifespan extension, and neuroprotective effect in *C. elegans* as *in vivo* model.

HT22 cells were used to study glutamate-induced oxidative stress. The glutamate can induced intracellular ROS and lead to oxidative stress in HT22 because they lack of ionotropic glutamate receptor, [19]. After that, the oxidative stress damages the nerve cells and results in cell death.

*C. elegans*, a free-living soil nematode, is widely used as a model of anti-aging, stress resistance, neuroscience, and longevity because they shared high homology with mammalian and human genes and biochemical pathways [20, 21]. The two major signaling pathways that regulate longevity and stress resistance in this nematode are DAF-16/FOXO pathway. Another pathway is SKN-1/NRF-2 pathway [22]. Several findings determined the antioxidant activities of plants that contained phenolic compounds, the secondary metabolite, [23-28]

Thus, the key research questions of this study were whether LRE, LRC and LRH can protect the neurotoxicity against glutamate-induced oxidative stress in HT22 cells and exhibited both the protective effect and lifespan extension in *C. elegans*. To test this hypothesis, the antioxidant properties of three extracts of LR were examined DPPH scavenging assay, ABTS scavenging assay, total flavonoid and total phenolic contents. In HT22 cells, cytotoxicity was determined by MTT assay. Apoptotic cells were assessed by annexin V-PI staining using flow cytometry analysis. The intracellular ROS accumulation level was detected using oxidized DCFDA. In addition, antioxidant gene expressions (CAT, SOD1, SOD2 and GPx) were determine by real-time PCR (qPCR). In *C. elegans*, the expression of stress-response proteins, such as heat shock protein (HSP-16.2), SOD-3, and GST-4, and transcription factors, such as DAF-16/FOXO transcription factor, and SKN-1/NRF-2 transcription factor were investigated. Aging marker, such as lipofuscin (an autofluorescent pigment) and pharyngeal pumping rate, were analyzed. The toxicity impacts (body length, and the number progeny) and lifespan were also assessed. In addition, neuroprotective effects against neurotoxicity were assessed by chemotaxis assay and polyQ40 aggregation. Therefore, our study would be suggested that LR extracts has a potent neuroprotective effect against toxicity on both HT22 cells and *C. elegans* as well as prolongation of lifespan in *C. elegans*.

## 2. Research questions

2.1 Whether the *Lignosus rhinocerus* (LR) extracts had neuroprotective effects against the oxidative stress in mouse hippocampal (HT22) neuronal cells and *Caenorhabditis elegans* (*C. elegans*) as well as lifespan extension in *Caenorhabditis elegans*.

2.2 What is the neuroprotective mechanism of *Lignosus rhinocerus* (LR) extracts in mouse hippocampal (HT22) neuronal cells and *Caenorhabditis elegans* model?

### 3. Research hypothesis

3.1 The *Lignosus rhinocerus* (LR) extracts had neuroprotective effects against the oxidative stress in mouse hippocampal (HT22) neuronal cells via a decrease in apoptotic cells and an increase in antioxidant gene expressions.

3.2 The *Lignosus rhinocerus* (LR) extracts exhibited both neuroprotective effects against oxidative stress and enhancing lifespan in *Caenorhabditis elegans* via DAF-16/FOXO signaling pathway and/or SKN-1/NRF- signaling pathway as well as a decrease in aging markers.

### 4. Research objectives

4.1 To investigate the biological activities of *Lignosus rhinocerus* (LR) extracts against oxidative stress in mouse hippocampal (HT22) neuronal cells and *Caenorhabditis elegans* (*C. elegans*) and lifespan extension in *Caenorhabditis elegans*.

4.2 To determine the neuroprotective mechanism of *Lignosus rhinocerus* (LR) extracts and in mouse hippocampal (HT22) neuronal cells and *Caenorhabditis elegans* as well as *C. elegans* longevity.

### 5. Research outcomes

Our findings suggest that *Lignosus rhinocerus* (LR) extracts have a potent neuroprotective effect against both glutamate-mediated neuronal cell death and neurotoxicity in *C. elegans*. In addition, they also extend *C. elegans* longevity (Figure 1). Therefore, this study implies that the *Lignosus rhinocerus* (LR) extracts might be a candidate for the prevention of neurodegeneration.

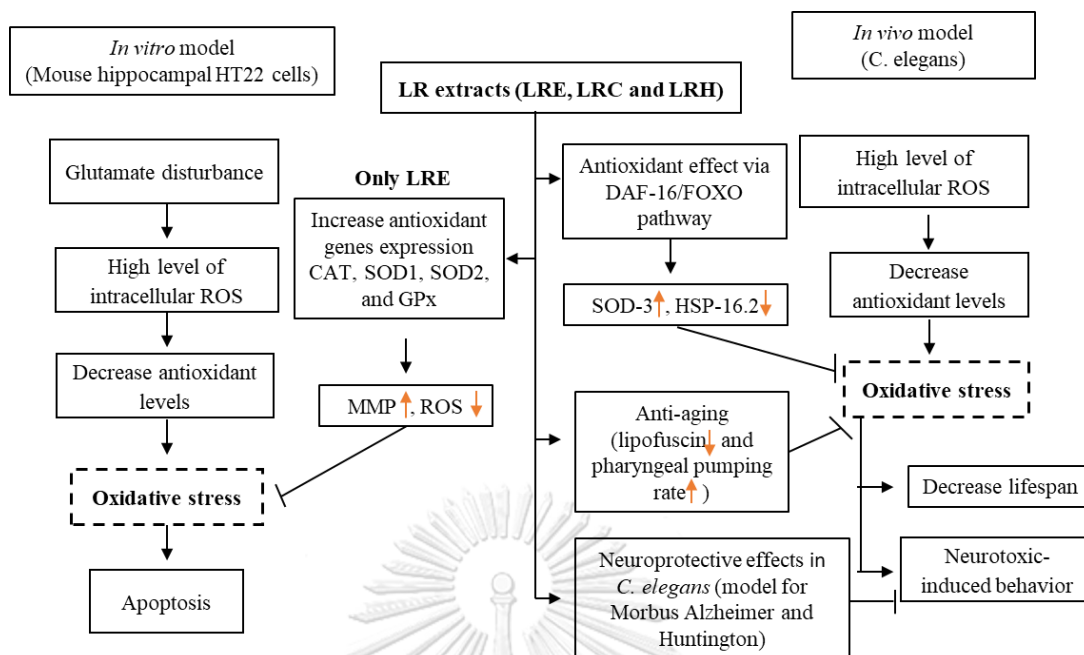
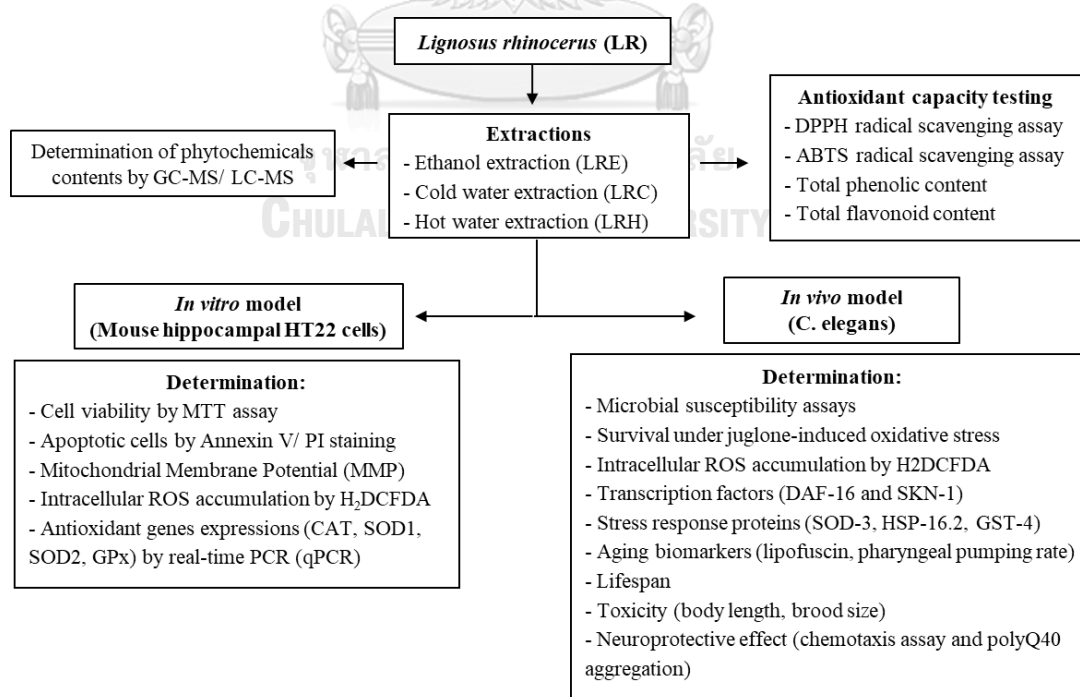


Figure 1 Model for the neuroprotective effect of LR extracts in HT22 cells and *C. elegans*

## 6. Conceptual Framework



## CHAPTER II

## Literature Review

## 2.1 Free radicals or reactive oxygen species (ROS) in aging.

Free radical or reactive oxygen species (ROS) are highly reactive molecules that consist of a number of diverse chemical species including superoxide anion ( $O_2^{\cdot-}$ ), hydroxyl radical ( $\cdot OH$ ), and hydrogen peroxide ( $H_2O_2$ ) [9]. They are produced by either extracellular stress factors including radiation, drugs, inflammation and trauma, or intracellular factor such as mitochondria metabolism. Many evidences show that mitochondrial dysfunction can produce more ROS formation (Figure 2). High ROS accumulation causes react with lipids, proteins, and nucleic acids causing oxidative damage or oxidative stress which accelerates aging [7, 29, 30].

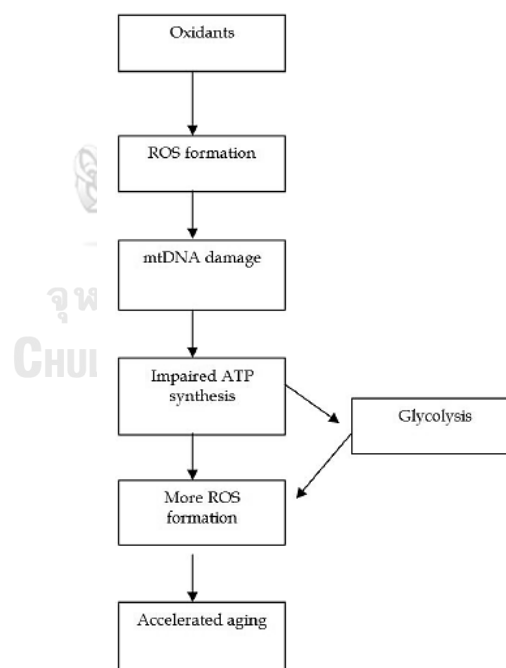


**Figure 2** Intracellular ROS production from mitochondria DNA damage which accelerate aging process [29].

## 2.2 Reactive oxygen species (ROS) in neurodegenerative diseases.

The intracellular ROS, especially superoxide anion ( $O_2^{\cdot-}$ ) mostly is generated in the mitochondrial respiratory chain [10]. It can induce oxidative stress by inducing lipid peroxidation because lipid which is mostly contained in the brain is polyunsaturated fatty acids (PUFAs) and highly susceptible to lipid peroxidation. Consequently, this process causes oxidative stress and cell damage leading to neurodegenerative diseases [31, 32] including Alzheimer's disease (AD) which is the most common form of dementia among worldwide older people over 65 years [6].

In addition, some studies found that accumulation of Amyloid beta ( $A\beta$ ), which is a main component protein of amyloid plaques and found in AD patient's brain, can insert into the neuronal and glial membrane bilayer and generate oxygen-dependent (and possibly redox metal ion-dependent) free radicals. Their actions result in lipid peroxidation and protein oxidation and lead to cellular dysfunction such as inhibition of glial cell  $Na^+$ -dependent glutamate uptake system with consequences on neuronal excitatory NMDA receptors, loss of protein transporter function, disruption of signaling pathways, and activation of nuclear transcription factors and apoptotic pathways. [33].

Therefore, imbalance between ROS and antioxidants in brain lead to brain dysfunction and death [11].

## 2.3 Role of antioxidant against oxidative stress

The antioxidants are the first defend mechanism and play a crucial role in detoxifying ROS. There are two main antioxidant systems to defense ROS including enzymatic and nonenzymatic antioxidants. The enzymatic antioxidants consist of superoxide dismutase (SOD) which is the first antioxidant to detoxify  $O_2^{\cdot-}$  into  $H_2O_2$  and  $O_2$ , catalase (CAT) which reacts very efficiently with  $H_2O_2$  to form water and oxygen molecular. In animals, hydrogen peroxide is detoxified by CAT and by glutathione peroxidase (GPx) [11], glutathione peroxidase (GPx) which is one of the most essential anti-oxidative defense mechanisms. It can catalyze hydroperoxides into water and oxygen by working together with oxidization of glutathione. On the



other hand, glutathione reductase (GR) can convert the oxidized glutathione to its reduced form (Figure 3) [34, 35]. The nonenzymatic antioxidants consist of vitamins C and E, phenolic, anthocyanin, flavonoids, and carotenoids which naturally present in foods and act as the secondary defense. In other words, they mostly enhance the function of endogenous enzymatic antioxidants [36-38].

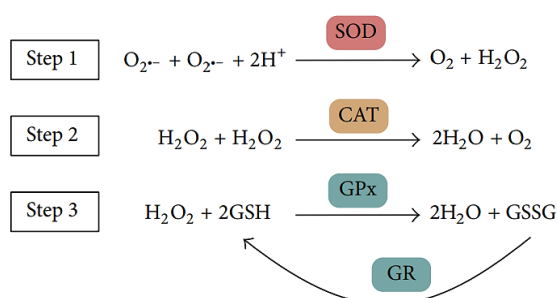


**Figure 3** Enzymatic antioxidant defense system [34].

Furthermore, the transcription factor that plays important role in resistance to oxidant stress is the nuclear factor erythroid 2-related factor 2 (Nrf2) which is responsible for phase II detoxification enzyme systems such as Glutathione peroxidase (GPx) [23]. It is also important for cell survival in role of anti-apoptotic signals in neuronal cells [39].

#### 2.4 *Lignosus rhinoceros* (LR) or Tiger Milk Mushroom

The *Lignosus rhinoceros* (*L. rhinocerotis*) is also known as *Lignosus rhinoceros* (*L. rhinoceros*) or Tiger Milk Mushroom because it is grown from the spot where the tiger dropped its milk while feeding the cubs. It belongs to family Polyporaceae in the division Basidiomycota (Figure 4). Normally, TMM has been found in Malaysia and other regions in South East Asia including Thailand. This mushroom consists of the pileus (cap), stipe (stem), and sclerotium (tuber) which is a compacted mass of fungal mycelium containing food reserves and a popular part that is extracted for medicinal uses (Figure 5) [15].

Scientific classification	
Kingdom:	Fungi
Division:	Basidiomycota
Class:	Agaricomycetes
Order:	Polyporales
Family:	Polyporaceae
Genus:	<i>Lignosus</i>
Species:	<i>L. rhinocerus</i>

**Figure 4** The scientific classification of *Lignosus rhinocerus* [15].

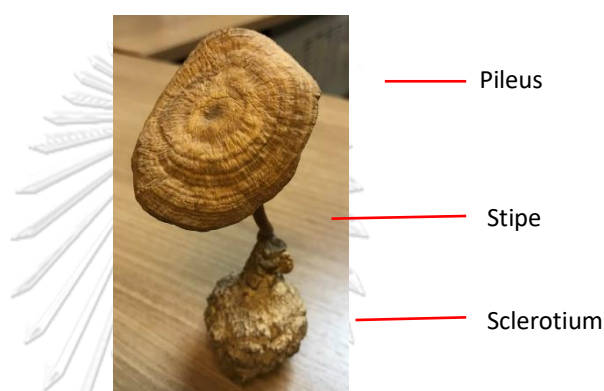


**Figure 5** The morphology of Tiger Milk Mushroom (*Lignosus rhinocerus*)

The Tiger Milk Mushroom have been used as the medicinal mushrooms and home remedies since ancient times for fever, inflammation, and respiratory disorders [15]. Several studies have been found that the cultivated Tiger Milk Mushroom sclerotia (TM02) is better and higher bioactive compounds than wild type [17, 40]. According to genomics and proteomics studies, the bioactive compounds of cultivated TMM sclerotia (TM02) consist of 1,3- $\beta$  - and 1,6- $\beta$  -glucans which is group of  $\beta$ -D-glucose polysaccharides, lectin which is a glycoprotein, laccase which is a copper-containing oxidase enzymes, and other fungal immune-modulatory proteins (FIPs), and antioxidant proteins (Figure 6) [41]. Besides carbohydrate and proteins, there are quinones, flavonoid-like compounds, cerebroside which is the common name for a group of glycosphingolipids and important components in animal muscle and nerve cell membranes, isoflavones, catechols, amines, triacylglycerols, sesquiterpenes and steroids [42].

Composition	<i>Lignosus rhinocerotis</i>	
	Wild strain (WT Rhino)	Commercial strain (TM02)
Energy (kcal/kg dry weight)	21.80 ± 1.20	32.19 ± 0.71
<b>NUTRITIONAL COMPOSITION (G/KG DRY WEIGHT)</b>		
Carbohydrate	8.84 ± 0.35	7.76 ± 0.04
Total sugar	0.07 ± 0.04	0.30 ± 0.10
Protein	0.38 ± 0.03	1.38 ± 0.02
Fat	0.03 ± 0.01	0.08 ± 0.00
<b>MINERAL (MG/KG DRY WEIGHT)</b>		
Calcium, Ca	0.37 ± 0.17	1.93 ± 0.60
Potassium, K	13.22 ± 0.56	20.32 ± 2.53
Sodium, Na	0.85 ± 0.07	0.88 ± 0.09
Magnesium, Mg	7.58 ± 0.37	14.79 ± 0.31
<b>Total glucans (mg/g extract)</b>	<b><i>Lignosus rhinocerotis</i> (KUM61075)</b>	
	<b>Hot water extract</b>	<b>Cold water extract</b>
α-glucan	10.37 ± 0.21	2.507 ± 0.30
β-glucans	38.93 ± 9.65	34.87 ± 8.18

**Figure 6** The chemical and nutritional of *Lignosus rhinocerus* (LR) [15]

In addition, the GC-MS analysis from LR extract showed that the majority groups of volatile compounds were fatty acids (68.58%), followed by esters (10.18%), sterols (6.26%), amides (5.76%), etc. The highest percentage constituent detected was linoleic acid (49.39%), followed by palmitic acid (11.29%), linolelaidic acid methyl ester (7.4%), oleic acid (6.51%), palmitoylethanolamide (3.69%), acetic acid (2.85%), etc. (Figure 7 ) [43]

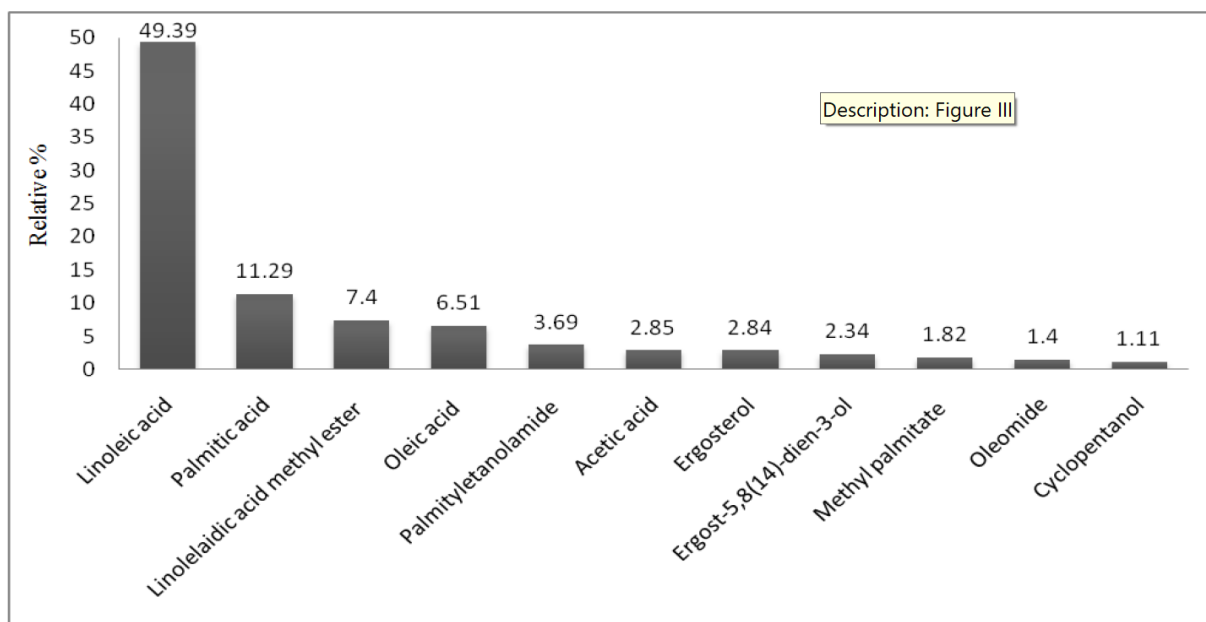


**Figure 7** Volatile compounds in *Lignosus rhinocerus* (LR) [43]

Previous studies have reported the various effects of LR extracts including the anti-asthmatic activity on rodent model of asthma by decrease levels of IgE and Th2 cytokines which is responsible for eosinophils recruitment [44].

Other activities including anti-coagulant and fibrinolytic activities showed that the protein fraction of the mushroom water extract consist of fibrinolytic enzyme with a specific activity of 151.61 U/mg [45].

Anti-inflammatory activity from hot aqueous, cold aqueous, and methanol crude extracts showed that the cold aqueous extract has the most potent extract and high-molecular-weight protein fraction was shown to inhibit tumor necrosis factor alpha (TNF- $\alpha$ ) production in lipopolysaccharide (LPS)-induced RAW 264.7 macrophage cells [46, 47]. Some finding found that the ethanol extract showed significant decrease of nitric oxide (NO) [48].

Anti-microbial activity, the methanol and aqueous extracts showed significant inhibition against the tested microbes except for *Streptococcus pyogenes* and *Serratia marcescens*. A qualitative phytochemical analysis showed the presence of alkaloids, protein, gums and mucilage, and flavonoids [49].

Anti-obesity and hepatoprotective activities, the result show that the aqueous extract of *L. rhinocerotis* mitigated non-alcoholic fatty liver disease in high-fat-diet induced obese hamsters. [50]

Antioxidant properties from cold water extract (CWE), hot water (HWE), and methanol extracts (ME) were test by DPPH• assay, ABTS•+ assay, Ferric reducing antioxidant power (FRAP) assay, and the total phenolic content (TPC). The results showed that phenolic compounds in HWE was highest, followed by CWE and ME, whereas FRAP value is higher in the ME compared to both HWE and CWE. It is possible that ME may present of other less polar components such as tocopherols and flavonoids, which might also contribute to their reducing/electron-donating ability [40]. In addition, several evidences show that  $\beta$ -glucans and polyphenol including flavonoid-like phenolic compounds contributed to the antioxidant activity [17, 40, 51, 52].

Anti-tumor or anti-cancer activities of hot aqueous and cold aqueous extract using 11 human cell lines, namely HL-60 (human acute promyelocytic leukemia cells), MCF7, MDA-MB-231 (human breast adenocarcinoma cells), HCT116 (human colorectal carcinoma cells), PC-3 (human prostate adenocarcinoma cells), A549 (human lung carcinoma cells), MRC-5 (human lung fibroblast cells), HepG2 (human hepatocellular carcinoma cells), WRL68 (human embryonic liver cells), HSC2 (human squamous carcinoma cells), and HK1 (human nasopharyngeal carcinoma cells). The cold aqueous extract was cytotoxic toward solid tumor cells with IC<sub>50</sub> of 37–120mg/mL, whereas the hot aqueous extract was inactive toward the solid tumor cells. [53-55].

Anti-viral activities from water extract showed inhibitory effect against dengue virus type-2 (DENV) by using the plaque reduction assay but the ethanol extract was inactive [56].

Neuritogenic activities, the results showed that the water extract increased the percentage of neurite bearing cells by 9.8 to 23.6% in PC12 cells and showed higher result than ethanol extract. Furthermore, other results showed that the aqueous

extract of sclerotium resulted in 38.1% of neurite bearing cells, which was approximately twice the number of NGF-treated neurite bearing cells in mouse neuroblastoma (N2a) cells [57, 58].

According to biological activities,  $\beta$ -glucans, that are natural cell wall polysaccharides of D-glucose monomers linked by  $\beta$ -glycosidic bonds and found high proportion in the aqueous extracts, are one of the main active components from mushrooms and play an important role in health promotion effects [59]. Normally, they are found from various sources including oat, barley, yeasts, mushrooms, some bacteria and seaweeds [60]. However, different sources of  $\beta$ -glucans show different branching pattern and biological effects. For example,  $\beta$ -glucans from oat and barley cause lowering cholesterol and blood sugar. Furthermore,  $\beta$ -glucans from barley exerted antioxidant activity by reducing of reactive oxygen species (ROS). Similar to barley,  $\beta$ -glucans from oat exerted an indirect antioxidant effect due to binding to specific membrane receptor of immune cells, especially antigen-presenting cells in animals with TNBS-induced colitis resulting in increased antioxidant response [61]. Whereas,  $\beta$ -glucans from mushroom mostly involved in modulating immune system, anti-inflammation, anti-cancer and antiviral activity [62-64].

## 2.5 Glutamate toxicity

Normally, Glutamate, an excitatory neurotransmitter, has a positive impact on several brain functions such as cognition, memory, and learning [65]. However, excess glutamate leads to glutamate toxicity, and the cause of neuronal apoptosis. There are two pathways for glutamate toxicity including receptor-initiated excitotoxicity [19, 66] and nonreceptor-mediated oxidative glutamate toxicity [67].

### 2.5.1 Receptor-initiated excitotoxicity

Exceed glutamate, resulting in excitotoxicity, is released into the synaptic space of brain and stimulates postsynaptic N-methyl-D-aspartate (NMDA) ionotropic glutamate receptors, leading to high influx of  $\text{Ca}^{2+}$  ion follow by increase in

depolarization of post synaptic membrane. These events activate caspase pathway and lead to neuronal apoptosis (Figure 8) [68].

#### 2.5.2 Nonreceptor-mediated oxidative glutamate toxicity

This pathway is linked to glutamate-induced toxicity in HT22 cells. HT22 cells are often used to study the neuroprotective effect against oxidative stress caused by glutamate toxicity because this immortalized cell line lacks of ionotropic glutamate receptor. High concentrations of extracellular glutamate ( $> 200\mu\text{M}$ ) have been shown to cause glutamate-mediated oxidative stress by preventing cysteine uptake into cells through a glutamate/cystine antiporter followed by depletion of intracellular cysteine resulting in glutathione decrease [69] which lead to ROS accumulation. Excessive ROS could damage cells and intracellular organelles such as Mitochondria and endoplasmic reticulum (ER) by several ways. For example, ROS interacts with mitochondrial membrane which lead to lipid peroxidation and membrane destabilization [70]. These processes alter mitochondrial membrane potential (MMP) which is a hallmark of mitochondrial dysfunction resulting in releasing mitochondrial cytochrome c and mitochondrial AIF. In addition, it also binds to mitochondrial DNA to induce fragmentation (Figure 8) [71, 72]. Interestingly, HT22 cells only activate of calpain and upregulation and translocation of AIF but they do not activate caspase-3 [73]. Thus, AIF translocation from mitochondria to the nucleus has been identified as the final step of caspase independent mitochondrial death signaling in neurons [74].

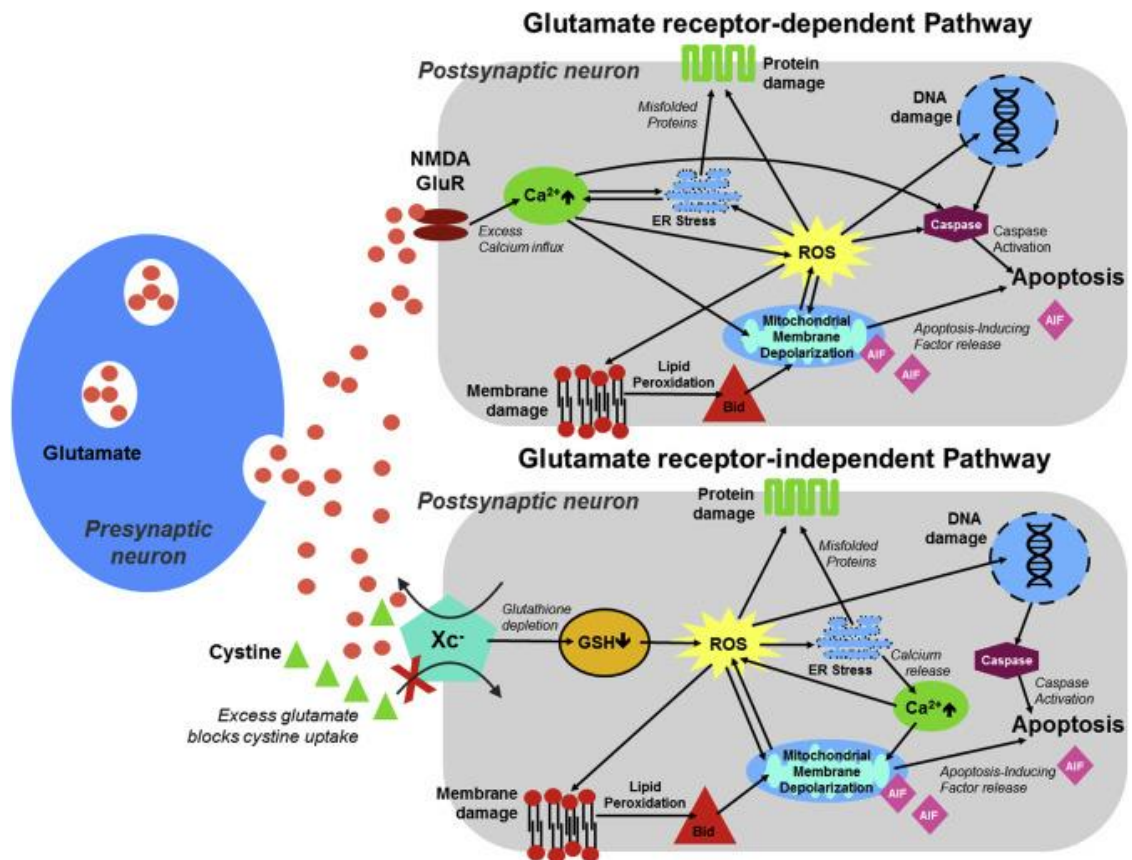


Figure 8 Glutamate-induced toxicity pathways [75]

## 2.6 *Caenorhabditis elegans* (*C. elegans*) models

### 2.6.1 Anatomy and life cycle

The *Caenorhabditis elegans* (*C. elegans*), which is a free-living transparent roundworm (not parasitic) (Figure 9), is widely used as a model organism for studying neuroscience and ageing because of a rapid reproduction rate, a short lifespan and easy to study the mechanism of drug or component [76]. There are two *C. elegans* sexes: a self-fertilizing hermaphrodite (XX) and a male (XO). Males arise infrequently (0.1%) by spontaneous non-disjunction in the hermaphrodite germ line and at higher frequency (up to 50%) through mating. Self-fertilization of the hermaphrodite allows for homozygous worms to generate genetically identical progeny, and male mating facilitates the isolation and maintenance of mutant strains as well as moving mutations between strains [77]. It reproduces with a life cycle of about 3 days under



optimal conditions. The animal can be maintained in the laboratory where it is grown on agar plates or liquid cultures with *E. coli* OP50 as the food source. The average lifespan ranges from 12 to 18 days at 20 °C. Normally, there are two *C. elegans* sexes: a self-fertilizing hermaphrodite (XX) and a male (XO). The postembryonic life cycle of *C. elegans* consists of four larval stages, L1–L4, and a reproductive stage. Under unfavorable conditions, the L2 stage can enter the dauer larval stage instead of developing into the regular L3 stage. The dauer larvae are stress-resistant they are thin, smaller body size and their mouths are sealed and cannot take in food, and they can remain in this stage for a few months. (Figure 10) [22].

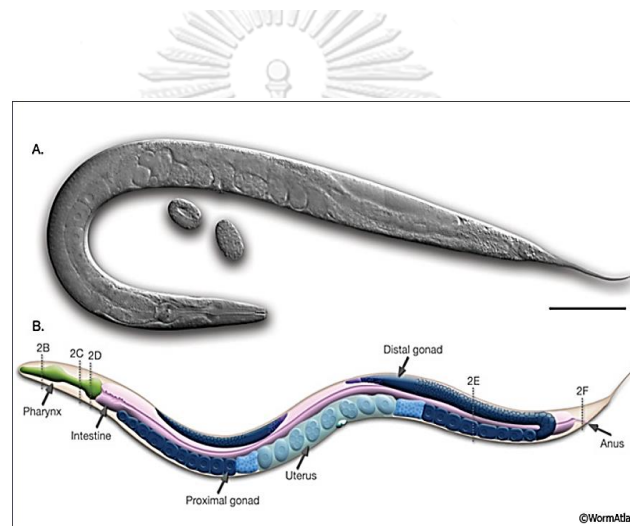
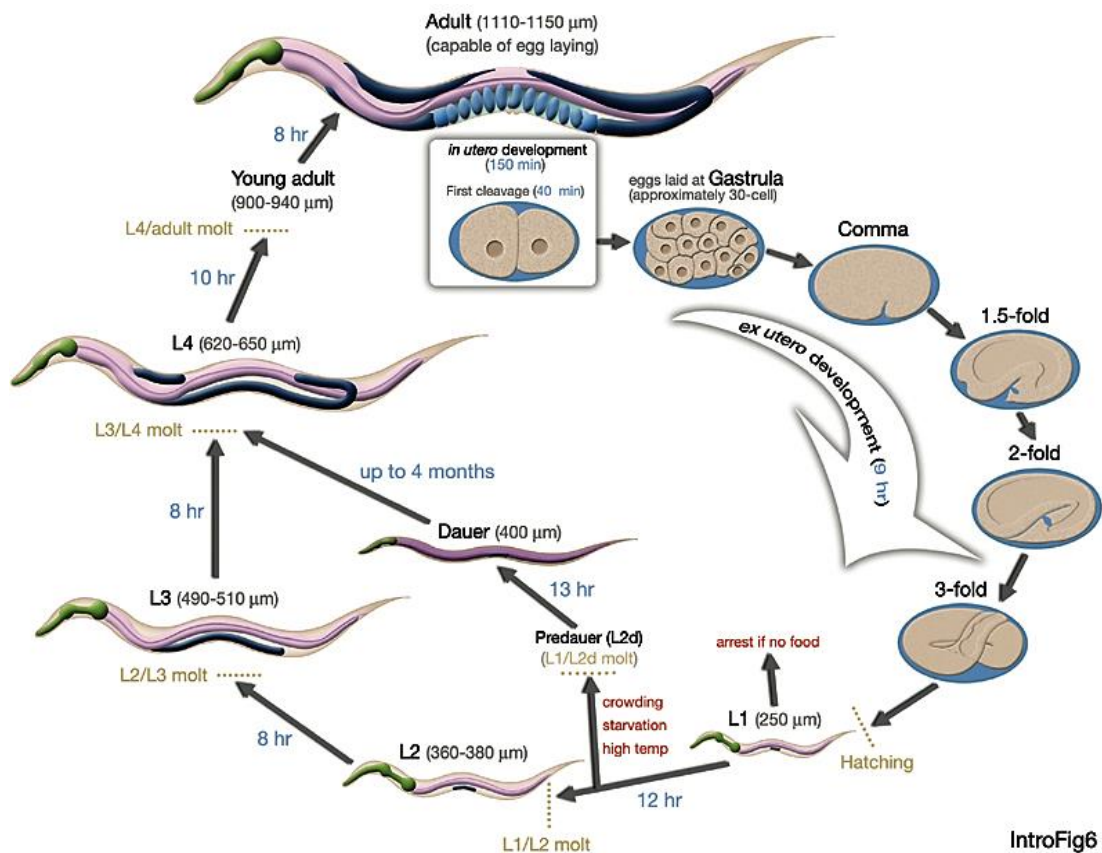


Figure 9 Anatomy of *C. elegans* [77].



IntroFig6

Figure 10 life cycle of *C. elegans* [77]

### 2.6.2 Stress resistance pathway

The major signalling pathways that regulate longevity and stress resistance in mammals (including human) are well conserved in this nematode (59). One of the best-studied pathways in *C. elegans* is the insulin/IGF-1 signaling (IIS) pathway, which regulates nutrient metabolism, growth, development, longevity, and behavior [78]. Under calorie restriction (CR) and oxidative stress, this pathway is inhibited and increase the function of DAF-16 and SKN-1 transcription factors. Thus, the two major signaling pathways that regulate longevity and stress resistance in this nematode are DAF-16/FOXO pathway. Another pathway is SKN-1/NRF-2 pathway [22]. In addition, there are several stressors to induced oxidative stress in *C. elegans* including juglone, H<sub>2</sub>O<sub>2</sub> [79], hypoxia[80],heat shock[81],UV irradiation[82], and heavy metal stress[83].

### 2.6.2.1 DAF-16/FOXO signalling pathway

The DAF-16 transcription factor is orthologue of mammalian Fork head box O family (FOXO) transcription factors. Normally, insulin/IGF-1 signaling (IIS) pathway, a central regulator of DAF-16 activity involves in growth, metabolism, reproduction in response to nutrient, and regulating aging. Activation IIS depends on the phosphorylation of DAF-2 receptor (Insulin/IGF-1 receptor homologue) in turn activates the phosphatidylinositol-3 OH kinase AGE-1 that catalyzes the conversion of phosphatidylinositol bisphosphate (PIP<sub>2</sub>) into phosphatidylinositol trisphosphate (PIP<sub>3</sub>). Then, PIP<sub>3</sub> phosphorylates the complex AKT-1/AKT-2 that leads to phosphorylates the transcription factor DAF-16. Therefore, DAF-16 is inhibited to translocate to nucleus. On the other hand, inhibition IIS by calorie restriction (CR) or oxidative stress promotes DAF-16 translocation to nucleus leading to stress response and lifespan extension in nematode (Figure 11) [84-86]. Activation of DAF-16 transcription factor can regulate many antioxidant genes including superoxide dismutase-3 (sod-3), catalase-1 (ctl-1), and small heat shock protein-16.2 (hsp-16.2) (Figure 12). In addition, several lines of evidence suggest that DAF-16 is also activated by other molecules for its activity including c-Jun N-terminal kinase (JNK), CST-1 or Ste20-like kinase and MST1 homolog, Sir2, The 14-3-3 proteins, Heat-shock factor (HSF),  $\beta$ -catenin, SMK-1, HCF-1 and SKN-1 [87].

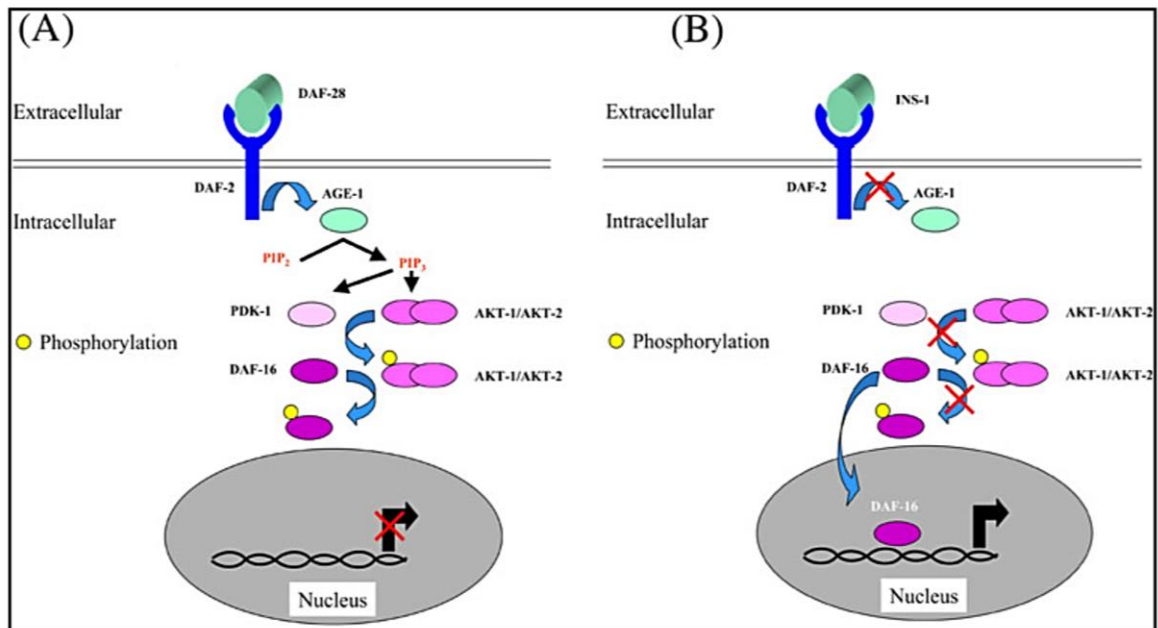


**Figure 11** IIS and DAF-16 pathway. Activation IIS pathway inhibits DAF-16 translocation to nucleus (A). Whereas, inhibition IIS signaling promotes DAF-16 translocation to nucleus [86]

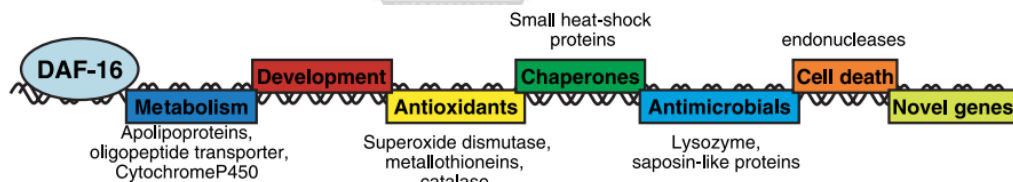


**Figure 5** Schematic presentation of DAF-16 target gene classes.

**Figure 12** Schematic of DAF-16 on target gene classes [88]

### 2.6.2.2 SKN-1/Nrf2 signalling pathway

Similar to DAF-16 activation, reducing of IIS pathway and under oxidative stress can also increase SKN-1 activities. The SKN-1 which is homologue of mammalian Nrf2 transcription factor responds to oxidative stress. The SKN-1/Nrf2 defends against oxidative stress by activating the conserved phase II detoxification enzymes including glutathione (GST-4) (Figure 13) [89].

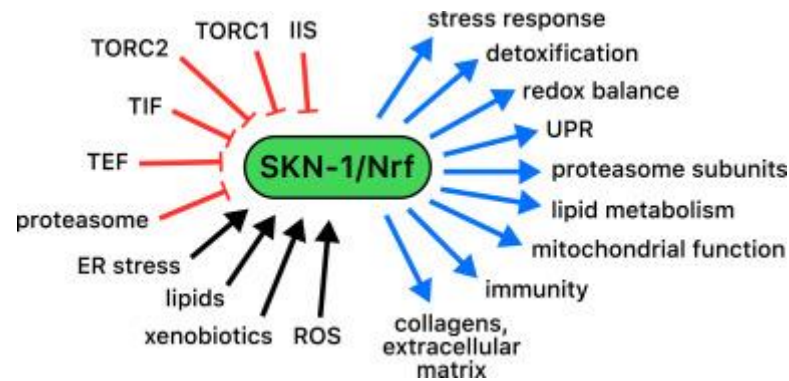


**Figure 13** Schematic of SKN-1 on target gene classes [90].

### 2.6.3 Biomarkers of aging in *C. elegans*

Besides antioxidant genes expression, another marker is lipofuscin, autofluorescent pigments or age pigments, is non-degradable and consists of oxidized, cross-linked proteins, lipids and saccharides. It is naturally produced and increased accumulation in intestinal lysosomes during aging due to cellular proteolytic mechanisms inability to degrade. [91, 92]. In addition, pharyngeal pumping rate is also related to aging. The aged worms also decline of both pharyngeal pumping rate and body movement. Moreover, measurements of these processes can be used to predict lifespan [93].

### 2.6.4 Neurotoxic-induced behaviour assessment

*C. elegans* became a more widely-used model in the neurotoxicology community. This was partly due to the simplicity of their nervous system, which is a relatively small neuronal network that is highly conserve with higher eukaryotes [94]. So, regulation of neurotoxicity and antioxidant stress responses in the worm provides critical insight into mechanisms of mammalian neurotoxicity. *C. elegans* has 302 neurons that signal through 890 electrical junctions, 1410 neuromuscular junctions and 6393 chemical synapses, using the same neurotransmitter systems including cholinergic, gamma amino butyric acid [GABAergic], glutamatergic, dopaminergic [DAergic] and serotonergic that are expressed in vertebrates [95]. Several studies

examining neurotoxicants from various toxicants, including pesticides [96], manganese (Mn) [97], cadmium (Cd), methylmercury (MeHg) and iron (Fe) by assess behavior-induced alterations including motility or locomotion behavior, chemotaxis behavior, feeding rate, feeding behavior, structural, reproduction, larval growth, gene expression and biochemical assay (Figure 14) [20, 94, 98, 99].

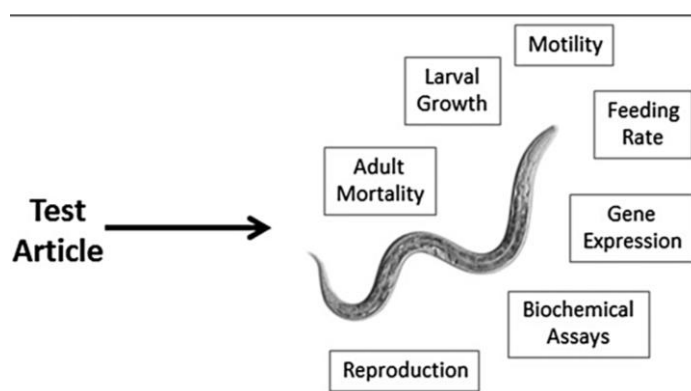


Figure 14 The test for toxicity assessment [20]

### 2.6.5 *C. elegans*-microbiomes interactions

Microbiomes are a community of microbiota including bacteria, fungi, and viruses present in a define environment, particularly in the gut. Gut microbiota played important roles in human health and diseases [100]. However, the underlying mechanisms of human-microbiota interaction are difficult and complex. Therefore, simple whole organism model such as *C. elegans* is useful to study how bacterial effects on host physiology. *C. elegans* in nature that live in soil and microorganism-rich rotting fruit and plant found diverse microbial community including Gammaproteobacteria (*Enterobacteriaceae*, *Pseudomonadaceae* and *Xanthomonadaceae*) and Bacteroidetes (*Sphingobacteriaceae*, *Weeksellaceae* and *Flavobacteriaceae*) [101, 102]. Similar to human gut microbiota, *C. elegans* gut microbiota involved in development, metabolism, immunity and lifespan [103, 104]. In addition, previous studies found that different strains of bacteria affect different *C. elegans*' biological activities. For examples, *B. megaterium* and *P. mendocina*

involved in immune-protective effect of *C. elegans* [105], *Pseudomonas* MYb11 had anti-fungal to protect nematodes from fungal [106], *Escherichia coli* mutations that increase ROS production found to activate host mitochondrial stress response, which delayed development in *C. elegans* [107], and *Bacillus subtilis* produced metabolites, nitric oxide, that extended the lifespan of nematodes through DAF-16 transcription [108-110].



## CHAPTER III

### Materials and Methods

#### Chemicals and Reagents

- 2,2'-Azino-bis (3- ethylbenzothiazoline-6-sulfonic acid) cation (ABTS) [Sigma-Aldrich, USA]
- Aluminum chloride Sigma-Aldrich, USA
- 5-(and-6)-carboxy-2',7'-dihydrofluorescein diacetate (H2DFFDA) [Thermo Scientific, USA]
- 2,2-Diphenyl-1-picrylhydrazyl (DPPH) [Merck, Germany]
- 3-(4,5-dimethylthiazol-2-yl)-2,5-diphenyl tetrazolium bromide (MTT) [Bio-basic, Canada]
- 2,7-dichlorofluorescein diacetate or H2DCF-DA [Fluka GmbH, Switzerland]
- Diethyl pyrocarbonate (DEPC) [Sigma-Aldrich, USA]
- Cholesterol [Sigma-Aldrich, Germany]
- Tryptone [Sigma-Aldrich, Germany]
- Yeast extract [Sigma-Aldrich, Germany]
- Potassium citrate [Sigma-Aldrich, Germany]
- Dimethyl Sulfoxide (DMSO) [Sigma-Aldrich, USA]
- DNA Ladder 100 bps [Fermentas, Lithuania]
- Dulbecco's modified Eagle medium (DMEM) [Sigma-Aldrich, USA]
- Ethanol RCI [Labscan, Thailand]
- Folin-Ciocalteu's phenol reagent [Sigma-Aldrich, USA]
- Gallic acid [Merck, Germany]



- Hydrochloric acid, 37% [Merck, Germany]
- Isopropanol [Sigma-Aldrich, USA]
- L-ascorbic acid [Calbiochem, USA]
- L-glutamic acid [Sigma-Aldrich, USA]
- Paraformaldehyde [Sigma-Aldrich, USA]
- Penicillin-Streptomycin solution [Corning Inc., USA]
- Phosphate Buffered Saline (PBS) [Hyclone, USA]
- Potassium persulfate [Sigma-Aldrich, USA]
- Primers [Bioneer, South Korea]
- Quercetin [Sigma-Aldrich, USA]
- RT Premix [Bioneer, South Korea]
- Sodium azide (AppliChem GmbH, Germany)
- Sodium acetate [Sigma-Aldrich, USA]
- Sodium carbonate [Merck, Germany]
- Sodium chloride [Merck, Germany]
- Dipotassium phosphate [Sigma-Aldrich, Germany]
- Potassium phosphate monobasic [Sigma-Aldrich, Germany]
- Magnesium Magnesium sulfate [Sigma-Aldrich, Germany]
- Juglone [Sigma-Aldrich GmbH, Germany]
- EGCG [Sigma-Aldrich, Germany]
- Sodium dodecyl sulfate (SDS) [Biobasics Inc., Canada]
- Sodium hydroxide [Merck, Germany]
- Trypsin-EDTA [Hyclone, USA]
- Trypan Blue Stain [Invitrogen, USA]

- Trizol Reagent [Invitrogen, USA]

### Equipments and Instruments

- Adhesive optical sealing film [Bioneer, South Korea]
- UV-Vis spectrophotometer (NanoDrop ND-1000) [Thermo Scientific, USA]
- Vortex [Scientific Industries, USA]
- Water bath [Mettmert, Germany]
- Analytical balances [MettlerToledo, Switzerland]
- Autoclave [Hirayama, Japan]
- Auto pipettes [Gilson, France]
- Exicycler real-time quantitative thermal block [Bioneer, South Korea]
- Filter tips [Thermo Scientific, USA]
- Flat bottom culture plate (6, 12, 96 well-plate) [Corning Inc., USA]
- Flow cytometer (BD FACSCalibur) [BD Biosciences, USA]
- Freezer (-20 °C) [Sanyo Electric, Japan]
- Freezer (-80 °C) [Lyofreeze, USA]
- Gel documentation (Geldoc) system [Syngene, UK]
- Gel electrophoresis apparatus [Bio-Rad, USA]
- Glasswares [Pyrex, USA]
- Hemocytometer [Hausser Scientific, USA]
- Incubator [Mettmert, Germany]
- Inverted microscope [Olympus, Japan]
- Laminar flow cabinet [Haier, China]
- Lamina flow clean bench [Esco, Singapore]
- Light microscope [Olympus , Japan]

- Liquid nitrogen tank [Taylor Wharton, USA]
- Magnetic stirrer [Daihan, South Korea]
- Microcentrifuge refrigerated machine [Vision, South Korea]
- Microplate reader (Enspire) [Perkin-Elmer, USA]
- Multichannel pipette [Gilson, France]
- pH meter [MettlerToledo, Switzerland]
- Pipette tips 10  $\mu$ L [Sorenson, USA]
- Pipette tips 20  $\mu$ L [Sorenson, USA]
- Pipette tips 200  $\mu$ L [Corning Inc., USA]
- Pipette tips 1000  $\mu$ L [Corning Inc., USA]
- PCR tube (0.2 mL) [Bioneer, South Korea]
- PVDF membrane [GE Healthcare, UK]
- Refrigerator (4  $^{\circ}$ C) [Sharp, Japan]
- Rotary evaporator [Heidolph, Germany]
- Soxhlet extraction apparatus [Lenz Laborglas, Germany]
- Benchtop centrifuge model Hettich Universal 320R [Sigma-Aldrich, USA]
- Centrifugal evaporator model miVac Quattro [Genevac, UK]
- Centrifuge tube (15, 50 mL.) [Corning Inc., USA]
- Cell culture flask (25, 75 CM<sup>2</sup>) [Corning Inc., USA]
- CO<sub>2</sub> incubator model Forma Series II 3110 [Thermo Scientific, USA]
- Cryovial tube (2 mL.) [Corning Inc., USA]
- Confocal laser scanning microscope (LSM 700) [Carl Zeiss, Germany]
- Fluorescence microscope BIOREVO BZ-9000 with a mercury lamp [Keyence, Germany]

- Disposal serological pipette (5, 10, 25 mL.) [SPL, South Korea]
- Electrophoresis power supply [Bio-Rad, USA]
- Extraction Thimble cellulose (Whatman) [GE Healthcare, UK]

## 1. Preparation of crude herbal extracts

A powder of cultivated strain TM02 of *Lignosus rhinocerus* (LR) or Tiger Milk Mushroom was obtained from LIGNO Biotech Sdn Bhd, Selangor, Malaysia. This powder was extracted into 3 fractions by ethanol, cold water and hot water using maceration technique. Briefly, the 100 g of LR powder was macerated with 1 L of ethanol and placed the extract on the shaker at 4 °C for 24 h. after that, filtered the extract by using Whatman® No.2 filter paper and ethanol was removed by rotary evaporation (Heidolph, Laborota 4011) to yield the crude ethanol extract (LRE). Cold water extraction, 100 g of LR powder was suspended in sterile water and placed it on the shaker at 4 °C for 24 h. For hot water extraction, the sclerotial powder was extracted with water at 95-100 °C for 2 h. After that, the mixture was filtered and freeze dried by lyophilizer (Modulyod freeze dryer, Thermo) to give the crude cold water extract (LRC) and the crude hot water extract (LRH), respectively. Finally, about 0.73 g, 11.07 g and 10.13 g were obtained from LRE, LRC and LRH, respectively.

## 2. Gas Chromatograph–Mass Spectrometer (GC-MS) Analysis

The LRE was analyzed from the Scientific and Technological Research Equipment Center (STREC) (Chulalongkorn University, Thailand). In brief, the GC-MS Triple Quad system was an Agilent 7890 series GC system coupled with an Agilent 7000C MS and a capillary column (HP-5MS 5% Phenyl Methyl Siloxane, length 30 m, i.d. 0.25 mm, phase thickness 0.25 µm). the carrier gas was helium (1 mL/min). The temperature of inlet was 250 °C and pressure set to 8.2317 psi. The volume of injection was 1.5 µL injection. The GC oven was kept at 60 °C and raised to 325 °C using linear gradient of 5 °C/min. Total running time was 14 min. The extracts (~10 mg) were dissolved in 1 mL of absolute ethanol and their obtained spectra were compared with NIST Mass Spectrometry Data Center to identify phytochemical

constituents. The others extracts were sent to analyze by colleague in our laboratory because we used the same powder and technique as colleague in our lab [18].

### 3. Assessment of antioxidant properties of LR *in vitro*

#### 3.1 Radical Scavenging Activity Assays: DPPH and ABTS

Principle of DPPH: The free radical scavenging assays are commonly used to evaluate the antioxidant potential of compounds or plant extracts, which can be easily determined by using an electron transfer/hydrogen donating-based assay. The stable 1,1-diphenyl-2-picrylhydrazyl (DPPH•) is one of the common used in determine antioxidant ability of plants. The compounds or plant extracts with electron transfer/hydrogen donating ability will change a dark purple color of DPPH radical into yellow color, which can be measured an absorbance at 517 nm (Figure 15).

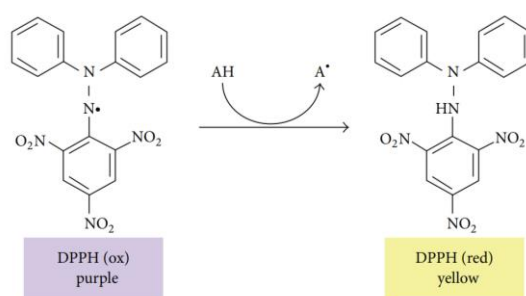


**Figure 15** Principle of DPPH radical scavenging capacity assay.

(<http://dx.doi.org/10.1155/2013/25175>)

Principle of ABTS: the ABTS radical scavenging assay is also commonly used. The principle is that p2,2'-azino-bis(3-ethylbenzothiazoline-6-sulfonate) radical cation (ABTS•+), the green-blue stable radical cationic chromophore, is produced by oxidation with potassium persulfate. During antioxidant reaction, the blue ABTS radical cation is converted back to its colorless. The absorption maximum at 734 nm [111]. The method is as same as DPPH radical scavenging assay (Figure 16).

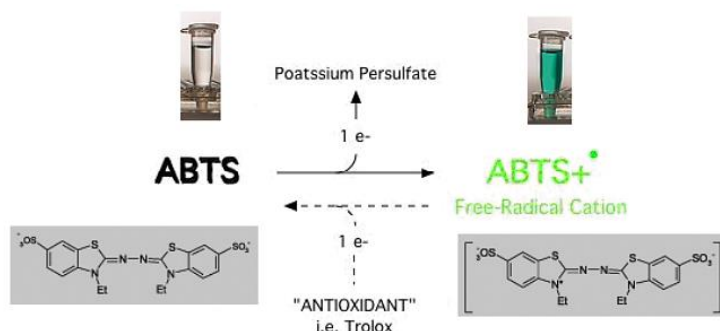


**Figure 16** Principle of ABTS radical scavenging capacity assay [112].

**Method:** the three extracts were prepared to a concentration 1 mg/mL Added them into a microplate and then added DPPH• or ABTS• + solution. The reactions were incubated at the dark place for 15 and 30 min, respectively. After that, the absorbance was measured by using microplate Reader (Perkin-Elmer) at 537 nm and 734 nm, respectively. Ascorbic acid (Vitamin C) was used as control for both assays. The antioxidant ability was showed in mg of vitamin C per g of dry weight extract. The equation for Radical scavenging activity is that:

$$\% \text{Inhibition} = 100 - \left[ \frac{(\text{Abs of sample} - \text{Abs of blank}) \times 100}{\text{Abs of control}} \right]$$

### 3.2 Folin–Ciocalteu Phenol Assay (FCP)

**Principle:** This technique was used to determine the total phenolic content in the extract. The Folin-Ciocalteu reagent is converted to reduced reagent by electron transfer from phenolic compounds to form a blue chromophore. The absorbance is measured at 760 nm. Garlic acid was used as standard (Figure 17).

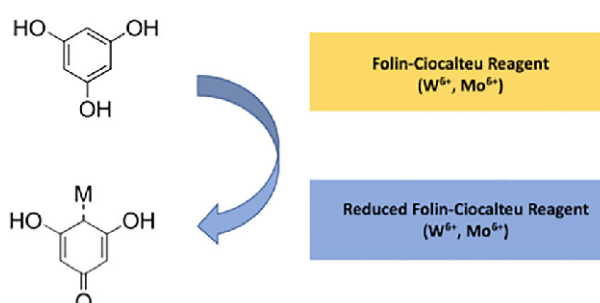


**Figure 17** Principle of Folin–Ciocalteu Phenol Assay  
(<https://onlinelibrary.wiley.com/doi/full/10.1002/pca.2851>)

Method: 10% Folin-Ciocalteu Phenol reagent (50  $\mu$ L) was used to react with the LRE, LRC and LRH extracts (50  $\mu$ L). After 20 min incubation, added 50  $\mu$ L sodium carbonate and incubated 20 min more. The absorbance was determined at 760 nm using EnSpire® Multimode Plate Reader (Perkin-Elmer). Garlic acid was used as standard and total phenolic content was expressed as mg of gallic acid equivalent (GAE) per g of dry weight extract.

### 3.3 Total Flavonoid content

Principle: The reaction between flavonoid and aluminum chloride ( $\text{AlCl}_3$ ) form a stable flavonoid- $\text{Al}^{3+}$  complex. The absorbance is measured at 415 nm. Quercetin was used as standard (Figure 18).

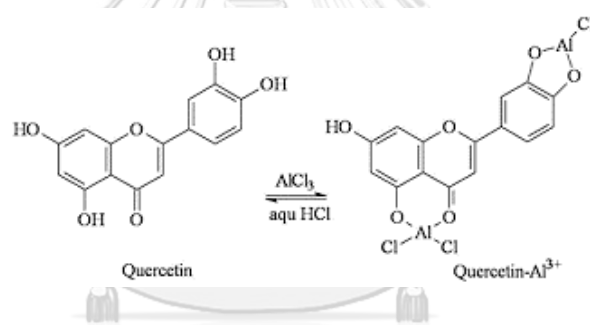


**Figure 18** Principle of total flavonoid content [113]

CHULALONGKORN UNIVERSITY

Method: 50  $\mu$ L of the LRE, LRC and LRH extracts were mixed with 10  $\mu$ L of 10% Aluminum chloride ( $\text{AlCl}_3$ ), 10  $\mu$ L Sodium acetate ( $\text{NaOAc}$ ) and 150  $\mu$ L of 95% ethanol. Then incubated at RT in dark place for 40 min. After that, the absorbance was measured at 415 nm using microplate reader. The standard for this test was a quercetin and results are expressed as mg of quercetin equivalent (QE) per g of dry weight plant extract.

#### 4. *In vitro* experiments

##### 4.1 Cell culture and treatments

Mouse hippocampal HT22 cells (a generous gift from Professor David Schubert at the Salk Institute, San Diego, CA, USA) were cultured in DMEM medium (Hyclone, Logan, UT), supplied with 10% fetal bovine serum, in a humidified atmosphere containing 5% CO<sub>2</sub> at 37 °C.

Treatment: The HT22 cells were divided into 10 groups including:

1. control group
2. DMSO-treated group
3. control herb groups
  - 3.1 LRE-treated groups (25, 50, 100, and 200 µg/mL)
  - 3.2 LRC-treated groups (25, 50, 100, and 200 µg/mL)
  - 3.3 LRH-treated groups (25, 50, 100, and 200 µg/mL)
4. 0.25 mM N-Acetylcysteine (NAC) as positive control
5. cotreatment groups
 

<ol style="list-style-type: none"> <li>5.1 LRE-treated groups (25, 50, 100, and 200 µg/mL)</li> <li>5.2 LRC-treated groups (25, 50, 100, and 200 µg/mL)</li> <li>5.3 LRH-treated groups (25, 50, 100, and 200 µg/mL)</li> <li>5.4 0.25 mM Nac</li> </ol>	}	+ 5mM Glutamate (GLU)
--	---	-----------------------

##### 4.2 3-(4,5-Dimethylthiazol-2-yl)-2,5-diphenyltetrazolium bromide tetrazolium (MTT) Assay

Principle: The yellow tetrazolium MTT (3-(4, 5-dimethylthiazolyl-2)-2,5-diphenyltetrazolium bromide) is reduced by metabolically active cells, in part by the action of dehydrogenase enzymes, to generate reducing equivalents such as NADH



and NADPH. The intracellular purple formazan can be solubilized and quantified by spectrophotometry. MTT assay, a colorimetric assay, is used to assess metabolic activity in the cells (Figure 19).

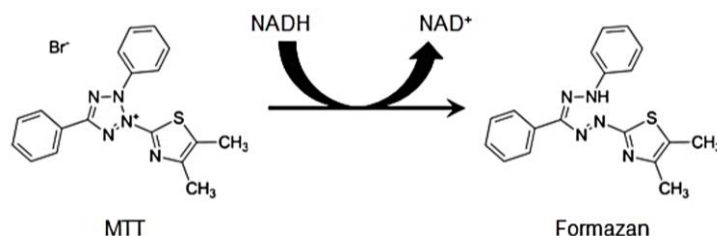


**Figure 19** MTT assay

(<https://www.aatbio.com/resources/faq-frequently-asked-questions/What-are-the-differences-between-MTT-and-WST-assays>)

Method: HT22 cells were seeded into 96-well plates and incubated overnight at 5% CO<sub>2</sub> at 37 °C. Next, the cells were treated with the group of treatments as mentioned above and incubate at 5% CO<sub>2</sub> at 37 °C for 14 h. After incubation, MTT solution was added to the each well and incubated 3 h more at the incubator. After that, the insoluble formazan was dissolved by 10% SDS and incubated in the incubator overnight. The MTT product was measured at 570 nm using a microplate reader. The percent of cell viability was calculated by the following formular.

$$\% \text{ Cell growth} = \frac{[(\text{Abs } 570 \text{ nm of treated group} - \text{blank}) / (\text{Abs } 5700 \text{ nm of control} - \text{blank})] \times 100}$$

#### 4.3 Assessment of apoptosis by Annexin V-FITC/propidium iodide (PI) staining using flow-cytometry

Principle: Annexin V is used for detect both early and late apoptotic cells because it interacts strongly and specifically with exposed phosphatidylserine (PS) which is the marker of early apoptosis. PI is used to evaluate necrosis (Figure 17). The level of oxidative stress-induced apoptotic cell death is quantified by the fluorescence intensity & monitored using flow cytometer (Figure 20).

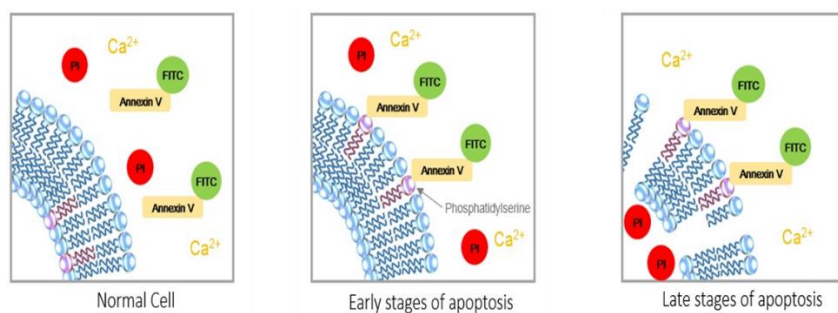


**Figure 20** Annexin V-FITC/propidium iodide (PI) staining at various stage of apoptosis. (<https://www.biocat.com/cell-biology/apoptosis/apoptosis-detection-phosphatidylserin-annexin-based>)

Method: HT22 cells ( $1 \times 10^5$  cells) were seeded in 12-well plate and incubated overnight at 5%  $\text{CO}_2$  at  $37^\circ\text{C}$ . Next, the cells were treated with the group of treatments as mentioned before and incubate in the incubator for 14 h more. After incubation, cells were harvested, washed and stained with annexin V/PI solution for 15 min in the dark. Live and dead cells were determined by using a BD FACSCalibur™ flow cytometer (BD Bioscience, Heidelberg, Germany). Data were collected at least 10,000 cells per group and results are shown as the percentage of apoptotic cells.

#### 4.4 Mitochondrial Membrane Potential (MMP) assay

Principle: The MMP is determined by using commercial kit (Cell Signaling) including the cationic dye TMRE (tetramethylrhodamine ethyl ester perchlorate) and a mitochondrial membrane potential disruptor CCCP (carbonylcyanide 3-chlorophenylhydrazone) as positive control for this test. TMRE, a cell membrane permeable fluorescent dye, is accumulated in the intact mitochondria. Depolarized or inactive mitochondria exhibits decreased membrane potential, resulting in reduced TMRE accumulation (Figure 21).

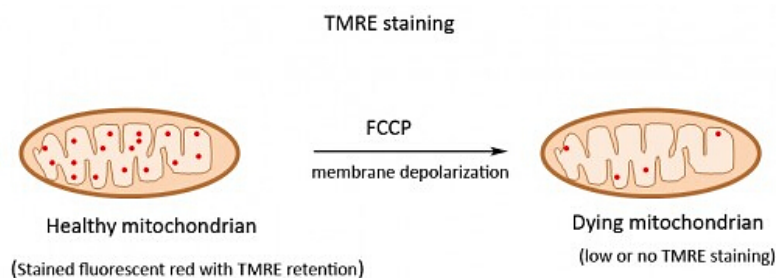


**Figure 21** Mitochondrial Membrane Potential (MMP) assay

(<https://www.webscientific.co.uk/product/tmre-mitochondrial-membrane-potential-assay>)

Method: Cells were seeded in 96-well plate and incubated overnight at 5% CO<sub>2</sub> at 37 °C. Next, the cells were treated with the group of treatments as mentioned before, except cells for CCCP group the get final volume 100 µl/well and incubated cells in the incubator for 14 h. After incubation, add CCCP in the positive control group to get final concentration of 50 µM, and then incubate cells at 37 °C for 15 min. After that, TMRE solution was added to each well to get a final concentration of 200 nM and place plate in an incubator (37°C and 5% CO<sub>2</sub>) for 20 min. Next, the solution was removed and washed cells with 1X PBS and then added 100 µl/well 1X PBS to the plate. The samples were measured by microplate reader at the excitation about 550 nm and emission about 580 nm.

#### 4.5 Assessment of intracellular ROS accumulation

Principle: Intracellular ROS is determined using the CM-H<sub>2</sub>DCFDA (general oxidative stress indicator). CM-H<sub>2</sub>DCFDA passively diffuses into cells, where its acetate groups are cleaved by intracellular esterases and its thiol-reactive chloromethyl group reacts with intracellular glutathione and other thiols. Subsequent oxidation yields a fluorescent that is monitored using flow cytometer. The ROS generation is quantified by the fluorescence intensity (Figure 22).

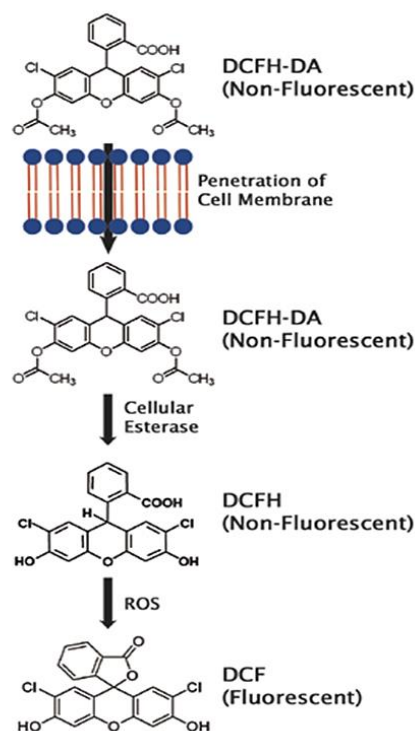


**Figure 22** Reactive oxygen species assay

(<https://www.cellbiolabs.com/reactive-oxygen-species-ros-assay>)

Method: Cells were seeded in 96-well plate and incubated overnight at 5% CO<sub>2</sub> at 37 °C. Then cells were treated with herbs according to mention before. After 14 h treatment, HT22 cells were added with 10 μM of H<sub>2</sub>DCFDA for 30 min at 37 °C, followed by washing three times with Phosphate Buffer Saline (PBS). The fluorescence intensity (excitation = 485 nm; emission = 535 nm) was measured using an EnSpire® Multimode Plate Reader (Perkin-Elmer) and the photographs were obtained using an Axio Observer A1 fluorescence microscope (Carl Zeiss, Jena, Germany).

#### 4.6 RNA isolation and assessment of antioxidant genes expression by real-time PCR (qPCR)

In brief, total RNA was isolated from specific treatment cells using Trizol reagent. 1 μg of total RNA was converted to cDNA by using Accupower RT Premix.

Quantitative real-time PCR reaction was performed by using Green Star PCR Master Mix that SYBR Green was included. Then, the specific genes including CAT, SOD1, SOD2, and Gpx were determined by the Exicycler Real Time Quantitative Thermal Block (Bioneer). The specific primers were previously reported by our research groups [114]. The relative expression of each gene was normalized to the internal control gene ( $\beta$ -actin).

## 5. *In vivo* experiments

### 5.1 *C. elegans* strains and maintenance

The *C. elegans* strains used in this study were wild type N2, CF1038 (*daf-16(mu86)I*), TJ375 (*gpls1[hsp-16.2::GFP]*), TJ356 (*zls356[daf-16p::daf-16a/b::GFP + rol-6]*), LD1 (*ldls7 [skn-1b/c::GFP + rol-6(su1006)]*), CF1553 (*mu1s84[pAD76(sod-3::GFP)]*), CL2166 (*dvls19[pAF15(gst-4::GFP::NLS)]*), BA17 (*fem-1(hc17)IV*), Strains CL2355 (*smg-1(cc546) dvls50 [pCL45 (snb-1::Abeta 1-42::3' UTR(long) + mtl-2::GFP] I*); CL2122 (*dvls15 [(pPD30.38)unc-54(vector)+(pCL26)mtl-2::GFP]*); and AM141 (*rmls133 [unc-54::54p::Q40::YFP]*). All worms were obtained from Caenorhabditis Genetics Center (University of Minnesota, Minneapolis, MN, USA) and were maintained on Nematode Growth Medium (NGM) agar containing *E. coli* OP50 as a food source and placed them in a 20 °C incubator. All strains and *E. coli* OP50 were obtained from Caenorhabditis Genetics Center (CGC), University of Minnesota, USA.

### 5.2 Synchronization and treatments

Synchronization was a technique to maintain worm in the same age-stage before beginning all experiments. In Brief, the worm's eggs on NGM agar were prepared by adding lysis solution containing 5M NaOH and 5% NaOCl as bleaching reagent. Then, vortexing for 10 min and centrifuging for 40 sec at 1300 rpm. Discarded the supernatant and wash the eggs with sterile water 2 times. Then, removed the water as much as possible. Added 8 mL M9 buffer in 60x15 mm petri dish and transferred the eggs into the dish. Placed them in a 20 °C incubator for 16 h.

the eggs in M9 buffer were hatched into L1 larvae stage because of no food. Before starting experiment, L1 larvae were transferred to S-medium containing *E. coli* OP50 (Figure 23).

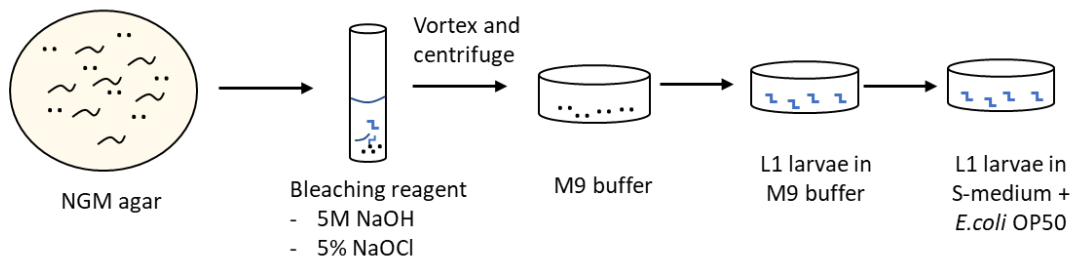


**Figure 23** Synchronization technique

Treatment: the worms were divided into 7 groups including:

1. control group
2. less than 1% DMSO group (solvent control)
3. LRE group (50, 100, and 200  $\mu\text{g}/\text{mL}$ )
4. LRC group (50, 100, and 200  $\mu\text{g}/\text{mL}$ )
5. LRH group (100, 200, and 300  $\mu\text{g}/\text{mL}$ )
6. 50  $\mu\text{g}/\text{mL}$  EGCG in DMSO (positive control for LRE group)
7. 50  $\mu\text{g}/\text{mL}$  EGCG in S-medium (positive control for LRC and LRH group).

### 5.3 Microbial susceptibility assays

Principle: To measure of an antibiotic or other substance to inhibit bacterial growth *in vitro*.

Method: A bacteria inoculum was prepared, dispensing *E. coli* OP50 in 0.9% NaCl solution, and adjusted the density to 0.5 McFarland, using the McFarland densitometer. The bacteria suspension was spread on LB plates. After letting them

dry for five minutes, prepared holes for LRE, LRC and LRH extracts at high dose (500, 1000  $\mu\text{g}/\text{mL}$ ), S-medium for control, DMSO for solvent control and the positive control, 200  $\mu\text{g}/\text{mL}$  ampicillin. Results were expressed as mean inhibition zone  $\pm$  SEM of three independent experiments. Each time fresh *E. coli* OP50 inoculum was prepared.

#### 5.4 Survival assay under Juglone-induced oxidative stress

Principle: To determine protective effect of the interested substances by observation of *C. elegans* survival under Juglone-induced oxidative stress.

Method: Age synchronized L1 larvae stage of wildtype N2 and transgenic CF1038 (DAF-16 loss-of-function mutant) worms were transferred to S-medium containing *E. coli* OP50 (OD600 = 1.0). they were divided into 7 groups. Each group contained around 80 worms and treated them with the extracts as mentioned before for 48 h. at 20  $^{\circ}\text{C}$ . After incubation time, added pro-oxidant juglone (a naphthoquinone from *Juglans regia*) to final concentration 80  $\mu\text{M}$  and incubated at 20  $^{\circ}\text{C}$  for 24 h. more. The surviving and dead worms were counted. The experiments were replicated three times.

#### 5.5 Measurement of intracellular ROS accumulation

Principle: Similar to *in vitro* ROS, intracellular ROS was determined using the CM-H<sub>2</sub>DCFDA (general oxidative stress indicator). CM-H<sub>2</sub>DCFDA passively diffuses into cells, where its acetate groups are cleaved by intracellular esterases and its thiol-reactive chloromethyl group reacts with intracellular glutathione and other thiols. Subsequent oxidation yields a fluorescent that is monitored using flow cytometer. The ROS generation is quantified by the fluorescence intensity.

Method: Age synchronized L1 larvae stage of wildtype N2 and transgenic CF1038 worms were transferred to S-medium containing *E. coli* OP50. Then, divided into 7 groups and transferred 100-200 worms to each group. Following by treated worms with all extracts for 48 h. at 20  $^{\circ}\text{C}$  incubator. After incubation time, H<sub>2</sub>DCF-DA was added (final concentration = 50  $\mu\text{M}$ ). Wrapped foil to avoid light and placed

them in 20 °C incubator for 1 h. Then, the worms were mounted on a glass slide and paralyzed by the addition of 10mM sodium azide, and at least 30 worms were randomly photographed using a fluorescence microscope BIOREVO BZ-9000 with a mercury lamp (Keyence Deutschland GmbH, Neu-Isenburg, Germany) with  $\lambda_{ex}$  480/20 nm,  $\lambda_{em}$  510/38 nm, 10X objective lens and constant exposure time. ImageJ software version 1.50i (National Institutes of Health, Bethesda, MD, USA). The relative fluorescence intensity of the full body was measured.

## 5.6 Transgenic reporter assays

### 5.6.1 Expression of HSP-16.2

Principle: To determine an expression of heat shock protein (HSP-16.2) that becomes active under oxidative stress.

Method: TJ375 transgenic worms were used in this experiment. This strain contained Hsp-16.2p::GFP reporter gene. The synchronized L1 worms were treated with all the extracts as mentioned above in S-medium for 48 h. at 20 °C incubator. After that, treated worms with 20  $\mu$ M Juglone in all groups for 24 h. at 20 °C. Then, mounted the worms on a glass slide with a drop of 10 mM sodium azide for paralysis and images of at least thirty worms per group. Fluorescent expression was detected by BIOREVO BZ-9000 fluorescence microscope (Keyence Deutschland GmbH, Neu-Isenburg, Germany) using 20X objective lens at constant exposure time. The mean relative fluorescence intensity of pharynx was analyzed using ImageJ software. The experiments were replicated three times.

### 5.6.2 Expression of GST-4

Principle: To determine an expression of glutathione S-transferase (GST-4) protein.

Method: Transgenic strain CL2166 was used in this experiment. This strain expressed GST-4::GFP fusion protein. The synchronized L1 worms were treated with all the extracts in S-medium for 48 h. at 20 °C. Then, 20  $\mu$ M was added to all groups for 24 h. at 20 °C. After that, the worms were mounted on the glass slide with 10



mM sodium azide and images of at least thirty worms per group. Fluorescent expression was detected by fluorescence microscope using 10X objective lens at constant exposure time. The mean relative fluorescence intensity was determined for three independent replications.

### 5.6.3 Expression of SOD-3

Principle: To determine an expression of superoxide dismutase (SOD-3) protein.

Method: Transgenic strain CF 1553, expressing SOD-3::GFP fusion protein were used. The synchronized L1 worms were treated with all the extracts in S-medium for 48 h. at 20 °C. After that, the worms were mounted on the glass slide with 10 mM sodium azide and images of at least thirty worms per group by fluorescence microscope using 10X objective lens at constant exposure time. The fluorescence intensity was analyzed for three repeats.

### 5.7 Subcellular DAF-16 localization

Principle: In TJ356 worms, the gene for the transcription factor DAF-16 is fused to GFP. Thus, the localization of DAF-16 can be studied by fluorescence microscopy. Only, when the transcription factors are translocated to the nucleus, genes for stress resistance and longevity become active.

Method: Synchronized TJ356 transgenic worms (L1 larvae), DAF-16::GFP fusion protein expression, were treated with all the extracts for 24 h. at 20 °C. Then, worms for all groups were analyzed by fluorescence microscope using 10X objective lens at constant exposure time. For analysis DAF-16 expression, there were three patterns: localization to nucleus, cytoplasm, or the intermediate region between the nucleus and cytoplasm. Worms were counted and sorted to each pattern. Three replicates were performed for each experiment.

### 5.8 Subcellular SKN-1 localization

Principle: In LD-1 worms, the gene for the transcription factor SKN-1 is fused to GFP. Thus, the localization of SKN-1 can be studied by fluorescence microscopy.

Only, when the transcription factors are translocated to the nucleus, genes for stress resistance and longevity become active.

Method: Synchronized L1 stage of LD-1 transgenic worms, SKN-1::GFP fusion protein expression, were treated with all the extracts for 48 h. at 20 °C. Then, worms for all groups were analyzed by fluorescence microscope using 10X objective lens at constant exposure time. For analysis SKN-1 expression, there were three patterns also: localization to nucleus, cytoplasm, or the intermediate region between the nucleus and cytoplasm. Worms were counted and classified into each pattern. Three replicates were performed for each experiment.

### 5.9 Lifespan assay

Principle: Lifespan assay is used to investigate the consequence of aging and death.

Method: This experiment used liquid culture system. Synchronized L1 larval wild-type (N2) worms were transferred to S-medium containing *E. coli* OP50 around 300 worms for each group of treatment and kept them at 20 °C. At day 1 of adulthood, the 40 adult worms from each group were transferred to individual new S-medium containing *E. coli* OP50 and treatments for 7 groups (three repeat for each group, n=120) as mentioned above. The worms were counted and recorded every day. They were transferred to new culture media every day for 5 days, after that, the worms were transferred every second day. The data was analyzed as a percentage of surviving worms.

### 5.10 Measurement of autofluorescent pigment (Lipofuscin)

Principle: Lipofuscin, a autofluorescent pigment, is a aging biomarker and accumulated in intestine during overage.

Method: The BA17 transgenic worms, temperature sensitive and recessive feminization strains (no laying eggs at 25 °C) were used to detect lipofuscin in this experiment. The Synchronized L1 worms were treated with all extracts in S-medium and kept they at 25 °C for 16 days. The media and treatments were change every

second day. At day 16, worms for all groups were analyzed by fluorescence microscope using 10X objective lens at constant exposure time. Three repeat experiments were performed by measuring the relative fluorescence intensity using ImageJ software.

### 5.11 Measurement of pharyngeal pumping rate

Principle: Pharyngeal pumping rate is the other aging biomarker that gets weaker overage.

Method: Wild type worms (N2 strain) were used for to determine the age-related decline in muscle function by pharyngeal pumping rate measurement. Synchronized adulthood N2 worms were transferred to NGM agar containing *E. coli* OP50 for control, and transferred to NGM agar containing *E. coli* OP50 with treatments for treatment groups. The adult worms were transferred to new NGM cultured agar every day during reproductive period. The pumping activities were analyzed on days 5, 10, 12, and 15 of adulthood. Each worm was recorded the pumping frequency for 60 s. The result is showed as pumps  $\text{min}^{-1}$  (mean  $\pm$  SEM)

### 5.12 Measurement of brood size and body length

Principle: Brood size and body length are used to investigate the toxicity of the interested substances. Under stress or toxic condition can reduce the number of progeny and the body size of *C. elegans*.

Method for brood size assay: L4 larvae worm was individually transferred to the new NGM agar plate containing *E. coli* OP50 with each treatment. The eggs were counted using a dissecting microscope every day until they stopped laying eggs to obtain a mean brood size.

Method for body length: wild type worms (N2 strain) were allowed to lay eggs into NGM agar plate with *E. coli* OP50 as a food source for 2-4 h before being picked worm out. And then, the remaining eggs were incubated at 20 °C for 48 h. Around 30 wild-type L4 larvae were randomly selected for each group, transferred to the solid NGM plates containing the corresponding concentration of all extracts and kept at 20

°C for 24 h. Adult day 1 worms were mounted on the glass slide with 10 mM sodium azide and images by bright-field microscope. the body length was determined using the software BZ-II Analyzer (Keyence Corp.). The results are presented as body length in micrometers (mean  $\pm$  SEM).

### 5.13 Assessment of neuroprotective effects in *C. elegans* model

#### 5.13.1 Chemotaxis assay

Principle: Chemotaxis assay is used to evaluate the neuroprotective effect of the interested substances on odorant response in *C. elegans*. Normal worms will move to the attractant position whereas the transgenic CL2355 worms express A $\beta$  in nerve cells (Alzheimer model). As a physiological response, these nematodes show a reduced ability for chemotaxis.

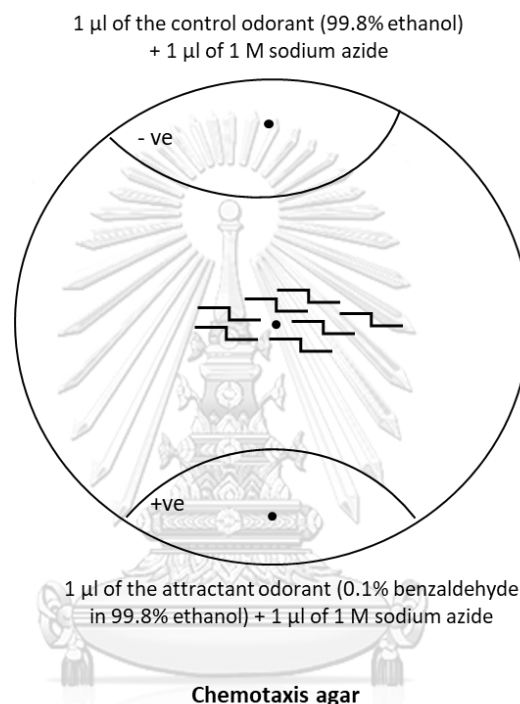
Method: The transgenic worms including CL2355, pan-neuronal expression of Human Abeta peptide, and CL2122, a control worm, were used. This assay slightly modified from Wu Y., et al [115]. The synchronized L1 worms both CL2355 and 2122 were transferred to S-medium containing *E. coli* OP 50 as a food source. Each strain of worms was divided into 7 groups. All worms were kept at 16 °C for 36 h, and then shift to 23 °C and incubated for 36 h more. The increased temperature is required for the pan-neuronal A $\beta$ 1–42 expression in the strain CL2355. After the incubation, the worms were washed three times with M9 buffer to completely remove *E. coli* OP50. Finally, around 40 worms were placed in the center of a chemotaxis agar plate (94 mm). Before placing the worms, 1  $\mu$ l of the attractant odorant (0.1% benzaldehyde in 99.8% ethanol) together with 1  $\mu$ l of 1 M sodium azide, used as worms paralyzing, were added to one side of the plate. On the other hand, 1  $\mu$ l of the control odorant (99.8% ethanol) along with 1  $\mu$ l of 1 M sodium azide were added (Figure 19). Then, all plates were kept at 23 °C for 1 h. After that, the worms were counted from both sides and calculated the chemotaxis index (CI) by the following formular:

$$CI = (Na - Nc) / Nt$$

Na: number of worms at the attractant position

Nc: number of worms at the control position

Nt: total number of worms on the plate



จุฬาลงกรณ์มหาวิทยาลัย  
Figure 24 Chemotaxis assay  
CHULALONGKORN UNIVERSITY

### 5.13.2 Assessment of PolyQ40 aggregation

Principle: The accumulation of PolyQ40 proteins in transgenic AM141 worms has been used as a model for Huntington's diseases. A soluble Q40::YFP distribution in body wall muscle cells immediately after hatching. As these worms age the rapid formation of foci is observed. When they reach adulthood, an entirely Q40::YFP aggregated phenotype is observed.

Method: The synchronized transgenic AM141, expressing polyQ40::YFP as a reporter gene, were treated as same as chemotaxis assay, Then, the worms were

incubated at 20 °C for 72 h. After incubation period, the worms were mounted on a glass slide with a drop of 10 mM sodium azide for paralysis and images of at least thirty worms per group. Fluorescent expression was detected by BIOREVO BZ-9000 fluorescence microscope (Keyence Deutschland GmbH, Neu-Isenburg, Germany) using 10X objective lens at constant exposure time. The numbers of PolyQ40 aggregation, located in the muscle cells of the worms, were counted manually. The mean  $\pm$  SEM was analyzed for three independent replications.

#### 5.14 Statistical Analysis

Data are presented as the mean of three independent experiments (the mean  $\pm$  SEM) and analyzed with GraphPad Prism 6. Statistical comparison between the control and treatments were performed using one-way ANOVA following Bonferroni's method (post-hoc). Lifespan data were determined by log-rank (Mantel-Cox) tests followed by the Gehan-Breslow-Wilcoxon test. All the experiments were performed at least three times. Differences with  $p < 0.05$  were considered statistically significant.

## CHAPTER IV

## Results

## 1. Antioxidant Properties and Total Phenolic and Flavonoid Contents

In this study, the antioxidant properties of three extractions of *Lignosus rhinocerus* (LR) were investigated by 2,2-diphenyl-1-picryl-hydrazyl-hydrate (DPPH) scavenging assay, 2,2'-azino-bis (3-ethylbenzthiazoline-6-sulphonic acid) (ABTS) scavenging assay. The results showed that % Radical scavenging activity in DPPH assay of *Lignosus rhinocerus* ethanol extract (LRE) was the highest. Next is *Lignosus rhinocerus* cold water extract (LRC) and *Lignosus rhinocerus* hot water extract (LRH) was the lowest at  $12.08 \pm 0.77\%$ ,  $5.88 \pm 1.13\%$  and  $4.78 \pm 1.21\%$ , respectively (Table 1). Similar to DPPH assay, % Radical scavenging activity of LRE was the highest follow by LRC and the LRH was the lowest at  $38.83 \pm 0.37$ ,  $31.66 \pm 0.35$  and  $23.56 \pm 4.71$ , respectively (Table 2). In addition, LRE found high phenolic content ( $19.78 \pm 0.18$ ). Next is LRC ( $7.38 \pm 0.03$ ) and LRH is the lowest ( $4.75 \pm 0.06$ ) (Table 3). On the other hand, LRH had the most flavonoid content ( $63.61 \pm 0.57$ ) follow by LRC ( $14.22 \pm 0.35$ ) and LRE is the lowest ( $9.39 \pm 0.50$ ) (Table 3)

**Table 1** Free radical scavenging capacity of three extractions of *Lignosus rhinocerus* (LR) using DPPH scavenging assay.

Sample	% Radical Scavenging Activity (of 1 mg/mL Extract)	mg VCEAC/g Dry Weight Sample
LRE	$12.08 \pm 0.77$	$33.67 \pm 1.45$
LRC	$5.88 \pm 1.13$	$22.01 \pm 2.13$
LRH	$4.78 \pm 1.21$	$19.93 \pm 2.28$

VCEAC: Vitamin C equivalent antioxidant capacity.

**Table 2** Free radical scavenging capacity of three extractions of *Lignosus rhinocerus* (LR) using ABTS scavenging assay.

Sample	% Radical Scavenging Activity (of 1 mg/mL Extract)	mg VCEAC/g Dry Weight Sample
LRE	38.83 ± 0.37	31.32 ± 0.39
LRC	31.66 ± 0.35	31.32 ± 0.39
LRH	23.56 ± 4.71	15.26 ± 4.95

VCEAC: Vitamin C equivalent antioxidant capacity.

**Table 3** Total phenolic and flavonoid contents of three extractions of *Lignosus rhinocerus* (LR)

Sample	Total Phenolic (mg(GA)/g of Dry Weight)	Total Flavonoid (mg(QE)/g of Dry Weight)
LRE	19.78 ± 0.18	9.39 ± 0.50
LRC	7.38 ± 0.03	14.22 ± 0.35
LRH	4.75 ± 0.06	63.61 ± 0.57

GA: Gallic acid; QE: Quercetin.

## 2. Phytochemical Constituents of LRE

Gas chromatograph–mass spectrometer (GC-MS) analysis showed the presence phytochemical compounds of LRE by detection and comparison the MS data with databases to identify chromatographic peaks as shown in chromatograms (Figure 25). In the percentage of compounds, we identified proposed phytochemical constituents of LRE that involved in antioxidant properties (Table 4) . For the others water extracts, the possible phytochemical constituents consist of high triglycerol, olenolic acid and betulinic acid [18].



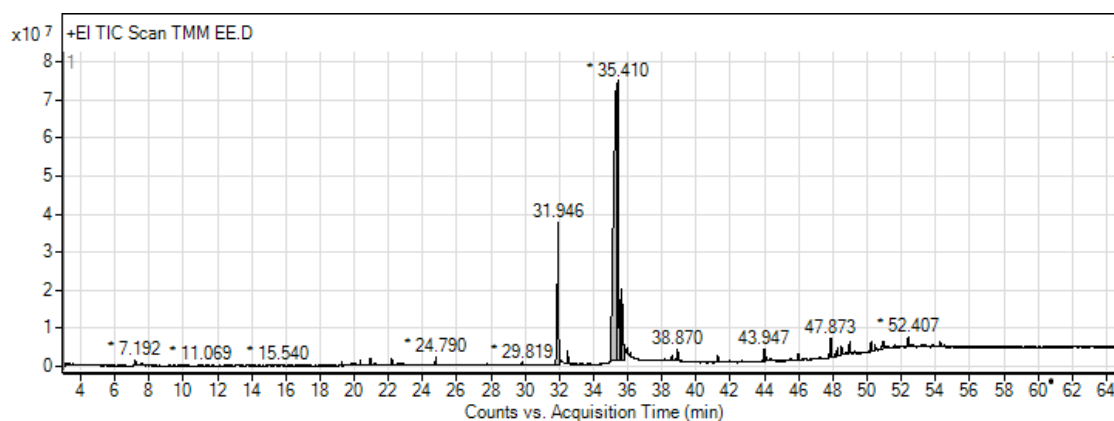


**Figure 25** Gas chromatograph–mass spectrometer (GC-MS) chromatogram of ethanol extraction of *Lignosus rhinocerus* (LRE). \* Peaks of proposed phytochemical constituents in LR were suggested by GC-MS.

**Table 4** Proposed phytochemical constituents in *Lignosus rhinocerus* (LRE)

Peak No.	RT	Area (%)	MF	MW	Name of Compound	Pharmacological activity	Ref
1	7.143	0.17	C <sub>3</sub> H <sub>8</sub> O <sub>3</sub>	92.09	Glycerin	n/a	
6	11.069	0.06	C <sub>11</sub> H <sub>24</sub>	156.31	Undecane	anti-allergic, anti-inflammatory	[116]
7	13.358	0.05	C <sub>10</sub> H <sub>18</sub> O	154.25	Terpinen-4-ol	antioxidant	[117]
11	15.540	0.08	C <sub>14</sub> H <sub>22</sub>	190.32	Benzene, 1,3-bis(1,1-dimethylethyl)-	n/a	
19	22.2	0.42	C <sub>6</sub> H <sub>6</sub> O	94.11	Phenol	antioxidant	[118]
20	24.790	1.04	C <sub>9</sub> H <sub>10</sub> O <sub>4</sub>	182.17	3,5-Dimethoxybenzoic acid	antibacterial	[119]
22	28.845	0.05	C <sub>9</sub> H <sub>11</sub> NO <sub>3</sub>	181.19	3,5-Dimethoxybenzamide	anticancer	[120]
23	29.819	0.16	C <sub>15</sub> H <sub>30</sub> O <sub>2</sub>	242.4	Pentadecanoic acid	antioxidant, antibacterial	[121, 122]
24	31.437	0.19	C <sub>18</sub> H <sub>34</sub> O <sub>2</sub>	282.47	Oleic acid	antioxidant	[123]
26	31.946	25.4	C <sub>16</sub> H <sub>30</sub> O <sub>2</sub>	254.41	Hexadecenoic acid	antifungal, antioxidant	[124]

Peak No.	RT	Area (%)	MF	MW	Name of Compound	Pharmacological activity	Ref
27	32.495	0.92	C <sub>17</sub> H <sub>30</sub> O <sub>2</sub>	266.4	7,10-Hexadecadienoic acid, methyl ester	antioxidant, anti-inflammatory,	[125]
28	33.709	0.22	C <sub>17</sub> H <sub>34</sub> O <sub>2</sub>	270.5	Heptadecanoic acid	antioxidant	[126]
29	34.368	0.12	C <sub>19</sub> H <sub>36</sub> O <sub>2</sub>	296.48	11-Octadecenoic acid, methyl ester	Antioxidant, antimicrobial	[127]
31	35.410	42.53	C <sub>18</sub> H <sub>34</sub> O <sub>2</sub>	282.5	9-octadecenoic acid	antioxidant	[127]
32	35.6	9.58	C <sub>20</sub> H <sub>36</sub> O <sub>2</sub>	308.5	Linoleic acid ethyl ester	antioxidant	[126]
34	38.870	1.01	C <sub>21</sub> H <sub>38</sub> O <sub>4</sub>	354.5	9,12-Octadecadienoic acid (Z,Z)-, 2,3-dihydroxypropyl ester	n/a	
40	47.873	1.77	C <sub>35</sub> H <sub>46</sub> O <sub>2</sub>	498.7	9(11)-Dehydroergosteryl benzoate	antimicrobial	[128]
46	50.939	1.72	C <sub>28</sub> H <sub>44</sub> O	396.6	Ergosterol	regulation of membrane fluidity and structure, developmental growth	[129, 130]

Rt: retention time; MF: molecular formula; MW: molecular weight

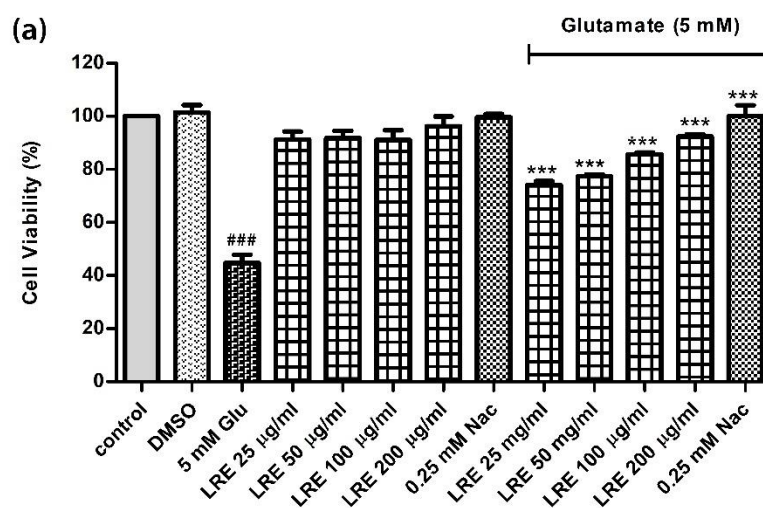
### 3. The biological activities of LR extract in mouse hippocampal HT22 cells (*in vitro*)

#### 3.1 Effect of LR extracts against glutamate-induced cytotoxicity

To evaluate cell cytotoxicity of three extractions of LR including LRE, LRC and LRH, the MTT assay was used. The results showed that HT-22 cells, induced with 5 mM glutamate, significantly reduced cell viability at  $44.71 \pm 3.15$  %;  $p < 0.001$  compared to control. However, LRE-treated cells at concentration 25, 50, 100 and 200  $\mu\text{g}/\text{mL}$  were not difference in cells viability compared to control. Similarly, 0.25 mM Nac-treated cells, as positive control, was not toxic to the cells compared to control. In addition, co-treatment cells with 25, 50, 100, and 200  $\mu\text{g}/\text{mL}$  of LRE and 5

mM glutamate showed significant protective effects against cell death in a dose-dependent manner at  $74.00 \pm 1.53\%$ ,  $77.33 \pm 0.67\%$ ,  $85.67 \pm 0.67\%$ , and  $92.33 \pm 0.88\%$ , respectively;  $p < 0.001$  compared to glutamate-treated cells. Likewise, co-treatment between 0.25 Nac and 5 mM glutamate significantly increased cell viability at  $94.67 \pm 1.76\%$ ,  $p < 0.001$  compared to glutamate-treated cells (Figure 26a).

Cell viability test of LRC-treated cells at concentration 25, 50, 100 and 200  $\mu\text{g/mL}$ , the results showed that they were not toxic to the cells compared to control. However, co-treatment cells with 25, 50, 100, and 200  $\mu\text{g/mL}$  of LRC and 5 mM glutamate decreased cell viability and they had no different in cell death compared to glutamate-treated cells (Figure 26b). Similarly, the results of cell viability of LRH-treated cells at concentration 25, 50, 100 and 200  $\mu\text{g/mL}$  were not toxic to the cells compared to control, whereas co-treatment cells between the same concentration of LRH with 5 mM glutamate failed to protect cell death compared to glutamate-induced cells (Figure 26c).



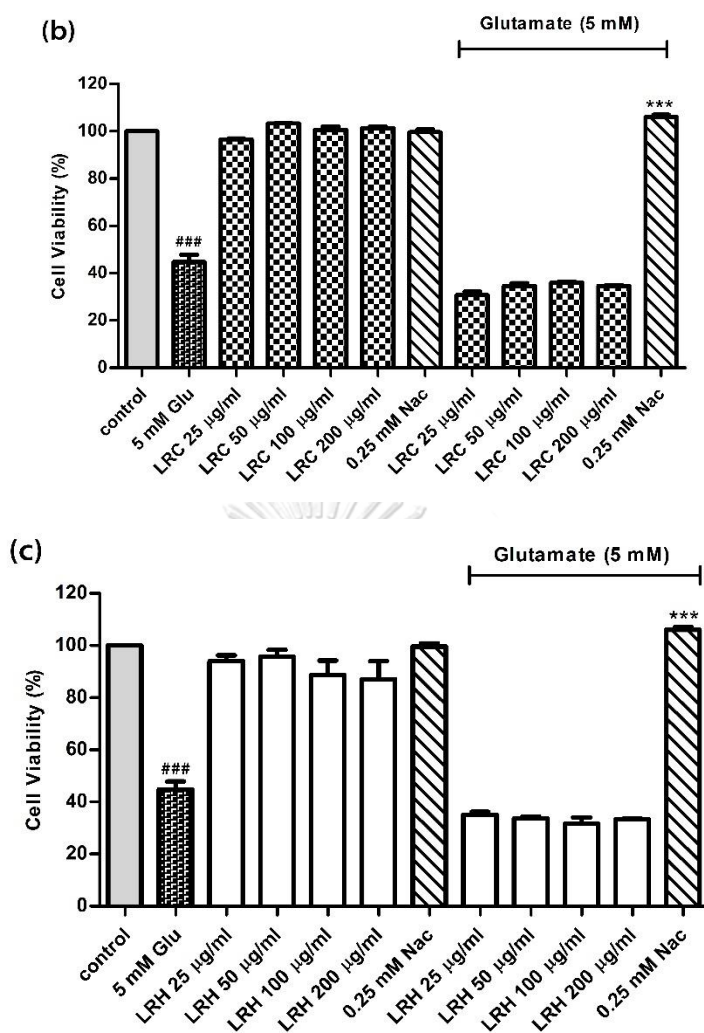
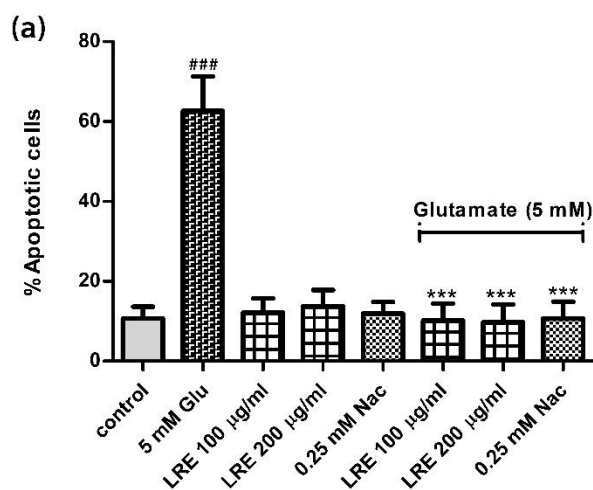


**Figure 26** Protective effect of different concentrations of LR extracts against glutamate-induced toxicity in HT22 cells. The percentage of cell viability of LRE cotreatment significantly increase and in a dose-dependent manner (a), The percentage of cell viability of LRC cotreatment (b), and LRH cotreatment (c) were not difference compared to glutamate-treated group. Values are mean  $\pm$  SEM of at least 3 independent runs. ###  $p < 0.001$  vs. control; \*  $p < 0.05$ , \*\*  $p < 0.01$ , and \*\*\*  $p < 0.001$  vs. glutamate alone.

### 3.2 Anti-apoptotic activity of LR extracts

According to MTT results, we chose 100 and 200  $\mu\text{g}/\text{mL}$  to test for other experiments because the cell viability after inducing with 5 mM glutamate had more

than 80%. To investigate the role of three extracts of LR in glutamate-induced apoptosis in HT22 cells, the cells were treated as mentioned in the method. We found that 5 mM glutamate-treated cells sharply increase the percentage of apoptotic cells at  $62.64 \pm 8.64\%$ ,  $p < 0.001$  compared to control ( $10.71 \pm 2.91\%$ ). On the other hand, LRE-treated cells at concentration 100 and 200  $\mu\text{g}/\text{mL}$  were not difference in the percentage of apoptotic cells compared to control as well as 0.25 mM Nac-treated cells. Moreover, co-treatment cells between 100 and 200  $\mu\text{g}/\text{mL}$  of LRE and 5 mM glutamate showed significantly decreased the percentage of apoptotic cells at  $10.18 \pm 4.266\%$ , and  $9.796 \pm 4.416\%$ , respectively;  $p < 0.001$  compared to glutamate-treated cells and also decrease in the percentage of apoptotic cells in 0.25 mM Nac-treated cells at  $10.73 \pm 4.175\%$ ,  $p < 0.001$  compared to control (Figure 27a). However, both LRC and LRH co-treated cells showed high percentage of apoptotic cells and they were not difference compared to 5 mM glutamate-treated cells alone (Figure 27b).



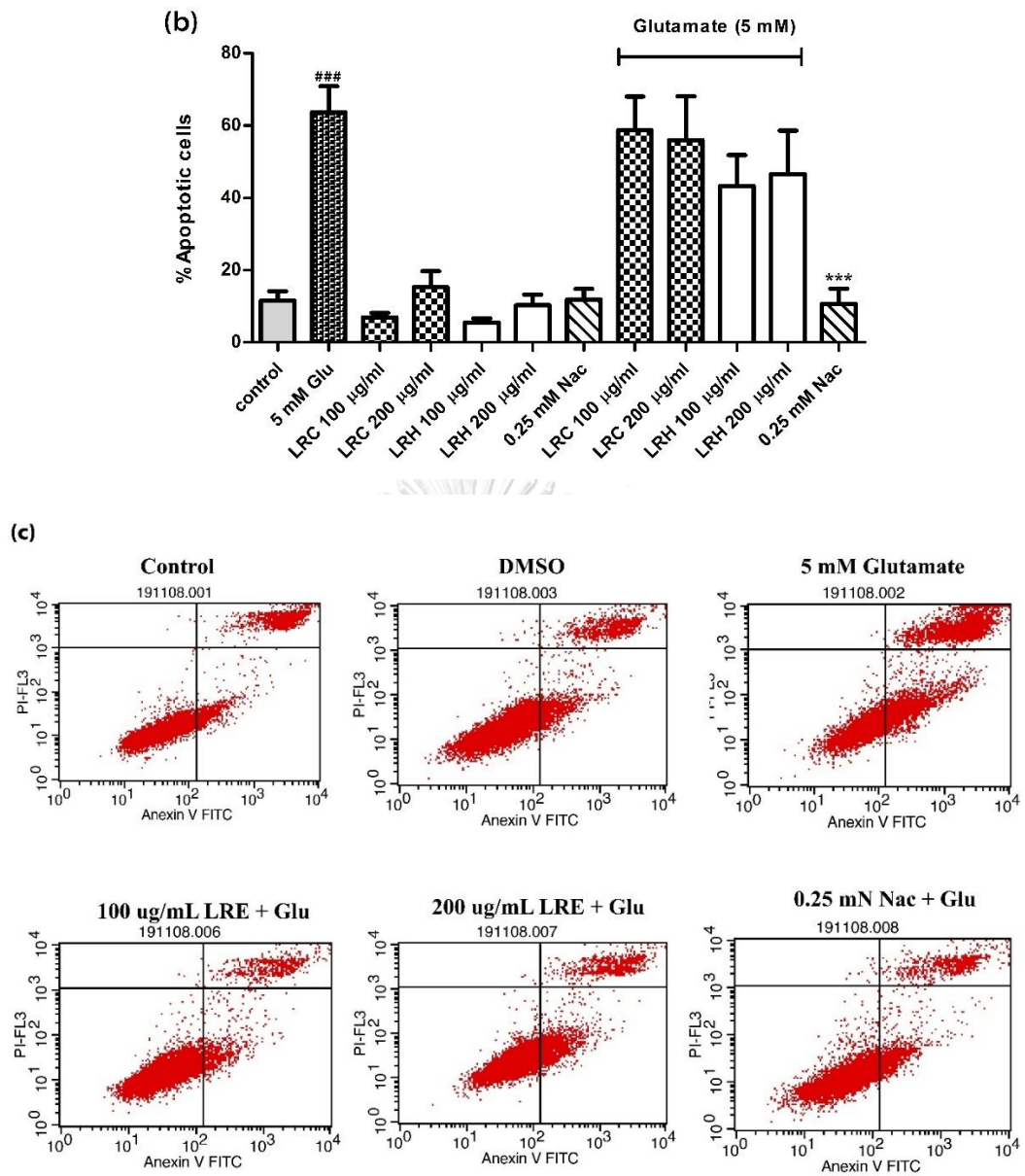
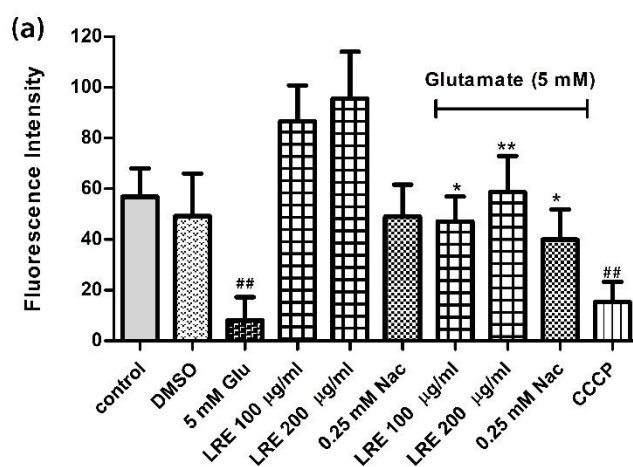


**Figure 27** Quantitative flow cytometric analysis of apoptotic cells using annexin V-FITC/PI staining in HT22 cells. Percentages of apoptotic cells were early stage (annexin V+/PI-, lower right quadrant) plus late stage (annexin V+/PI+, upper right quadrant). The percentages of apoptotic cells of LRE cotreatment (a) significantly decrease. Whereas, the percentages of apoptotic cells of LRC and LRH cotreatment (b) were not difference compared to glutamate alone. Representative scatter plots show the distribution of annexin V and PI staining for control (c). 0.25 mM Nac was

positive control. Values are mean  $\pm$  SEM of at least 3 independent runs. ###  $p < 0.001$  vs. control; and \*\*\*  $p < 0.001$  vs. glutamate alone.

### 3.3 Effect of LR extracts on Mitochondrial Membrane Potential (MMP)

The HT-22 cells, treated with only 5 mM glutamate, importantly reduced fluorescence intensity of TMRE at  $8.00 \pm 9.23$ ,  $p < 0.001$  compared to control ( $56.81 \pm 11.28$ ). Similarly, the cells, treated with CCCP as positive control for this test, showed significant decrease in fluorescence intensity compared to control at  $15.29 \pm 7.947$ ;  $p < 0.01$ . However, the cells LRE-treated cells at concentration 100 and 200  $\mu\text{g}/\text{mL}$  were not difference in the fluorescence intensity like 0.25 mM Nac-treated cells compared to control. Furthermore, the cells were co-treated between 100, and 200  $\mu\text{g}/\text{mL}$  of LRE and 5 mM glutamate significantly improved the TMRE fluorescence intensity in a dose-dependent manner compared to glutamate-treated cells at  $47.19 \pm 9.774$ , and  $58.62 \pm 14.36$ ;  $p < 0.01$ , respectively as well as co-treated 0.25 mM Nac and 5 mM glutamate ( $39.95 \pm 11.89$ ,  $p < 0.05$ ) (Figure 28a). The cotreatment of LRC or LRH (100, and 200  $\mu\text{g}/\text{mL}$ ) with 5 mM glutamate showed low fluorescence intensity of TMRE and were not difference from 5 mM glutamate-treated cells (Figure 28b)



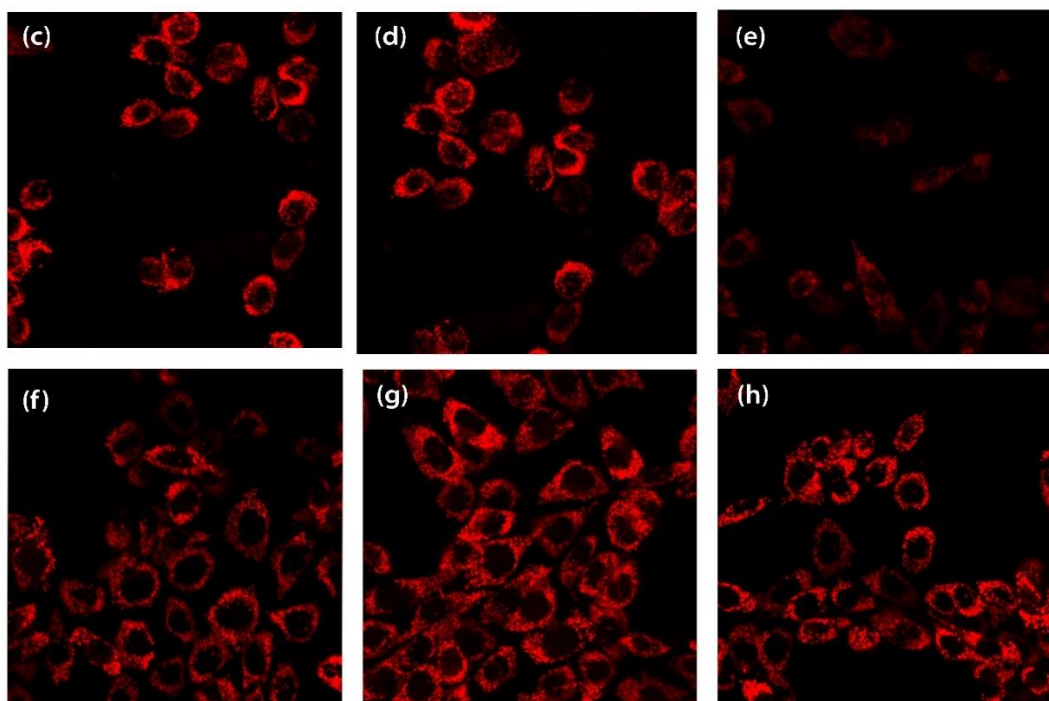
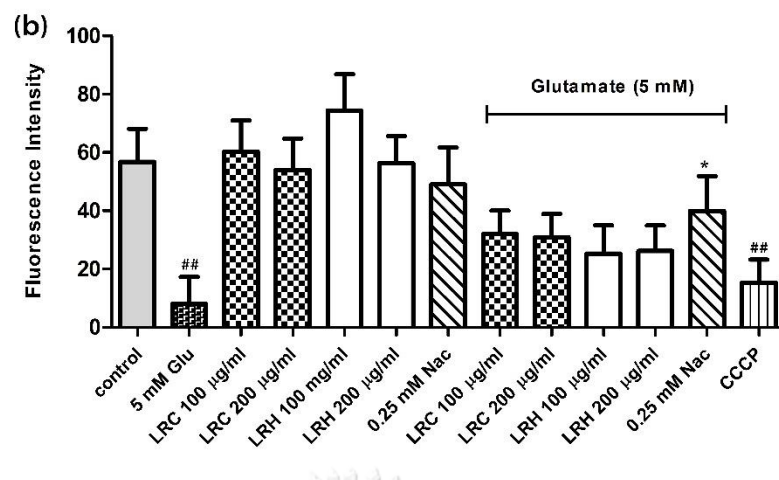
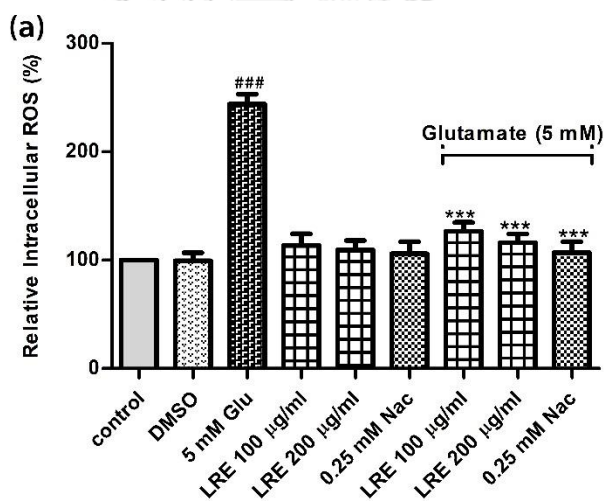


**Figure 28** Protective effect of different concentrations of LR extracts on MMP in HT22 cells. The cells in LRE cotreatment group significantly increase MMP in a dose-dependent manner compared to glutamate alone (a). Whereas, the cells in LRC and LRH cotreatment group were no difference compared to glutamate-treated group (b). Representative fluorescence micrographs with TMRE staining under a fluorescence microscope of the cells control group (c); DMSO group (d); 5 mM glutamate group (e); 100 µg/mL (f) and 200 µg/mL (g) of LRE cotreatment groups; and 0.25 Nac group (h). Values are mean  $\pm$  SEM of at least 3 independent runs. ##  $p < 0.01$  vs. control; \*  $p < 0.05$ , and \*\*  $p < 0.01$  vs. glutamate alone.



### 3.4 Effect of LR extracts on intracellular ROS level

From the results, HT-22 cells, treated with 5mM of glutamate alone, significantly increased ROS generation at  $243.9 \pm 9.22\%$ ;  $p < 0.001$  compared to control. Whereas, the cells treated between 100, and 200  $\mu\text{g/mL}$  of LRE and 5 mM glutamate cotreatment significantly decreased intracellular ROS accumulation in a dose-dependent manner compared to control at  $126.6 \pm 8.39\%$ , and  $116.1 \pm 7.99\%$ ;  $p < 0.001$ , respectively as well as co-treated 0.25 mM Nac and 5 mM glutamate ( $106.9 \pm 10.33\%$ ;  $p < 0.001$ ) (Figure 29a). On the contrary, co-treated cells with LRC or LRH (100, and 200  $\mu\text{g/mL}$ ) together with 5 mM glutamate showed high level of intracellular ROS expression and the results were not difference from 5 mM glutamate-treated cells alone (Figure 29b).



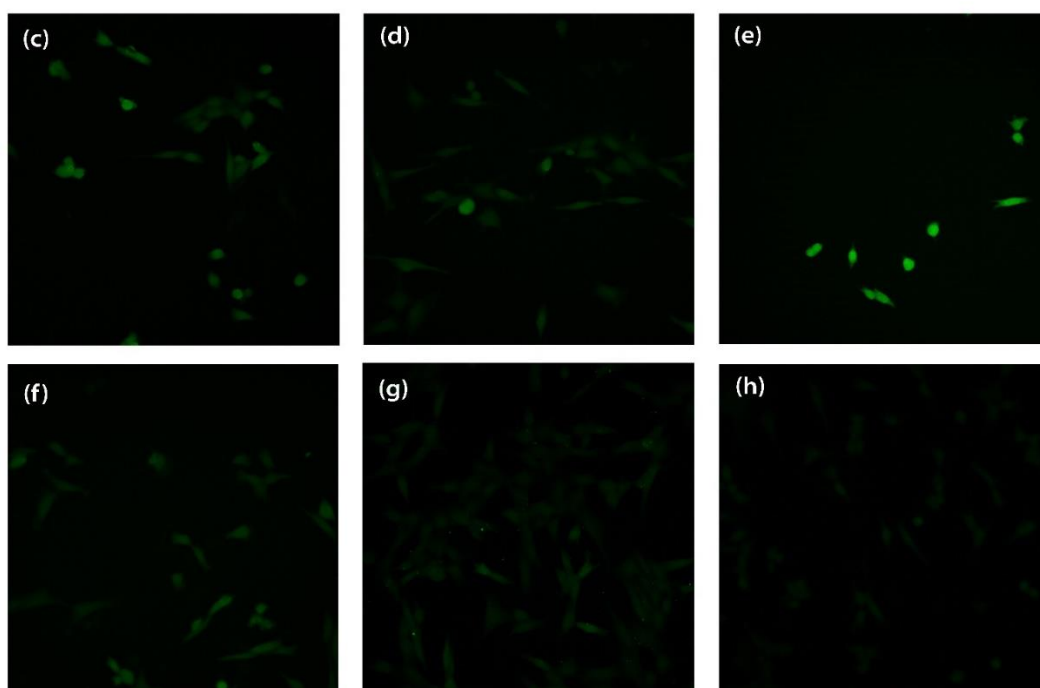
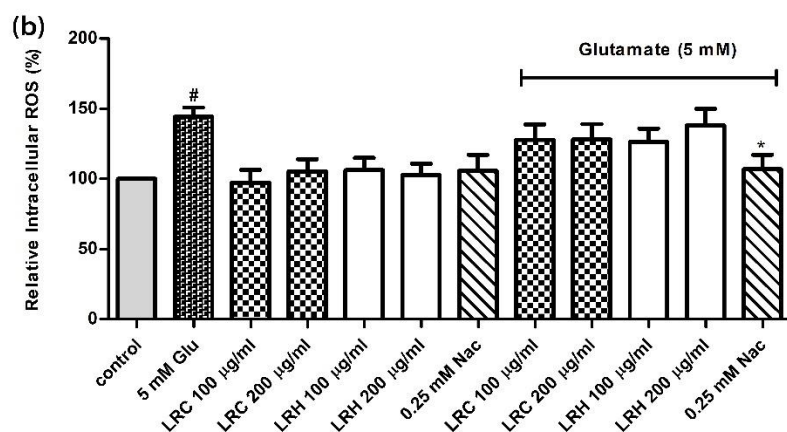


**Figure 29** The effect of different concentration of LR extracts on intracellular ROS accumulation in HT22 cells. The cells in LRE cotreatment group significantly decrease in ROS level in a dose-dependent manner compared to glutamate alone (a). Whereas, the cells in LRC and LRH cotreatment group were not difference in ROS level compared to glutamate-treated group (b). Representative fluorescence micrographs with DCFH-DA staining under a fluorescence microscope of the cells control group (c); DMSO group (d); 5 mM glutamate group (e); 100 µg/mL (f) and 200 µg/mL (g) of LRE cotreatment groups; and 0.25 mM Nac group (h). Values are mean  $\pm$  SEM

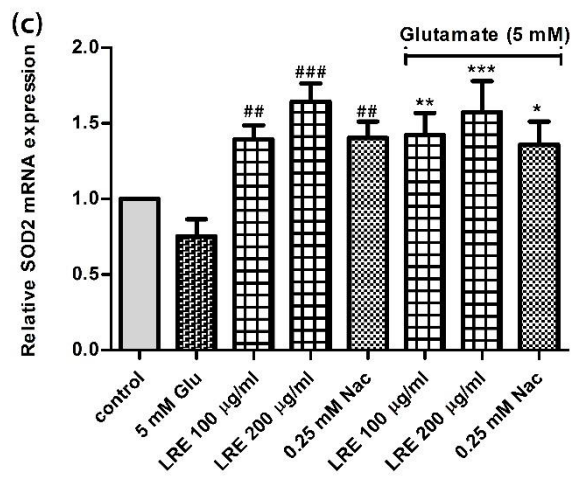
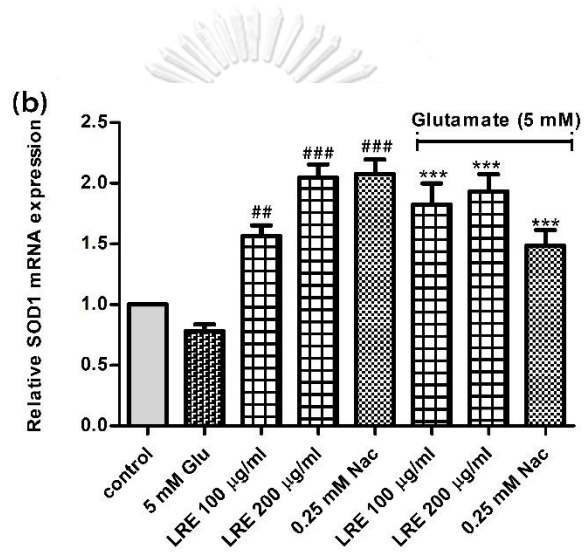
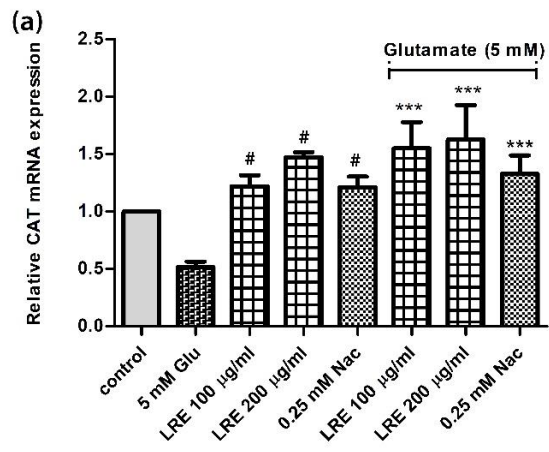
of at least 3 independent experiments. ###  $p < 0.001$  vs. control; \*  $p < 0.05$ , and \*\*\*  $p < 0.001$  vs. glutamate alone.

### 3.5 Effect of LR extracts on antioxidant gene expressions

According to the protective effect of LRE in previous experiments, so we focus on LRE extract to test in further experiments. For the expression of CAT genes, the results showed that 5 mM glutamate-treated cells caused reduction of CAT gene expression, whereas the expression of CAT of the cells were co-treated between 100, and 200  $\mu\text{g}/\text{mL}$  of LRE and 5 mM glutamate significantly enhanced 3-fold and 3.2-fold, respectively like 0.25 mM Nac-cotreated cells 2.6-fold enhancing, in comparison to glutamate-treated cells (Figure 30a).

Similarly, the cells, with 100, and 200  $\mu\text{g}/\text{mL}$  of LRE- glutamate cotreatment, the 100, and 200  $\mu\text{g}/\text{mL}$  of LRE-treated cells importantly increased the SOD1 expression 2.25-fold, and 2.38-fold, respectively when compared to glutamate-treated cells. The cotreatment of 0.25 mM Nac also increased 1.88-fold compared to glutamate-treated cells (Figure 30b). In addition, cotreatment of 100  $\mu\text{g}/\text{mL}$  of LRE, 200  $\mu\text{g}/\text{mL}$  of LRE and 0.25 mM Nac also significantly increased SOD2 expression by 1.75-fold, 2-fold, and 1.75-fold, respectively compared to glutamate-treated cells (Figure 30c).

However, 5 mM glutamate-treated cells showed significant decrease in GPx expression but cotreatment of 100  $\mu\text{g}/\text{mL}$  of LRE, 200  $\mu\text{g}/\text{mL}$  of LRE and 0.25 mM Nac showed significant increase by 3.7-fold, 4-fold, and 3.7-fold, respectively, in a comparison to glutamate-treated cells (Figure 30d).



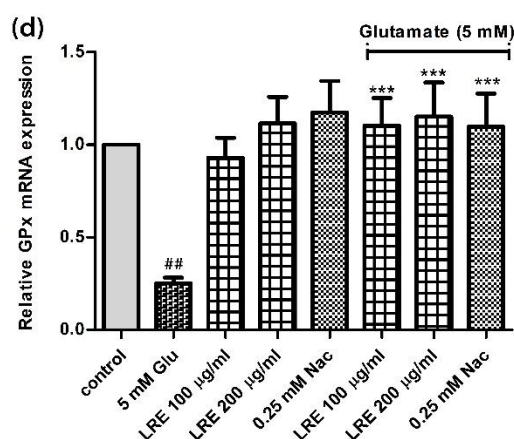


**Figure 30** The effect of different concentrations of LRE extracts on antioxidant gene expressions in HT22 cells. The cells of LRE cotreatment significantly increase in CAT gene expression (a); SOD1 gene expression (b); SOD2 gene expression (c); and GPx gene expression (d) compared to glutamate alone. Values are mean  $\pm$  SEM of at least 3 independent runs. ##  $p < 0.01$  vs. control; \*  $p < 0.05$ , \*\*  $p < 0.01$ , and \*\*\*  $p < 0.001$  vs. glutamate alone.

#### 4. The biological activities of LR extract in *C. elegans* (*in vivo*)

##### 4.1 Microbial susceptibility assays

From the result, all the extracts even in high dose (1000  $\mu\text{g}/\text{mL}$ ) did not impact on *E. coli* OP50 compared with Ampicilin (Table 5, Figure 31).

**Table 5** Microbial susceptibility test

Test	Mean inhibition zone $\pm$ SEM
S-medium	0.6 $\pm$ 0
DMSO	0.73 $\pm$ 0.23
LRE 500 $\mu\text{g}/\text{mL}$	0.73 $\pm$ 0.23
LRE 1000 $\mu\text{g}/\text{mL}$	0.73 $\pm$ 0.23
LRC 500 $\mu\text{g}/\text{mL}$	0.6 $\pm$ 0
LRC 1000 $\mu\text{g}/\text{mL}$	0.6 $\pm$ 0
LRH 500 $\mu\text{g}/\text{mL}$	0.6 $\pm$ 0
LRH 1000 $\mu\text{g}/\text{mL}$	0.6 $\pm$ 0
Ampicilin 200 $\mu\text{g}/\text{mL}$	3.52 $\pm$ 0.13

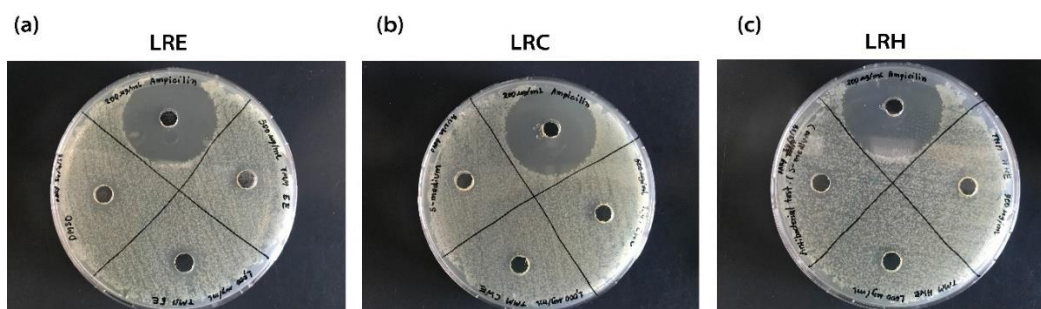


**Figure 31** Microbial susceptibility test for LRE (a), LRC (b), and LRH (c)

#### 4.2 Effect of LR extracts against juglone-induced oxidative stress in wild type

From the results, the age synchronized N2 worms were exposed to 80  $\mu\text{M}$  juglone. Only  $19.37 \pm 4.41$  % of untreated control could survive. Whereas, The survival rate of N2 worms that treated with LRE (50, 100 and 200  $\mu\text{g}/\text{mL}$ ) significantly increased and were dose-dependent at  $79.78 \pm 9.42$  % ( $p < 0.05$ ),  $85.32 \pm 8.72$  % ( $p < 0.01$ ),  $87.46 \pm 9.09$  % ( $p < 0.001$ ), respectively compared to DMSO ( $20.54 \pm 7.8$  % ). Similarly, the worms treated with 50  $\mu\text{g}/\text{mL}$  EGCG in DMSO significantly increased compared to DMSO ( $60.91 \pm 1.28$  %,  $p < 0.05$ ) (Figure 32a).

The worms were treated with different dose of LRC (50,100 and 200  $\mu\text{g}/\text{mL}$ ) significantly increased the survival rates by dose dependent at  $54.86 \pm 5.87$  ( $p < 0.05$ ),  $66.13 \pm 5.81$  ( $p < 0.01$ ) and  $79.07 \pm 6.54$  ( $p < 0.001$ ) compared to control, respectively (Figure 32b). Similarly, LRH (100, 200 and 300  $\mu\text{g}/\text{mL}$ ) significantly enhanced the survival rate at  $52.66 \pm 0.76$  ( $p < 0.05$ ),  $60.45 \pm 4.57$  ( $p < 0.01$ ), and  $69.5 \pm 11.8$  ( $p < 0.001$ ) compared to control, respectively (Figure 32b). For EGCG in S-medium (50  $\mu\text{g}/\text{mL}$ ) treatment, the survival worms were significant increase compared to control ( $53.33 \pm 1.93$ ,  $p < 0.05$ ).

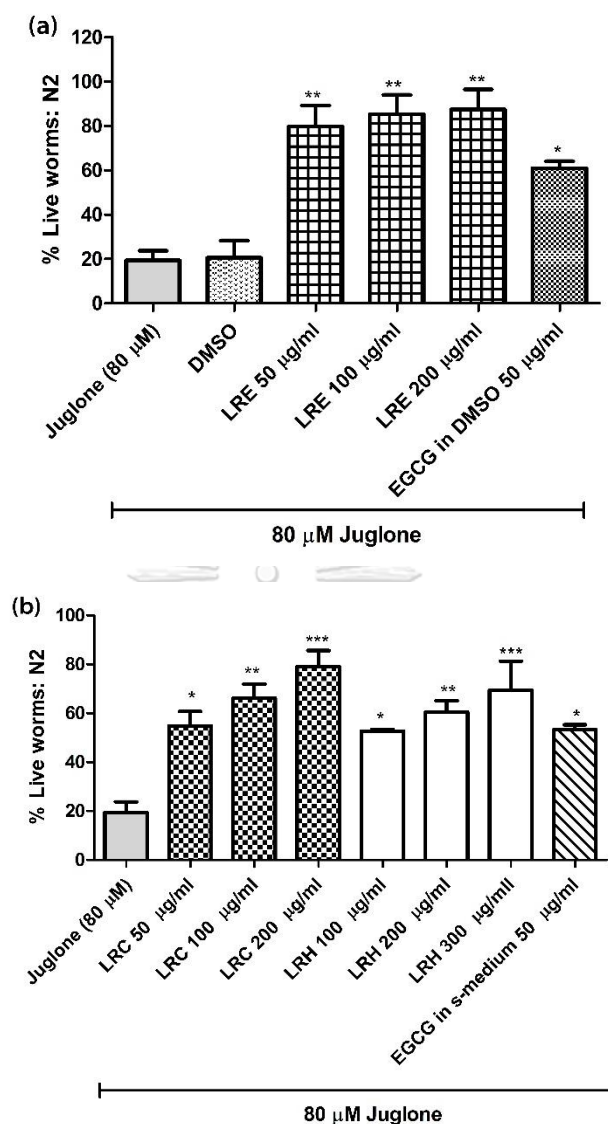


**Figure 32** Effect of different concentrations of LR extracts on survival rate against juglone-induced oxidative stress in N2 worms. The survival rate was significantly increase and dose dependent after LRE treatments (a) and LRC or LRH treatment (b). Values are mean  $\pm$  SEM of at least 3 independent runs. \*  $p < 0.05$ , \*\*  $p < 0.01$ , and \*\*\*  $p < 0.001$ .

#### 4.3 Effect of LR extracts on intracellular ROS accumulation in wild type

After wild type worms (N2) were treated with LR extracts. The results showed that LRE (50, 100 and 200  $\mu$ g/mL) significantly reduced intracellular ROS by reducing

fluorescence intensity and the reduce effects were dose-dependent at  $45.07 \pm 1.38$  % ( $p < 0.001$ ),  $27.96 \pm 0.89$  % ( $p < 0.001$ ),  $11.47 \pm 1.12$ % ( $p < 0.001$ ) compared to DMSO, respectively. Likewise, the worms were treated with 50  $\mu\text{g}/\text{mL}$  EGCG in DMSO significantly declined ROS accumulation compared to DMSO ( $31.92 \pm 2.03$ ,  $p < 0.001$ ) (Figure 33).

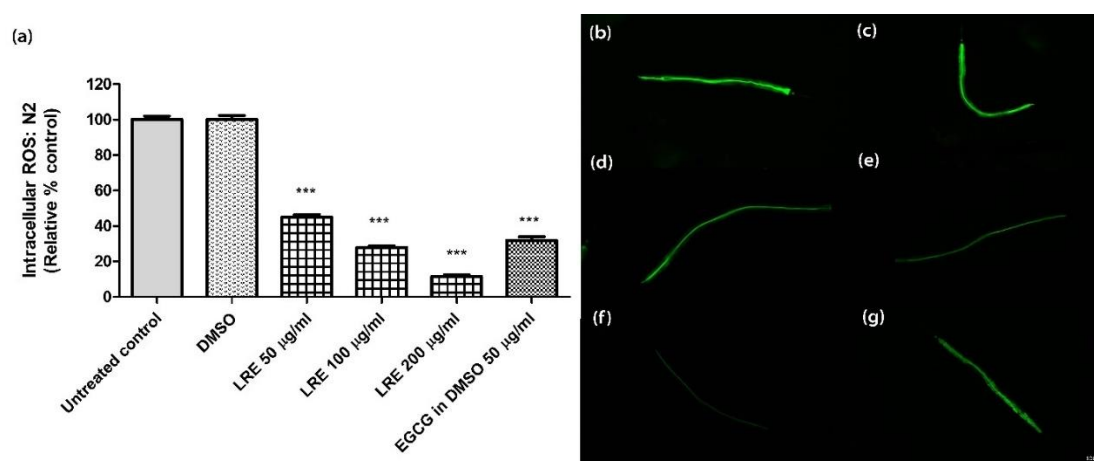


**Figure 33** Effect of different concentrations of LRE extracts and positive control (EGCG) on intracellular ROS accumulation in N2 worms. Intracellular ROS was significantly decreased after LRE and EGCG treatments (a). The fluorescent of ROS of control worms (b); DMSO treated worms (c); LRE at 50,100 and 200  $\mu\text{g}/\text{mL}$  treated worms (d-f, respectively); EGCG treated worms (g). Values are mean  $\pm$  SEM of at least 3 independent runs. \*\*\*  $p < 0.001$  compared to DMSO.

The age synchronized N2 worms were treated with 50, 100, and 200  $\mu\text{g}/\text{mL}$  of LRC showed low level of intracellular ROS dosed dependent at  $59.21 \pm 1.33$  %,  $40.12 \pm 1.58$  %, and  $25.58 \pm 1.50$  %;  $p < 0.001$  compared to control, respectively (Figure 4). Similar to LRC groups, the worms were treated with 50, 100, and 200  $\mu\text{g}/\text{mL}$  of LRC showed significant decrease in intracellular ROS expression at  $50.65 \pm 1.44$  %,  $38.7 \pm 1.55$  %, and  $20.35 \pm 1.14$  %;  $p < 0.001$  compared to control, respectively. For 50  $\mu\text{g}/\text{mL}$  EGCG in S-medium, the worms significantly decreased ( $25.3 \pm 1.92$ ,  $p < 0.001$ ) compared to control ( $100 \pm 2.09$ ) (Figure 34).



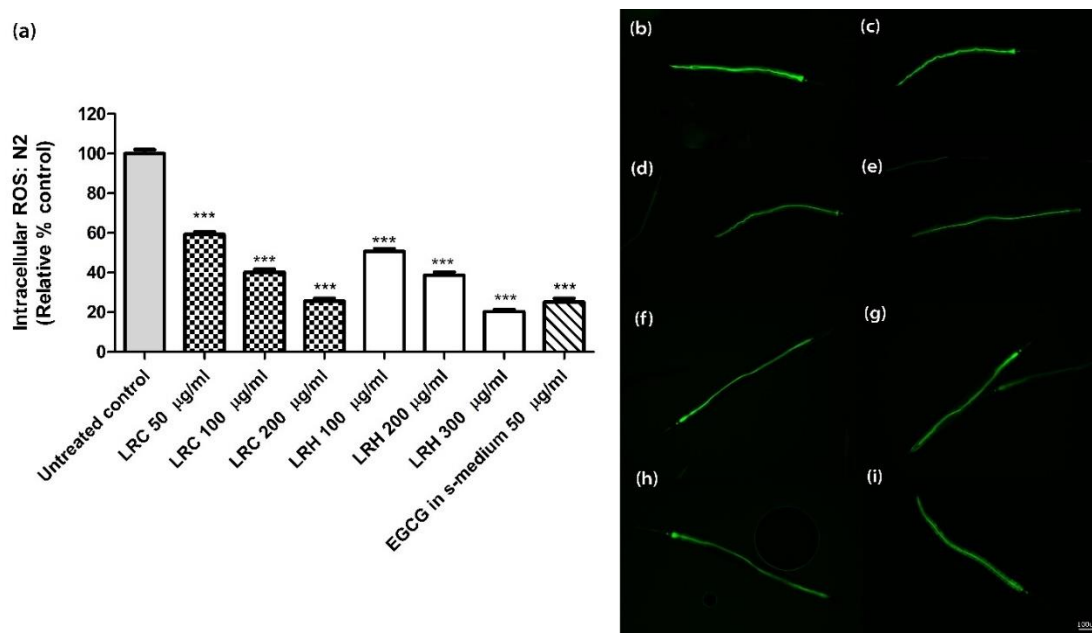


**Figure 34** Effect of different concentrations of LRC, LRH extracts and positive control (EGCG) on intracellular ROS accumulation in N2 worms. Intracellular ROS was significantly decrease after LRC, LRH extracts and EGCG treatments (a). The fluorescent of ROS of control N2 worms (b); LRC at 50,100 and 200 µg/mL treated worms (c-e, respectively); LRH at 100,200 and 300 µg/mL treated worms (f-h, respectively); and EGCG treated worms (i). Values are mean ± SEM of at least 3 independent runs. \*\*\*  $p < 0.001$  compared to control.

CHULALONGKORN UNIVERSITY

#### 4.4 Effect of LR extracts on HSP-16.2 expression

The synchronized TJ375 transgenic worms, treated with LRE with various concentrations (50, 100, and 200 µg/mL), significantly decreased the level of heat shock protein (HSP-16.2) after induced with 20 µM juglone and were dose dependence compared to DMSO at  $33.03 \pm 1.18$  %,  $17.86 \pm 0.90$  %, and  $10.33 \pm 1.15$  % ( $p < 0.001$ ). For 50 µg/mL EGCG in DMSO treated group, the worms also significantly reduced the HSP-16.2 expression levels compare to DMSO ( $9.18 \pm 0.49$ ,  $p < 0.001$ ) (Figure 35).

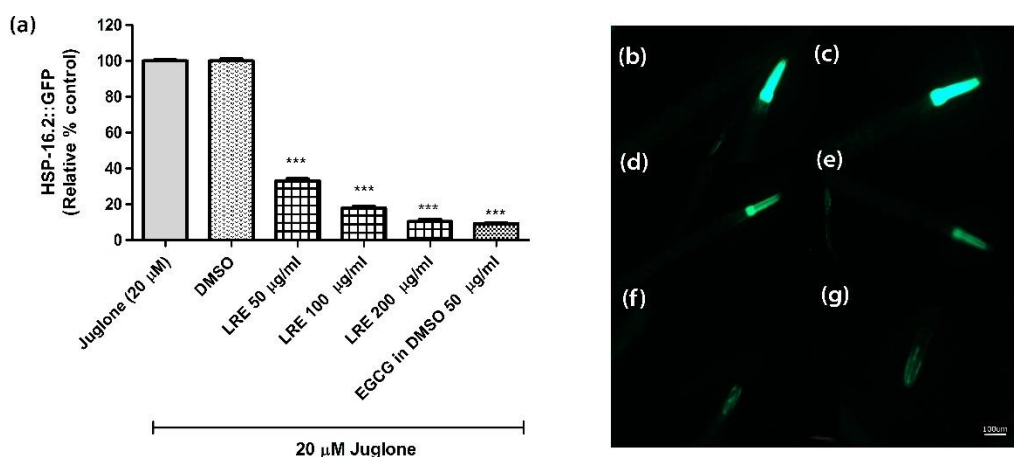


**Figure 35** Effect of different concentrations of LRE extracts and positive control (EGCG) on HSP-16.2 expression in TJ375 transgenic worms. The HSP-16.2 expression in TJ375 transgenic worms was significantly decrease after treated with LRE and EGCG treatments (a). The fluorescent of HSP-16.2 expression of control TJ375 worms (b); treated with DMSO (c); LRE at 50, 100 and 200  $\mu$ g/mL (d-f, respectively); and treated with EGCG (g). Values are mean  $\pm$  SEM of at least 3 independent runs. \*\*\*  $p < 0.001$  vs. DMSO.

The mutant worms, treated with LRC (50, 100, and 200  $\mu$ g/mL) significantly reduced HSP-16.2 expression at  $30.73 \pm 1.54\%$ ,  $17.77 \pm 0.72\%$ , and  $7.61 \pm 0.36\%$ ,  $p < 0.001$ , respectively. The mutant worms, treated with LRH (50, 100, and 200  $\mu$ g/mL) showed significant decrease at  $21.64 \pm 1.21\%$ ,  $11.88 \pm 1.25\%$ , and  $6.74 \pm 0.82\%$  ( $p < 0.001$ ) compared to control ( $10.27 \pm 0.39\%$ ) (Figure 36).

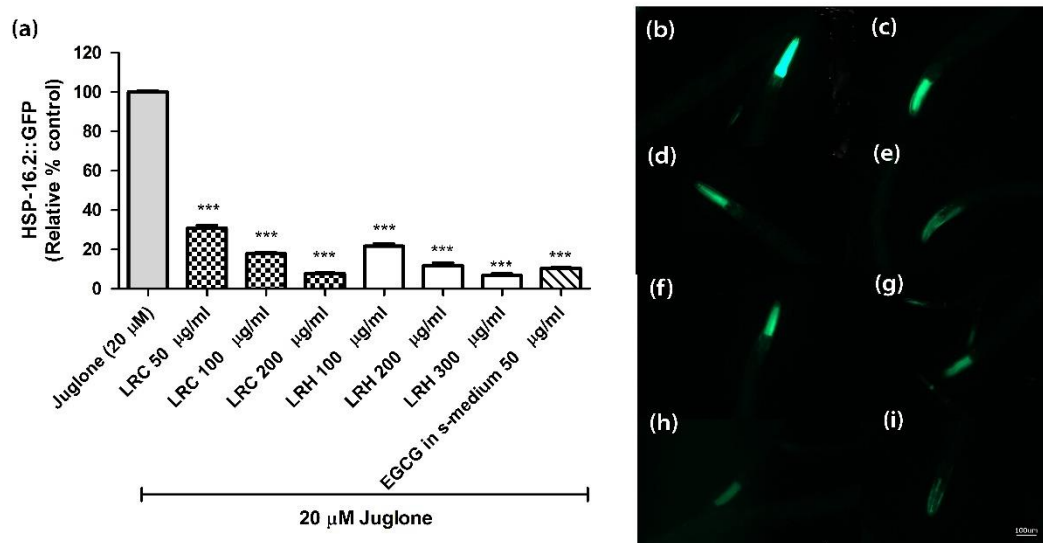


**Figure 36** Effect of different concentrations of LRC, LRH extracts and positive control (EGCG) on HSP-16.2 expression in TJ375 transgenic worms. The HSP-16.2 expression in TJ375 transgenic worms was significantly decreased after LRC, LRH and EGCG treatments (a). The fluorescent of HSP-16.2 expression of control TJ375 worms (b); treated with LRC at 50,100 and 200  $\mu$ g/mL (c-e, respectively); treated with LRH at 100, 200 and 300  $\mu$ g/mL (f-h, respectively); and treated with EGCG (i). Values are mean  $\pm$  SEM of at least 3 independent runs. \*\*\*  $p < 0.001$  vs. control.

#### 4.5 Effect of LR extracts on GST-4 expression

The results show that the CL2166 transgenic worms, treated with LRE and EGCG had no effect on the expression of GST-4 in CL2166 worms when compared to DMSO (Figure 37a). Similarly, the worms treated with LRC, LRH and EGCG in S-medium had no effect on the expression of GST-4 worms when compared to control (Figure 37b).

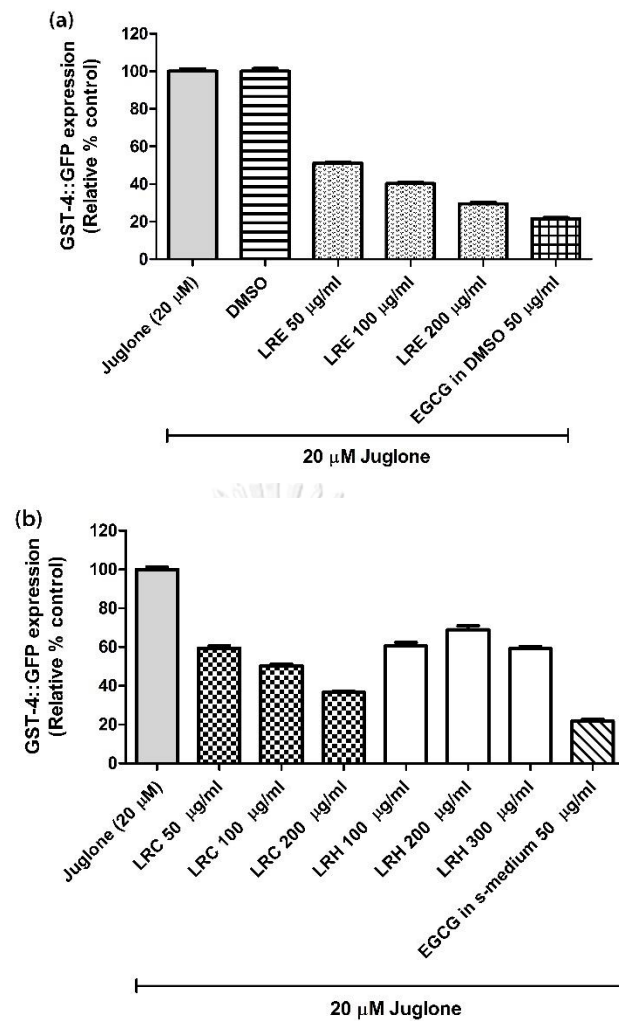


**Figure 37** Effect of different concentrations of LR extracts on GST-4 expression in CL2166 transgenic worms. The survival rate was significantly increase and dose dependent after LRE treatments (a) and LRC or LRH treatment (b). Values are mean  $\pm$  SEM of at least 3 independent experiments.

#### 4.6 Effect of LR extracts on SOD-3 expression

The synchronized CF1553 transgenic worms, treated with 50, 100, and 200  $\mu$ g/mL of LRE, significantly enhanced SOD-3 expression at  $169.1 \pm 1.72$  %,  $202.3 \pm 2.67$  %, and  $238.9 \pm 2.83$  %,  $p < 0.0001$ , respectively compared to DMSO. Similar to LRE, 50  $\mu$ M EGCG in DMSO significantly reduced at  $21.6 \pm 0.58$  % (Figure 38).

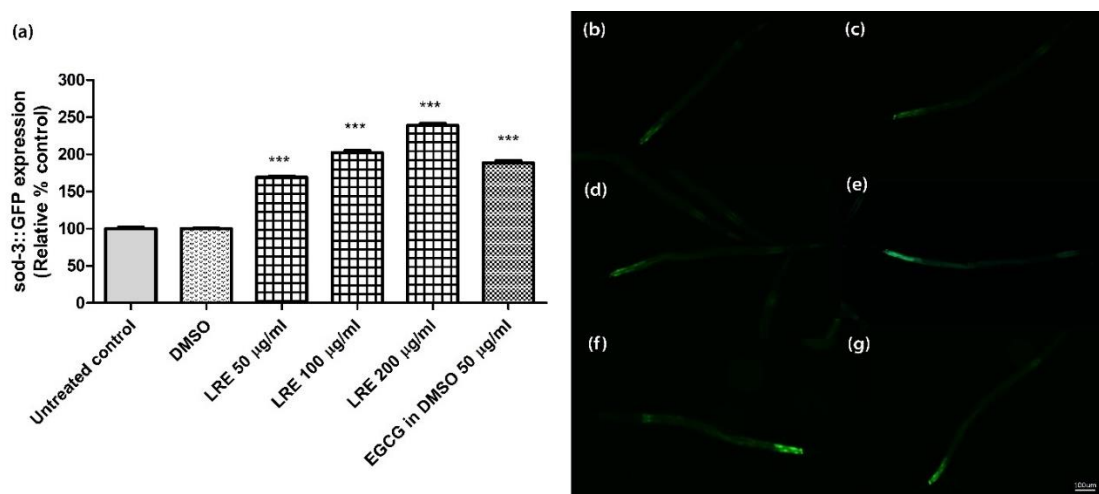


**Figure 38** Effect of different concentrations of LRE extracts and positive control (EGCG) on SOD-3 expression in CF1553 transgenic worms. SOD-3 expression was significantly increase after LRE and EGCG treatments (a). The fluorescent of SOD-3 expression of control CF1553 transgenic worms (b); DMSO treated worms (c); LRE at 50,100 and 200 µg/mL treated worms (d-f, respectively) ; and EGCG treated worms (g). Values are mean  $\pm$  SEM of at least 3 independent runs. \*\*\*  $p < 0.001$  vs. DMSO.

Similar to LRE, the worms, treated with 50, 100, and 200 µg/mL of LRC showed significant increase at  $156.6 \pm 1.53$  %,  $194.9 \pm 1.94$  %, and  $223.8 \pm 4.34$  %;  $p < 0.001$ , respectively, compared to control. The worms, treated with 100, 200 ,and 300 of LRH, significantly increased at  $169.8 \pm 1.94$  %,  $208.6 \pm 2.248$ ,  $247.4 \pm 4.49$  %;  $p < 0.001$  respectively, compared to control. In addition, the worms, treated with 50 µM EGCG in S-medium, significantly increased SOD-3 expression by  $166.3 \pm 2.35$  %,  $p < 0.001$  (Figure 39).

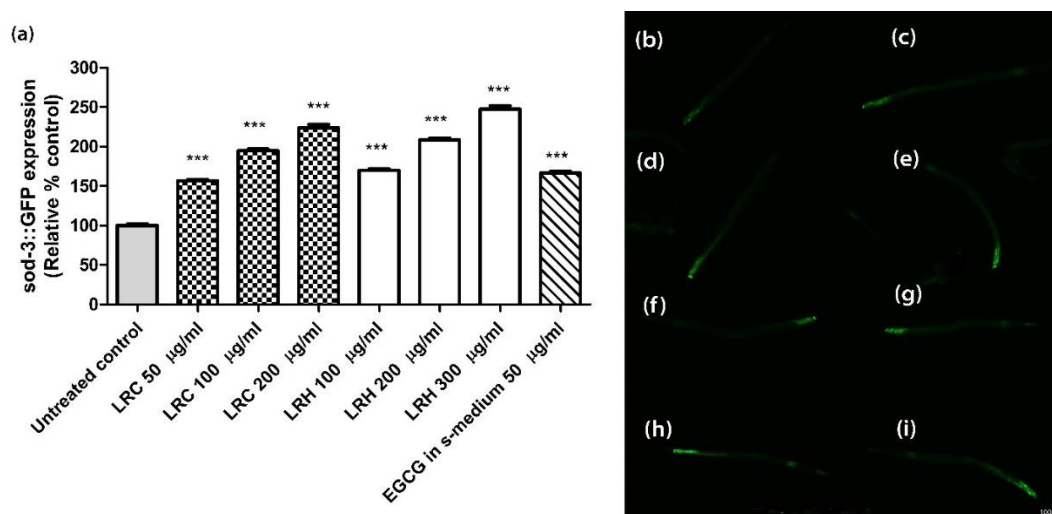


**Figure 39** Effect of different concentrations of LRC, LRH extracts and positive control (EGCG) on SOD-3 expression in CF1553 transgenic worms. SOD-3 expression was significantly increased after LRC, LRH and EGCG treatments (a). The fluorescent of SOD-3 expression of control CF1553 transgenic worms (b); LRC at 50, 100, and 200 µg/mL treated worms (c-e, respectively); LRH at 100, 200, and 300 µg/mL treated worms (f-h, respectively); and EGCG treated worms (i). Values are mean  $\pm$  SEM of at least 3 independent runs. \*\*\*  $p < 0.001$  vs. control.

#### 4.7 Effect of LR extracts on DAF-16/FOXO pathway

The age synchronized TJ356 transgenic worms, treated with 50, 100, and 200 µg/mL of LRE, significantly enhanced DAF-16 translocation to nucleus. The percentage of nuclear subcellular localization were  $48.7 \pm 7.51$  % ( $p < 0.01$ ),  $63.09 \pm 9.07$  % ( $p < 0.001$ ), and  $72.77 \pm 11.20$  % ( $p < 0.001$ ) compared to DMSO ( $3.74 \pm 0.41$ ). For 50 µM EGCG in DMSO treatment, the result showed significantly enhanced DAF-16 translocation to nucleus compared to DMSO ( $40.24 \pm 4.89$ ,  $p < 0.05$ ) (Figure 40a).

Similar to LRE, the synchronized worms, treated with LRC (50, 100, and 200 µg/mL) showed significant increase in DAF-16 nuclear localization compared to control at  $39.05 \pm 0.68$ % ( $p < 0.05$ ),  $40.85 \pm 0.72$ % ( $p < 0.05$ ), and  $54.0 \pm 3.51$ %, ( $p < 0.001$ ), respectively. The result of LRH treatment showed significant increase in DAF-16 nuclear localization compared to control at  $39.83 \pm 7.29$ %, ( $p < 0.05$ ),  $54.48 \pm$

8.79%, ( $p < 0.001$ ), and  $59.76 \pm 10.00\%$  ( $p < 0.001$ ), respectively. The worms of  $50 \mu\text{M}$  EGCG in S-medium treatment showed significantly enhanced DAF-16 translocation to nucleus compared to control ( $41.29 \pm 12.04$ ,  $p < 0.05$ ) (Figure 40b).

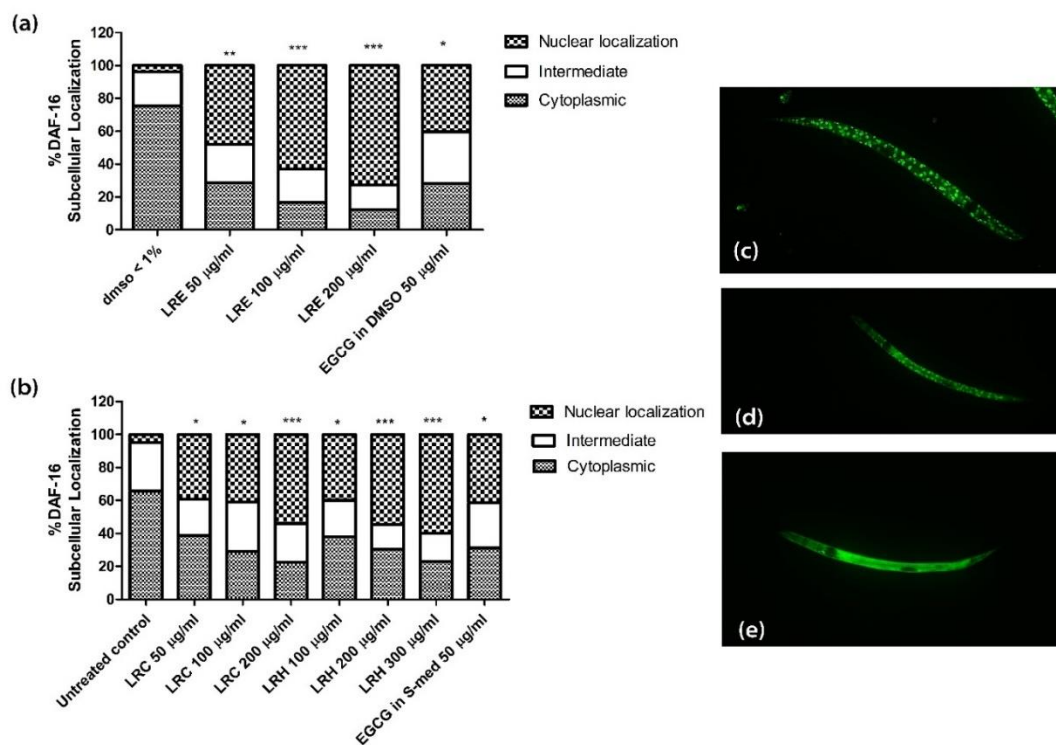


**Figure 40** Effect of different concentrations of the extracts on DAF-16 nuclear localization in TJ356 transgenic worms. DAF-16 nuclear localization was significant increase after LRE treatment (a), LRC, and LRH treatments (b). DAF-16 locations in TJ356 worms: nucleus (c), intermediate (d) and cytosol (e). Values are mean  $\pm$  SEM of at least 3 independent runs. \*  $p < 0.05$ ; \*\*  $p < 0.01$ ; and \*\*\*  $p < 0.001$  vs. control.

#### 4.7.1 Effect of LR extracts against juglone-induced oxidative stress in CF1038

To confirm whether all extracts activated the antioxidant activities via DAF-16/FoxO pathway. The CF1038 transgenic worms were treated with all concentrations of LRE, LRC, LRH and EGCG. From the results, *there were no difference of the % survival worms both all concentration of LRE extracts compared*

to DMSO (Figure 41a) and all concentration of LRC, LRH extracts compared to control (Figure 41b).

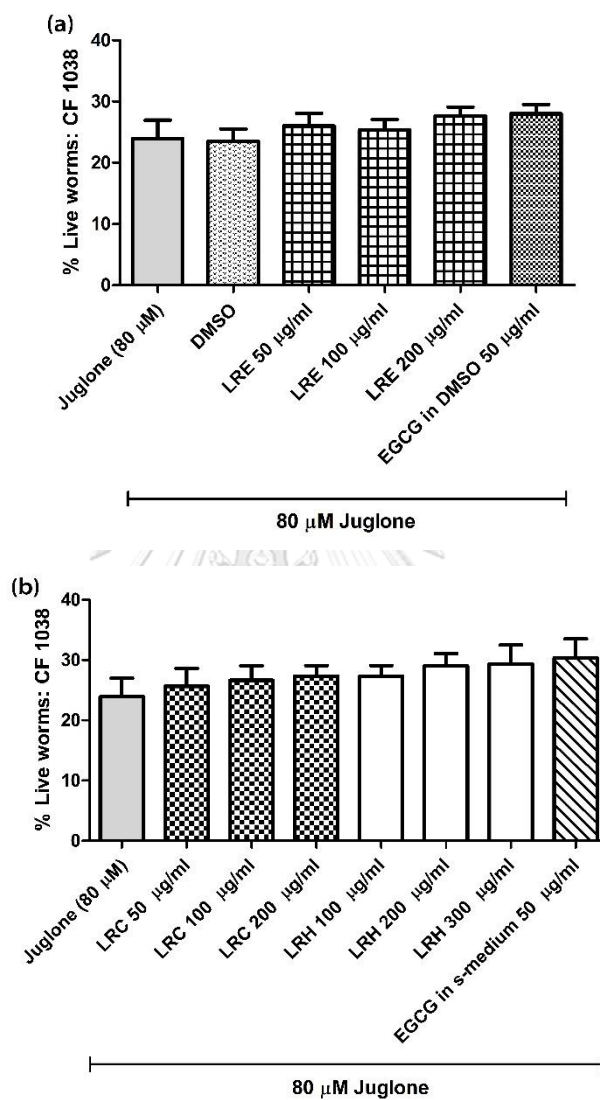


**Figure 41** Effect of different concentrations of LR extracts on survival rate against juglone-induced oxidative stress in CE1038 worms. The survival rate no difference after treated LRE extracts (a) and LRC or LRH extract (b). Values are mean  $\pm$  SEM of at least 3 independent runs.



#### 4.7.2 Effect of LR extracts on intracellular ROS accumulation in CF1038

Similar to oxidative stress results, there were no difference of intracellular ROS accumulation in CF1038 worms both all concentration of LRE extracts compared to DMSO (Figure 42a) and all concentration of LRC, LRH extracts compared to control (Figure 42b).

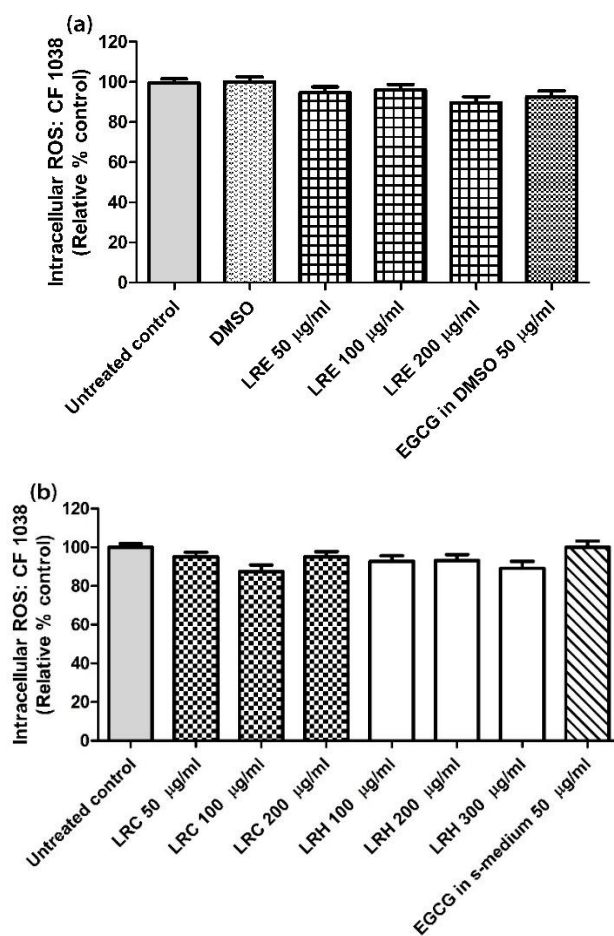


**Figure 42** Effect of different concentrations of LR extracts on intracellular ROS accumulation in CF1038 worms. The results showed no difference after treated LRE extracts (a) and LRC or LRH extract (b). Values are mean  $\pm$  SEM of at least 3 independent runs.

#### 4.8 Effect of LR extracts on SKN-1/NRF-2 pathway

The LD-1 transgenic worms were treated with all the extracts. From the result, the SKN-1 nuclear translocation of LD-1 had no differences between all concentration of LRE and EGCG compared to DMSO group (Figure 43a). In addition, the worms had no differences between all concentration of LRC, LRH and EGCG compared to control (Figure 43b).

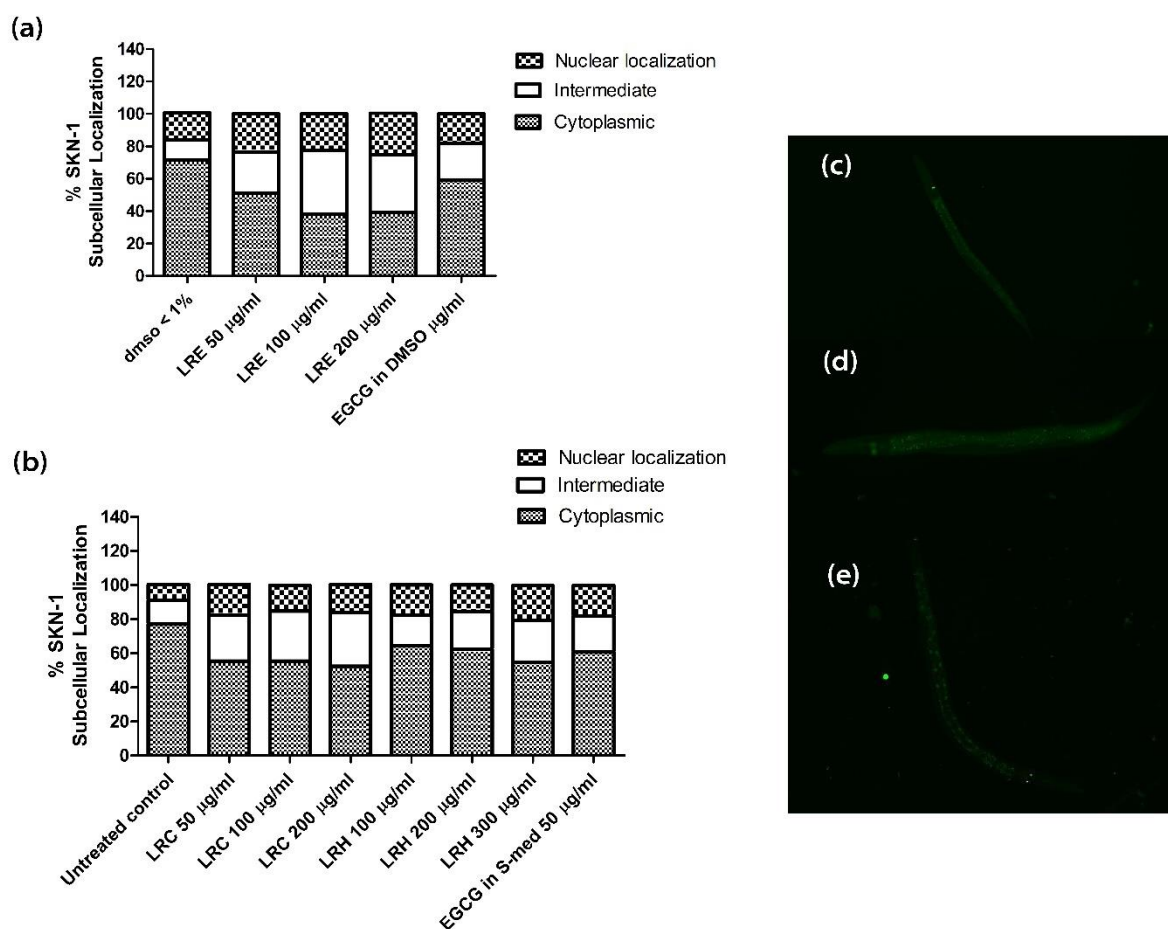


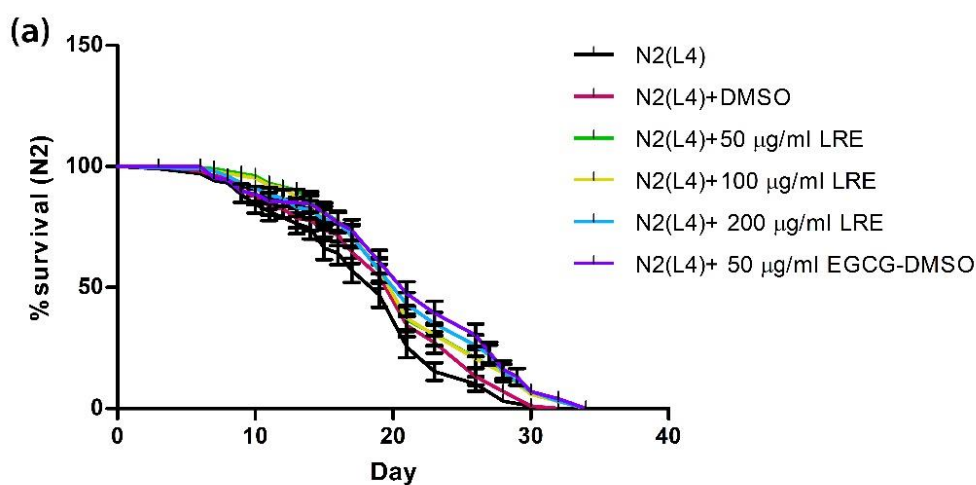
**Figure 43** Effect of different concentrations of the extracts on SKN-1 nuclear localization in LD1 transgenic worms. The LD1 worms showed no difference after LRE treatment (a), LRC, LRH and EGCG treatments (b) compare to control. SKN-1 locations in LD1 worms: cytosol (c), intermediate (d) and nucleus (e). Values are mean  $\pm$  SEM of at least 3 independent runs.

#### 4.9 Effect of LR extracts on lifespan extension

The age synchronized N2 worms, treated with different concentration of LRE significantly enhanced the survival of N2 worms compared to DMSO control. The mean lifespan of the 50, 100 and 200  $\mu\text{g/ml}$  extract-treated worms were  $20.98 \pm 0.61$ ,  $21.06 \pm 0.64$ , and  $21.09 \pm 0.69$ ;  $p < 0.01$ , compared to control, respectively. For 50  $\mu\text{M}$  EGCG in DMSO-treated worms, the mean lifespan was significant increase compared to DMSO ( $21.42 \pm 0.73$ ;  $p < 0.01$ ) (Figure 44a and Table 6).

Similarly, the age synchronized N2 worms, treated with 50, 100 and 200  $\mu\text{g/ml}$  LRC significantly enhanced the survival of N2 worms compared to control group at  $20.34 \pm 0.66$  ( $p < 0.05$ ),  $20.95 \pm 0.76$  ( $p < 0.05$ ), and  $20.95 \pm 0.76$  ( $p < 0.001$ ), respectively (Figure 44b and Table 6).

In addition, the age synchronized N2 worms, treated with 100, 200 and 300  $\mu\text{g/ml}$  LRH significantly enhanced the survival of N2 worms compared to control group at  $20.28 \pm 0.72$  ( $p < 0.05$ ),  $20.66 \pm 0.71$  ( $p < 0.05$ ), and  $20.93 \pm 0.76$  ( $p < 0.001$ ), respectively. The worms, treated with 50  $\mu\text{M}$  EGCG in S-medium, showed that the mean lifespan was significant increase compared to control ( $21.42 \pm 0.73$ ;  $p < 0.01$ ) (Figure 44c and Table 6)



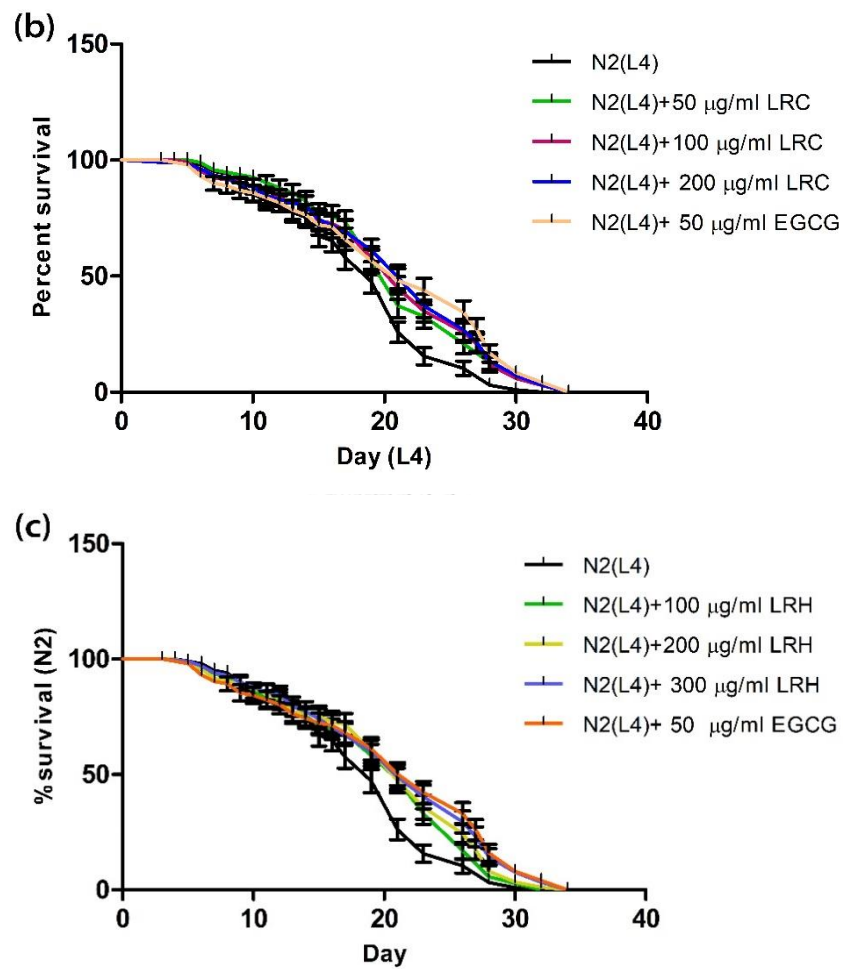


**Figure 44** Effect of different concentrations of LR extracts on Longevity. The N2 worm-treated with 50, 100, and 200 µg/mL LRE (a); 50, 100, and 200 µg/mL LRC (b); and 100, 200, and 300 µg/mL LRH (c). Lifespan extension after LRE, LRC and LRH extract treatment showed in cumulative survival plots.

**Table 6** Results and statistical analyses of *C. elegans* lifespan assay

Treatment: N2	Mean lifespan (day) $\pm$ SEM	% increased lifespan (vs. control)	p-value (vs. control)	p-value summary	Number of worms
Control	18.23 $\pm$ 0.64				99
DMSO	19.65 $\pm$ 0.62	7.79	0.1137	ns	106
LRE 50 $\mu$ g/ml	20.98 $\pm$ 0.61	15.09	0.002	**	100
LRE 100 $\mu$ g/ml	21.06 $\pm$ 0.64	15.52	0.002	**	102
LRE 200 $\mu$ g/ml	21.09 $\pm$ 0.69	15.69	0.0028	**	100
EGCG in DMSO 50 $\mu$ g/ml	21.42 $\pm$ 0.73	17.50	0.0012	**	100
LRC 50 $\mu$ g/ml	20.34 $\pm$ 0.66	11.57	0.0225	*	100
LRC 100 $\mu$ g/ml	20.71 $\pm$ 0.75	13.60	0.0125	*	100
LRC 200 $\mu$ g/ml	20.95 $\pm$ 0.76	14.92	0.0067	**	100
LRH 100 $\mu$ g/ml	20.28 $\pm$ 0.72	11.25	0.0362	*	104
LRH 200 $\mu$ g/ml	20.66 $\pm$ 0.71	13.33	0.0124	*	102
LRH 300 $\mu$ g/ml	20.93 $\pm$ 0.76	14.81	0.0072	**	98
EGCG in S-medium 50 $\mu$ g/ml	21.17 $\pm$ 0.82	16.13	0.0052	**	101

The lifespan assay was carried out with wild type (N2) worms at 20 °C. Mean lifespan in days is the average number of days the worms survived in each group. The treatment group was compared to the control by log-rank (Mantel – Cox) tests followed by the Gehan – Breslow – Wilcoxon test

#### 4.10 Effect of LR extracts on Lipofuscin level

The synchronized BA17 transgenic worms that were temperature sensitive and recessive feminization strains (no laying eggs at 25 °C, treated with 50, 100, and 200  $\mu$ g/mL of LRE, significantly attenuated lipofuscin accumulation at  $62.00 \pm 1.34$

%,  $53.06 \pm 1.50$  %, and  $60.44 \pm 1.00$  %;  $p < 0.0001$ , respectively compared to DMSO. Similarly, 50  $\mu\text{M}$  EGCG in DMSO-treated worms significantly reduced lipofuscin level at  $60.10 \pm 1.42$  %;  $p < 0.001$  compared to DMSO (Figure 45a).

Like LRE, the worms, treated with 50, 100, and 200  $\mu\text{g}/\text{mL}$  of LRC showed significant decrease lipofuscin level at  $59.38 \pm 11.20$  %,  $52.72 \pm 0.96$  %, and  $49.85 \pm 1.20$  %;  $p < 0.001$ , respectively, compared to control. The worms, treated with 100, 200 ,and 300 of LRH, significantly decreased in autofluorescent at  $54.12 \pm 0.85$  %,  $47.83 \pm 1.68$ , and  $45.17 \pm 0.87$  %;  $p < 0.001$  respectively, compared to control. In addition, the worms, treated with 50  $\mu\text{M}$  EGCG in S-medium, significantly decreased lipofuscin expression at  $50.55 \pm 1.59$  %,  $p < 0.001$  (Figure 45b).



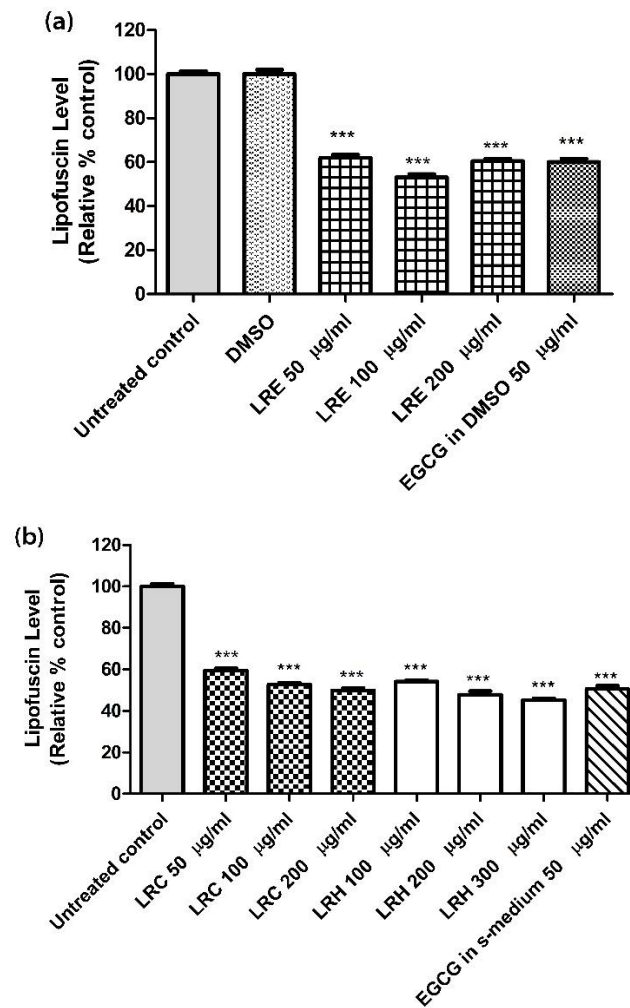


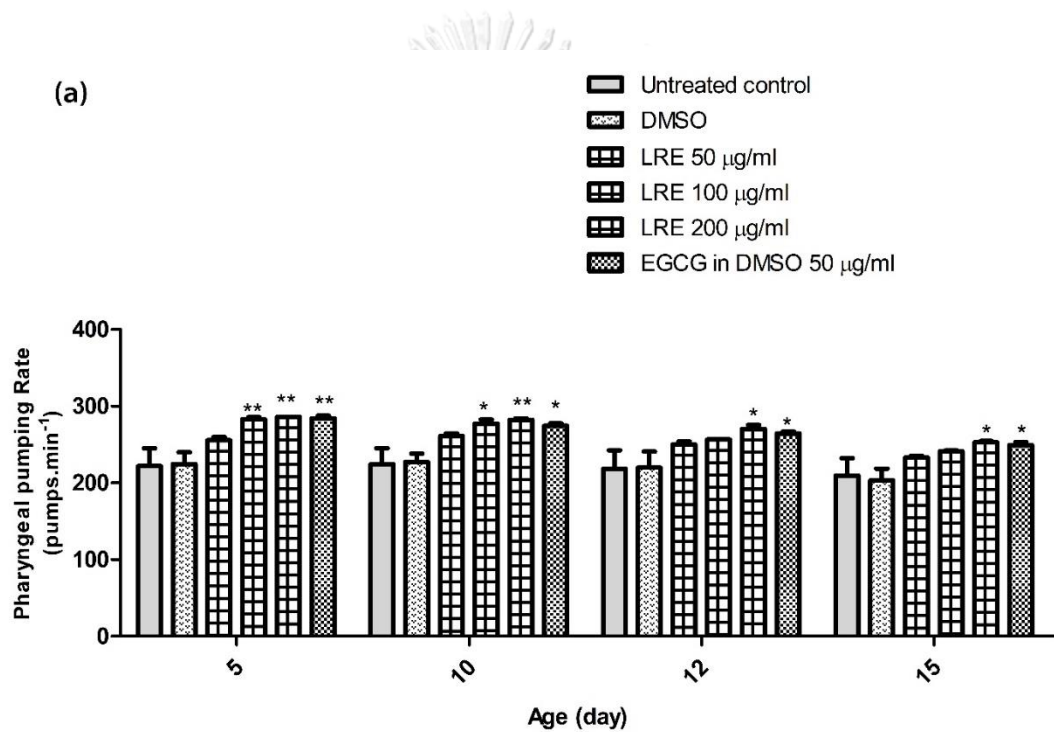
**Figure 45** Effect of different concentrations of LR extracts on lipofuscin level in BA17 worms. The worms, treated with LRE extracts 50, 100 and 200 µg/ml significantly attenuated lipofuscin level (a). The worms, treated with 50, 100 and 200 µg/ml LRC, and 100, 200 and 300 µg/ml LRH extracts significantly decreased lipofuscin level (b). Values are mean  $\pm$  SEM of at least 3 independent runs. \*\*\*  $p < 0.001$  vs. control.

#### 4.11 Effect of LR extracts on pharyngeal pumping rate

The age synchronized N2 worms, treated with 100 of LRE, significantly improved pharyngeal pumping rate of adult worms on days 5 and 10 compared to DMSO. Whereas, the worms treated with 200 µg/mL were significant increase in pharyngeal pumping rate on day 5, 10, 12 and 15. Similarly, the worms, treated with

50  $\mu\text{M}$  EGCG in DMSO significantly improved pharyngeal pumping rate on day 5, 10, 12 and 15 compared to DMSO (Figure 46a).

The worms, treated with LRC (200  $\mu\text{g}/\text{mL}$ ) LRH (200 and 300  $\mu\text{g}/\text{mL}$ ) showed significant increase pharyngeal pumping rate on days 5 and 10 compared to control. Whereas, the worms, treated with 50  $\mu\text{M}$  EGCG in S-medium, significantly increased pharyngeal pumping rate on day 5, 10, 12 and 15 compare to control (Figure 46b).





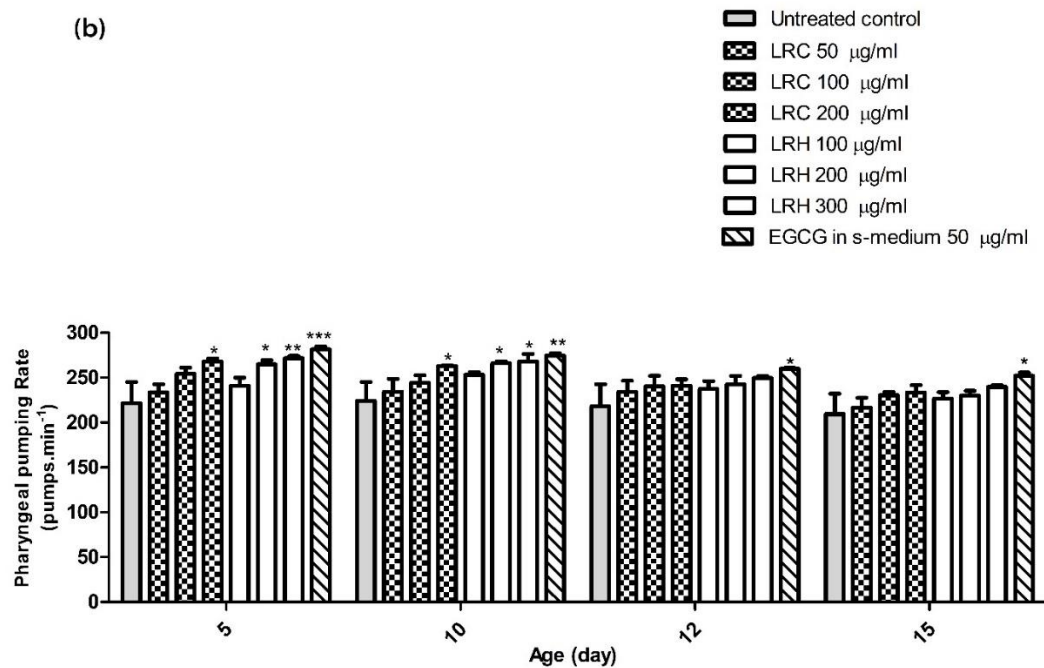


**Figure 46** Effect of different concentrations of LR extracts on pharyngeal pumping rate in N2 worms. The worms, treated with 100 µg/mL LRE significantly improved pumping rate on day 5 and 10, whereas, 200 µg/mL LRE and EGCG treated groups increase pharyngeal pumping rate on day 5, 10, 12 and 15 (a). LRC or LRH treatment significantly improved pumping rate on day 5 and 10, except EGCG improved rate until day 15 (b). Values are mean  $\pm$  SEM of at least 3 independent runs. \*\*\*  $p < 0.001$  vs. control.

จุฬาลงกรณ์มหาวิทยาลัย  
CHULALONGKORN UNIVERSITY

#### 4.12 Effect of LR extracts on body length and Brood size

The N2 worms were treated with all concentrations of LRE, LRC, LRH and EGCG. From the results, there were no difference of body length both all concentration of LRE extracts compared to DMSO (Figure 47a) and all concentration of LRC, LRH extracts compared to control (Figure 47b).

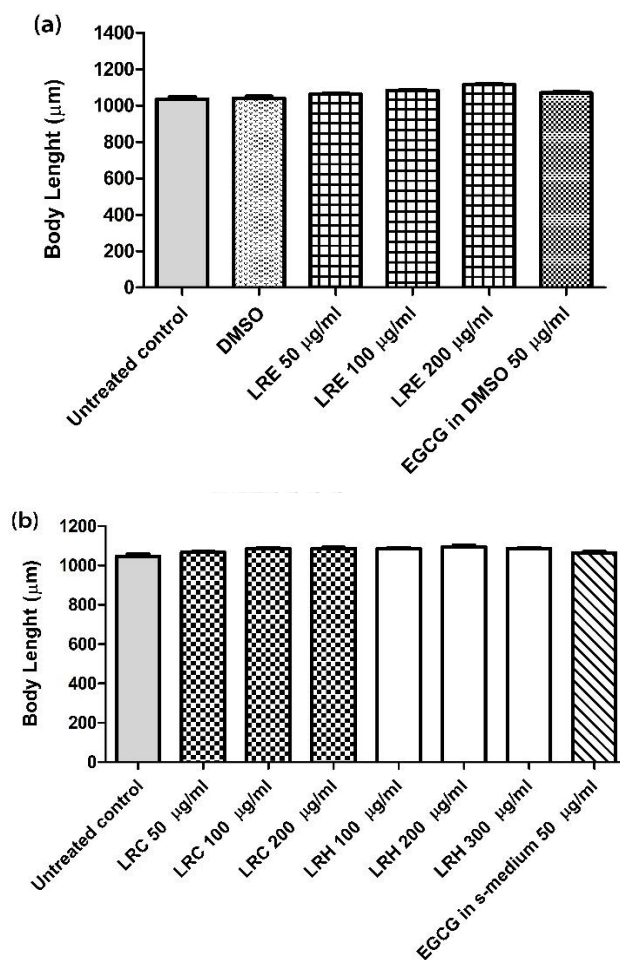


**Figure 47** Effect of different concentrations of LR extracts on body length in N2 worms. The worms, treated with LRE extracts (a); and treated LRC, LRH and EGCG (b) were not different in body length compared to control. Values are mean  $\pm$  SEM of at least 3 independent runs.

Furthermore, There were no difference of the amount of progeny both all concentration of LRE extracts compared to DMSO (Figure 48a) and all concentration of LRC, LRH extracts compared to control (Figure 48b).

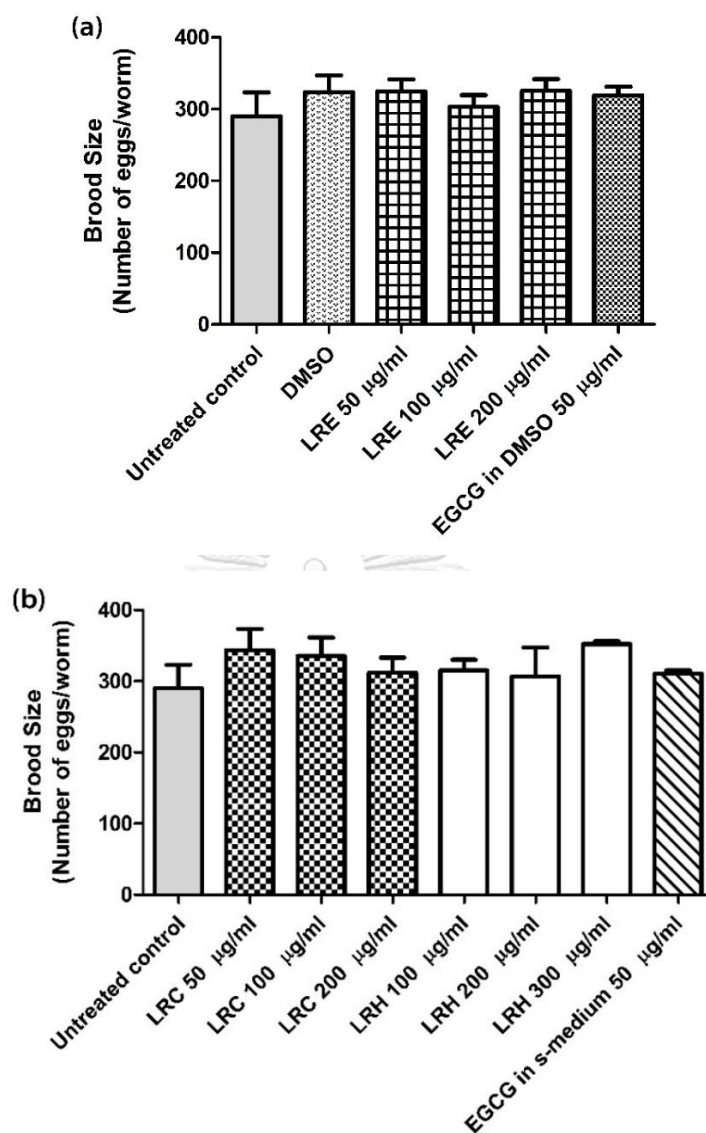


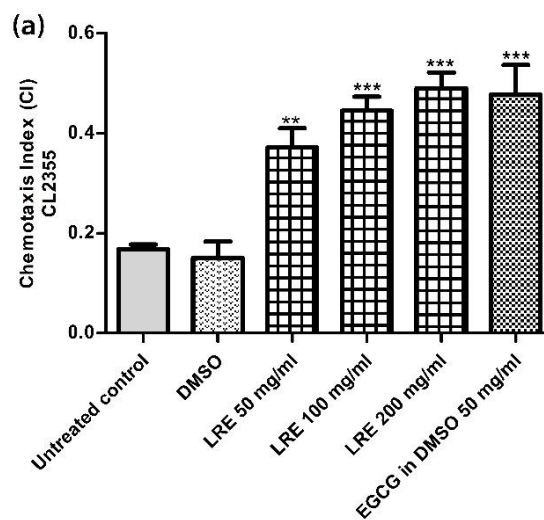
**Figure 48** Effect of different concentrations of LR extracts on brood size in N2 worms. The worms, treated with LRE extracts (a); and treated LRC, LRH and EGCG (b) were not different in amount of progeny compared to control. Values are mean  $\pm$  SEM of at least three independent runs.

#### 4.13 Neuroprotective effect of LR extracts against A $\beta$ -induced deficit in chemotaxis behavior in *C. elegans*

The result showed that the transgenic CL2355 worms, A $\beta$ -induced deficit in chemotaxis behavior, significant increase in Chemotaxis Index (CI) when treated with

(50, 100, and 200  $\mu\text{g}/\text{mL}$ ) LRE in a dose-dependent manner at  $0.37 \pm 0.04$  ( $p < 0.01$ ),  $0.45 \pm 0.03$  ( $p < 0.001$ ), and  $0.49 \pm 0.03$  ( $p < 0.001$ ), respectively as well as 50  $\mu\text{g}/\text{mL}$  EGCG group ( $0.48 \pm 0.06$ ;  $p < 0.001$ ) compared to DMSO ( $0.1506 \pm 0.03$ ) (Figure 49a). However, there were no difference in CI in transgenic CL2122 worms (no A $\beta$ ) when treated with LRE and 50  $\mu\text{g}/\text{mL}$  EGCG compared to DMSO control (Figure 49b).

Moreover, transgenic CL2355 worms, treated with 50, 100, and 200  $\mu\text{g}/\text{mL}$  of LRC, significant increase in Chemotaxis Index (CI) at  $0.63 \pm 0.03$  ( $p < 0.05$ ),  $0.75 \pm 0.04$  ( $p < 0.001$ ), and  $0.72 \pm 0.04$  ( $p < 0.01$ ), respectively. Similarly, the transgenic worms, treated with 100, 200, and 300  $\mu\text{g}/\text{mL}$  of LRH significantly enhanced CI at  $0.63 \pm 0.03$  ( $p < 0.05$ ),  $0.74 \pm 0.02$  ( $p < 0.001$ ), and  $0.74 \pm 0.04$  ( $p < 0.001$ ), respectively as well as 50  $\mu\text{g}/\text{mL}$  EGCG group ( $0.79 \pm 0.05$ ;  $p < 0.001$ ) compared to control ( $0.47 \pm 0.04$ ) (Figure 49c). However, they were also no difference in CI in transgenic CL2122 worms (no A $\beta$ ) when treated with LRC, LRH, and 50  $\mu\text{g}/\text{mL}$  EGCG compared to control (Figure 49d).



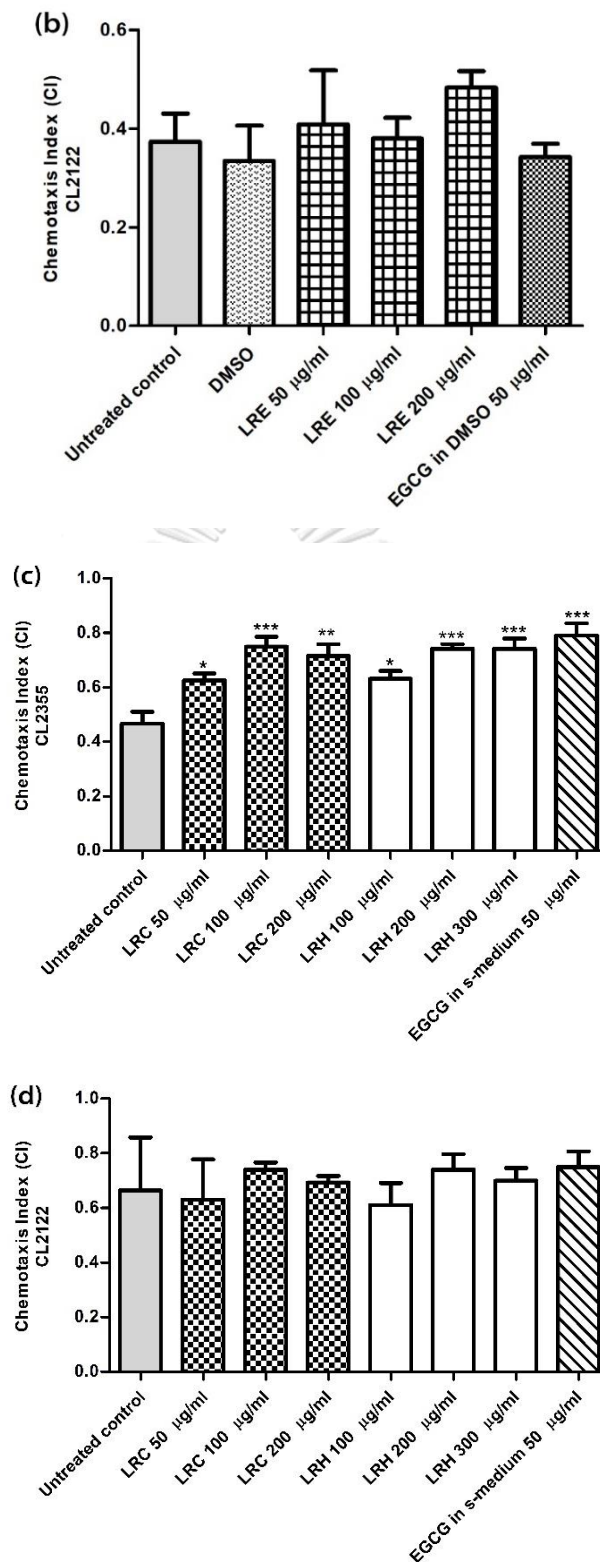
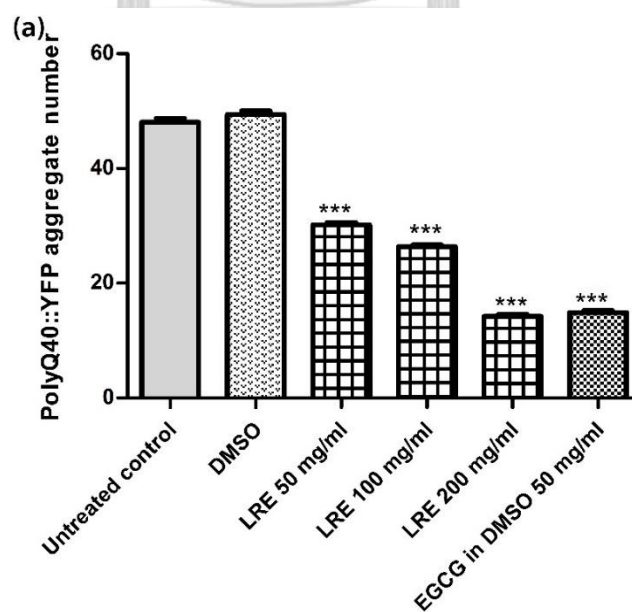


**Figure 49** The effect of different concentrations of LRE extracts against  $A\beta$ -induced deficit in chemotaxis behavior in *C. elegans*. The transgenic CL2355 worms ( $A\beta+$ ) after

treat with 50, 100, and 200  $\mu\text{g}/\text{mL}$  of LRE significantly increase in CI compared to DMSO (a). The transgenic CL2122 worms ( $A\beta$ -) after treat with 50, 100, and 200  $\mu\text{g}/\text{mL}$  of LRE were not difference in CI compared to DMSO (b). In addition, the transgenic CL2355 worms, treated with (50, 100, and 200  $\mu\text{g}/\text{mL}$ ) LRC and (100, 200, and 300  $\mu\text{g}/\text{mL}$ ) LRH significantly increase in CI compared to control (c). However, the transgenic CL2122 worms, treated with both LRC and LRH were not difference in CI compared to control (d). Values are mean  $\pm$  SEM of at least 3 independent tests. \* $p < 0.05$ , \*\*  $p < 0.01$ , and \*\*\*  $p < 0.001$  vs. DMSO.

#### 4.14 Neuroprotective effect of LR extracts on PolyQ40 aggregation

The result showed that the transgenic AM141 worms, treated with 50, 100, and 200  $\mu\text{g}/\text{mL}$  LRE significantly reduced the number of polyQ40 aggregation in a dose-dependent manner at  $30.18 \pm 0.41$ ,  $26.38 \pm 0.28$ , and  $14.21 \pm 0.36$ ;  $p < 0.001$ , respectively compared to DMSO ( $49.40 \pm 0.65$ ). Similarly, the worms treated with 50  $\mu\text{g}/\text{mL}$  EGCG significantly reduced polyQ40 aggregation at  $14.87 \pm 0.37$ ;  $p < 0.001$  compared to DMSO (Figure 50).



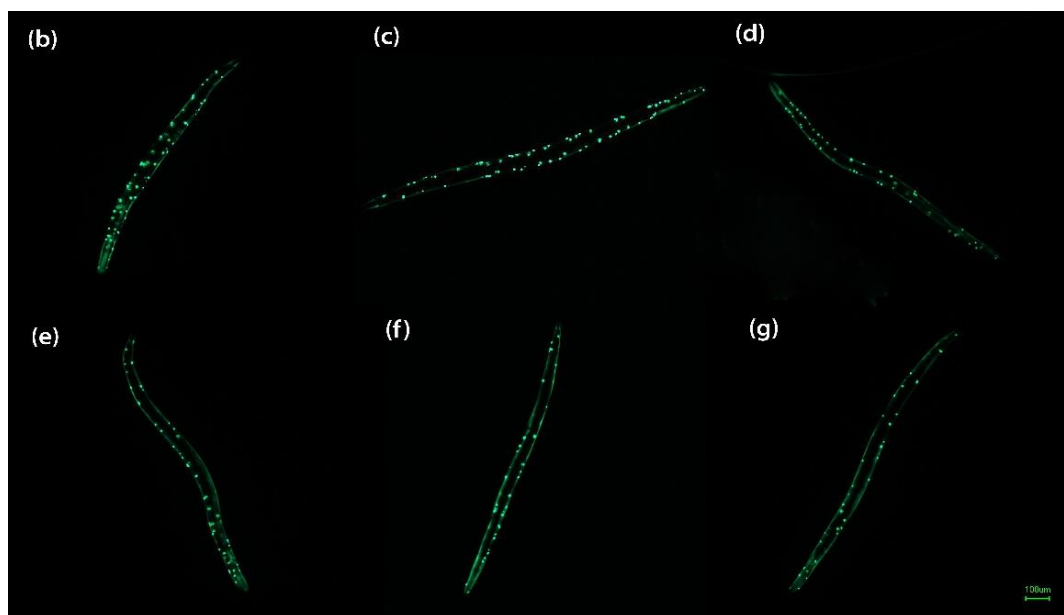


**Figure 50** The effect of different concentrations of LRE extracts against PolyQ40 aggregation in *C. elegans*. The transgenic AM141 worms after treat with of different concentration of LRE significantly decrease in PolyQ40 formation (a). PolyQ40 formation under a fluorescence microscope of control worms (b); DMSO treated worms (c); after treated with 50, 100, and 200 µg/mL of LRE (d-f); and 50 µg/mL of EGCG treated worms (g). Values are mean  $\pm$  SEM of at least 3 independent runs. \*\*\*  $p < 0.001$  vs. DMSO.

In addition, the result showed that the transgenic AM141 worms, treated with 50, 100, and 200 µg/mL LRC, significantly reduced the number of polyQ40 aggregation in a dose-dependent manner at  $28.29 \pm 0.44$ ,  $22.20 \pm 0.39$ , and  $16.40 \pm 0.41$ ;  $p < 0.001$ , respectively compared to control ( $48.08 \pm 0.63$ ). Similarly, the worms, treated with 100, 200, and 300 µg/mL LRH, significantly reduced the number of polyQ40 aggregation at  $24.5 \pm 0.40$ ,  $16.23 \pm 0.33$ , and  $14.52 \pm 0.41$ ;  $p < 0.001$ , respectively as well as the worms treated with 50 µg/mL EGCG ( $17.74 \pm 0.44$ ) compared to control (Figure 51).

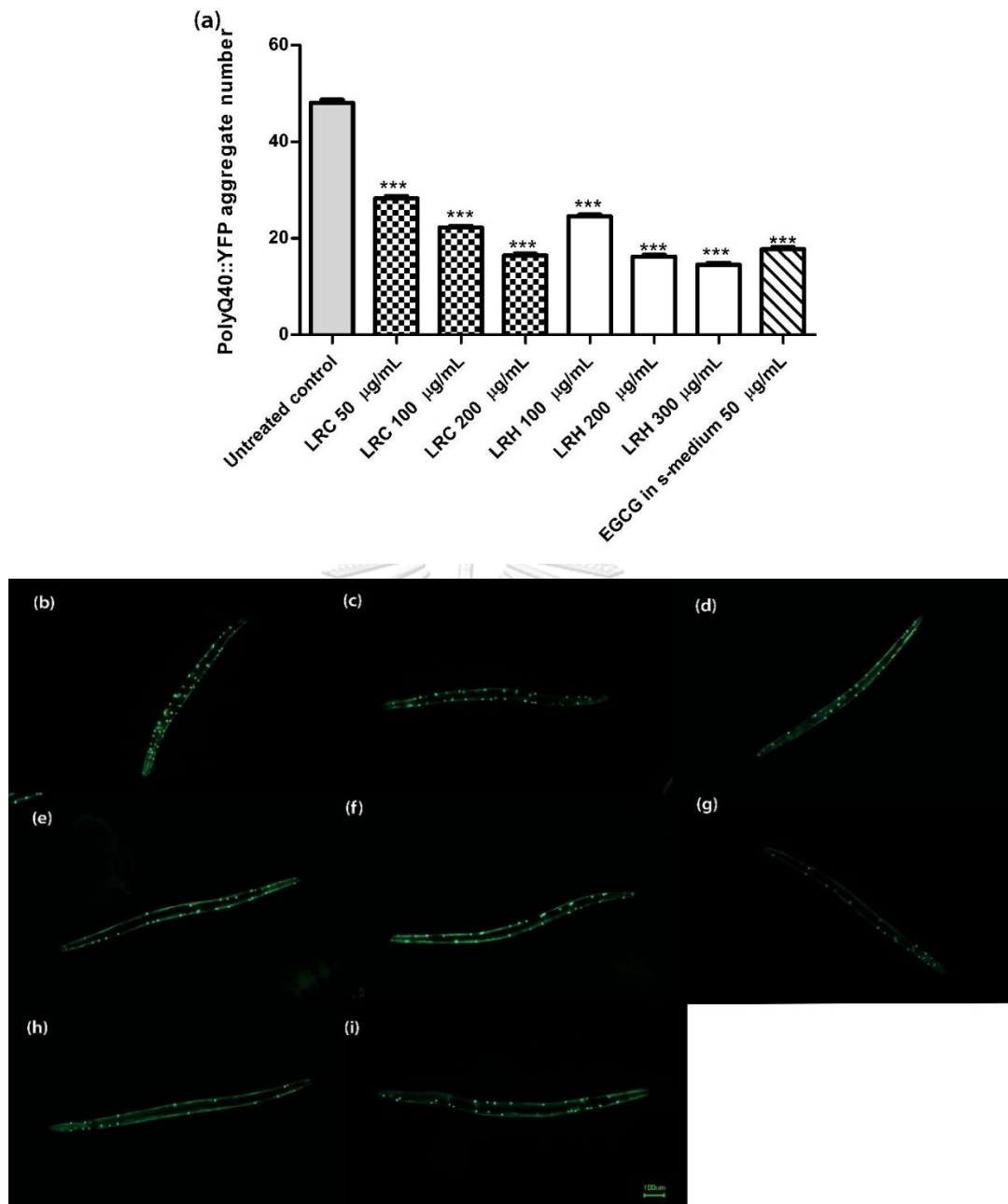


**Figure 51** The effect of different concentrations of LRC and LRH against PolyQ40 aggregation in *C. elegans*. The transgenic AM141 worms after treat with of different concentration of LRC and LRH significantly decrease in PolyQ40 formation (a). PolyQ40 formation under a fluorescence microscope of control worms (b); LRC at 50, 100, and 200 µg/mL treated worms (c-e); LRH at 100, 200, and 300 µg/mL treated worms (f-h); and 50 µg/mL of EGCG treated worms (i). Values are mean  $\pm$  SEM of at least 3 independent runs. \*\*\*  $p < 0.001$  vs. DMSO.



## CHAPTER V

### Discussion and Conclusion

Age-associated diseases such as neurodegenerative disorders including Alzheimer's disease (AD), Parkinson's disease (PD), and Huntington's Disease (HD) are related to increase in the intracellular reactive oxygen species (ROS) accumulation [131, 132]. Excessive ROS cause oxidative stress that leads to cellular or neuronal injury and neuronal apoptosis. Glutamate-induced oxidative stress is also one of the factors that play complex role in neurodegenerative diseases. Normally, glutamate, an excitatory neurotransmitter, has a positive impact on several brain and functions such as cognition, memory and learning [65]. However, excess glutamate leads to glutamate toxicity, and cause of neuronal apoptosis [19]. There are two pathways for glutamate toxicity including glutamate-receptor dependent pathway that involves in over activation of ionotropic (NMDA) receptor resulting in massive influx of calcium ions ( $\text{Ca}^{2+}$ ) and subsequent excessive ROS production leading to oxidative stress [66, 68]. The other pathway is glutamate receptor-independent pathway, often called oxidative glutamate toxicity or oxytosis. The ROS accumulation results from intracellular GSH depletion that contributes to oxidative stress, mitochondrial damage, and ultimately cell death [67]. However, different neuronal cell lines response differently to glutamate. Most of them express ionotropic glutamate receptor that is the greatest majority of neurodegenerative disorders but they also co-existing to CySS/glutamate antiporters and metabotropic glutamate receptors, supporting the assumption that excitotoxicity effect in these cells is accumulative [72]. Therefore, to study glutamate-induced oxidative stress resulting in neural injury, HT22 cells serves as appropriate model system in this study. Since, this immortalized cell line lacks of ionotropic glutamate receptor, toxicity in this model occurs mainly through oxytosis. Therefore, the endogenous enzymes including SOD, CAT and GPx play an important role in ROS detoxification. Recently, plants or natural products were widely studied because most of them contained phytochemical constituents

that involved in antioxidant activities which were safe and had low side effects [133-136]. *Lignosus rhinocerus* (LR) or Tiger Milk Mushroom, folk medicinal mushroom has been reported about several pharmacological effects. In this present study, we report, for the first time to our knowledge, the neuroprotective of LR extracts against glutamate-induced oxidative stress in HT22 cells. In this cell line we induced the oxidative stress by using 5 mM glutamate which has been reported to reduce approximately 50% of the cells [114, 137]. Interestingly, our finding found that only LRE prevented cells from undergoing apoptosis after cotreatment by using Annexin V/PI staining that interacts strongly and specifically with exposed phosphatidylserine (PS), the marker of apoptosis [138]. The protective effect of LRE correlated with increasing MMP, antioxidant gene expressions (CAT, SOD1, SOD2, and GPx) and decreasing intracellular ROS accumulation. Studied on the chemical constituents of LR have been shown that bioactive compounds from ethanol extracts performed better activities than aqueous extractions because ethanol extract contained high phenolic compounds and other lipids such as linoleic, oleic and palmitic acid which were volatile organics and acted as the antioxidants. Whereas, aqueous extracts contained high proportion of polysaccharides,  $\beta$ -glucan and water-soluble components [12, 43, 50, 139]. Some findings reported that aqueous extracts of LR showed the antioxidant properties *in vitro* including DPPH and ABTS scavenging assay and contained and total phenolic compounds [15, 40, 41]. However, several findings found that mushroom  $\beta$ -glucan from aqueous extract involved in modulating immune system, anti-inflammation, anti-cancer and antiviral activity [62-64]. Unlike  $\beta$ -glucan in mushroom,  $\beta$ -glucan in barley showed free radical scavenging property higher than in oats and yeast [140]. In addition,  $\beta$ -glucan in oats exert indirect antioxidant effect on immune cells [61]. Therefore, it could be possible that glucan in LRC and LRH unlikely to be the major component that was responsible for protection HT22 cells from glutamate-induced oxidative stress. Furthermore, according to our finding, the antioxidant system is important for the rescue of neuronal cells from oxidative stress not only through glutamate receptor-independent pathway but also glutamate receptor-dependent pathway [141, 142].

Therefore, LRE may exert neuroprotective effect on increasing endogenous antioxidant system through glutamate receptor pathway.

To further investigate a potential antioxidant activity of LRE, LRC and LRH *in vivo*, *C. elegans* was obtained as organism model and *E.coli* OP50 was supplied as a food source [22]. *C. elegans* was widely used as a model of anti-aging, antioxidant, and longevity because they shared high homology with mammalian and human genes and biochemical pathways [21, 134, 143]. A juglone, a yellow pigmented from *Juglans regia*, was one of the stressors and commonly used to generate ROS for inducing oxidative stress leading to increase intracellular ROS and [79, 144]. From the results, all the extracts exhibited the protective effect against juglone-induced oxidative stress resulting in enhancing the survival rate, reducing both intracellular ROS accumulation and HSP-16.2 expression that is widely used as a marker of oxidative stress because it was expressed under pernicious condition e.g. high temperature, presence of oxidant (juglone) [145, 146]

To investigate the underlying mechanism that involved in stress resistance and longevity, two major signaling pathways including DAF-16/FOXO signaling pathway and SKN-1/NRF-2 signaling pathway were observed in this study. Normally, insulin/IGF-1 signaling (IIS) pathway is a central regulator of DAF-16 activity. DAF-16 transcription factor in *C. elegans* homologue to mammalian Fork head box O (FOXO) transcription factor. Activation IIS causes phosphorylation of DAF-16 transcription factor that turns into inactive form and locates in cytosol. On the contrary, inactivation IIS by starvation or oxidative stress can activate DAF-16 transcription factor to translocate into nucleus by dephosphorylation [84, 85, 147]. The active form of DAF-16 regulates transcriptions of several antioxidant genes including superoxide dismutase-3 (SOD-3) and catalase-1 (CTL-1) [88, 148, 149]. The other pathway is SKN-1/Nrf2. The SKN-1 transcription factor is homologue to mammalian NRF-2 transcription factor. This transcription factor defends against oxidative stress by activating the conserved phase II detoxification enzymes including glutathione [89]. So, GST-4, an isoform of the glutathione S-transferases, is the key protein in this pathway.

In this current study, we monitored the increase in translocation of DAF-16 transcription factors into nucleus after treatment with all LR extracts. Furthermore, transcription factor paralleled with their target gene expression, SOD-3. On the other hand, the localization of SKN-1 was not affected. Similarly, all LR extracts were not affected the GST-4 expression. Therefore, the antioxidant effects of LRE, LRC and LRH exert their effect via activation of DAF-16/FOXO signaling pathway. In addition, there were several findings found that the phenolic compounds involved in antioxidant systems via DAF-16/FOXO pathway [8, 25, 27, 150-152], similar to oleic,  $\alpha$ -linolenic acid, palmitic acid, and benzoic acid [123, 153].

Increasing ROS accumulation and oxidative stress also correlated to lifespan and aging. We observed that LRE, LRC and LRH treatments extended the life span *C. elegans*. Therefore, these results suggest that lifespan prolongation resulted from activation of DAF-16/FOXO pathway and subsequent decrease ROS accumulation and increase SOD-3 expression. This longevity could exclude from dietary restriction (DR) due to no impact on body length and the number of progenies, similar to polyphenol effect from other findings [27, 150, 154].

Similarly, aging process also correlated to ROS and oxidative stress, we observed the two biomarkers of aging including lipofuscin which is an autofluorescent pigment, located in intestinal cells during overage. Lipofuscin accumulation is related to aging [92, 155]. The other is pharyngeal pumping rate. Normally, aging causes pharyngeal muscle decline through time resulting in slow in pharyngeal pumping rate [155-157]. We found that LRE, LRC and LRH treatment exhibited anti-aging effect by reducing lipofuscin accumulation. Whereas, high dose of LRE, LRC and LRH improve the pharyngeal pumping rate. The results are similar to antioxidant (polyphenolic) compound reduce aging [158, 159]. However, this technique used manual counting that caused an error counting easily. The precision count prefers to counting machine.

Furthermore, LRE exerted the neuroprotective effect against A $\beta$ -induced deficit in chemotaxis behavior in *C. elegans* leading to increasing in CI of CL 2355 transgenic strains, contained human A $\beta$  peptide that is also known as a hallmark of

AD [160]. Olfactory dysfunction is early biomarker or preclinical symptoms observed in AD [161]. Similarly, LRE also showed decrease in polyQ40 aggregation that is related to the neurodegenerative diseases including Huntington's disease and other polyglutamine diseases [162]. The aggregation of these protein is induced by oxidative stress resulting in oxidation of proteins and related to pathogenesis of this disease [163]. Our finding correlated to several studies previously about phenolic compounds that have been found in plants or natural products and reported their effectiveness to prevent many diseases including neurodegenerative diseases [25, 52, 114, 137, 150, 151, 164-171].

Although LRC and LRH had no effect on HT22 cells, they exhibited the protective effect on *C. elegans*. As mentioned before, the aqueous components of LR extracts were reported that they rich in high molecular weight polysaccharides including glucans. Especially,  $\beta$ -glucan was found the effect of improved lifespan in *C. elegans* via DAF-16 as well as phenolic compounds [172]. However, *C. elegans* was a whole organism, it is possible to hypothesize that LRC and LRH may indirectly involve in *C. elegans*' microbiome (bacteria, fungi, and viruses) that plays a complex roles in *C. elegans* development, metabolism, immunity and lifespan [103, 104]. However, the limitation of *C. elegans* model is that the biological effects in *C. elegans* are still far from mammals or human. Some molecular pathways do not exist in the worms. Therefore, the other animal models such as murine model are required to study.

In conclusion, *Lignosus rhinocerus* (LR) extracts exhibited antioxidant and anti-aging properties via DAF-16/FoxO signaling pathway leading to increase in stress resistance; decrease in intracellular ROS accumulation; and lifespan extension in *C. elegans*. In addition, they also had the neuroprotective effect against neurotoxicity in *C. elegans*. However, only LRE showed the neuroprotective effect in hippocampal neuronal cells which is mediated via inhibition of intracellular ROS accumulation and increase in both MMP and expression of antioxidant genes. Therefore, our finding suggested that LRE may be a new candidate for prevention of neurodegeneration. However, further studies of identify the bioactive components and exact mechanism

of LR extracts are required to support their ability in order to development of neuroprotective supplement in the future.



## REFERENCES



จุฬาลงกรณ์มหาวิทยาลัย  
**CHULALONGKORN UNIVERSITY**

1. Kitada M, Kume S, Takeda-Watanabe A, Kanasaki K, Koya D. Sirtuins and renal diseases: relationship with aging and diabetic nephropathy. *Clin Sci (Lond)*. 2013;124(3):153-64.
2. de Magalhaes JP. How ageing processes influence cancer. *Nat Rev Cancer*. 2013;13(5):357-65.
3. Falandry C, Bonnefoy M, Freyer G, Gilson E. Biology of cancer and aging: a complex association with cellular senescence. *J Clin Oncol*. 2014;32(24):2604-10.
4. Jove M, Portero-Otin M, Naudi A, Ferrer I, Pamplona R. Metabolomics of human brain aging and age-related neurodegenerative diseases. *J Neuropathol Exp Neurol*. 2014;73(7):640-57.
5. Budni J, Bellettini-Santos T, Mina F, Garcez ML, Zugno AI. The involvement of BDNF, NGF and GDNF in aging and Alzheimer's disease. *Aging Dis*. 2015;6(5):331-41.
6. Duthey B. Priority Medicines for Europe and the World "A Public Health Approach to Innovation" 2013 [Available from: [http://www.who.int/medicines/areas/priority\\_medicines/BP6\\_11Alzheimer.pdf](http://www.who.int/medicines/areas/priority_medicines/BP6_11Alzheimer.pdf).
7. Harman D. The free radical theory of aging. *Antioxidants and Redox Signaling*. 2003;5(5):557-61.
8. Larsen PL. Aging and resistance to oxidative damage in *Caenorhabditis elegans*. *Proceedings of the National Academy of Sciences*. 1993;90(19):8905-9.
9. Lushchak VI. Free radicals, reactive oxygen species, oxidative stress and its classification. *Chemico-Biological Interactions*. 2014;224:164-75.
10. Cui H, Kong Y, Zhang H. Oxidative Stress, Mitochondrial Dysfunction, and Aging. *Journal of Signal Transduction*. 2012;2012:646354.
11. Matés JM, Pérez-Gómez C, De Castro IN. Antioxidant enzymes and human diseases. *Clinical biochemistry*. 1999;32(8):595-603.



12. Phan C-W, David P, Sabaratnam V. Edible and medicinal mushrooms: emerging brain food for the mitigation of neurodegenerative diseases. *Journal of medicinal food*. 2017;20(1):1-10.
13. Phan C-W, David P, Naidu M, Wong K-H, Sabaratnam V. Therapeutic potential of culinary-medicinal mushrooms for the management of neurodegenerative diseases: diversity, metabolite, and mechanism. *Critical reviews in biotechnology*. 2015;35(3):355-68.
14. Johnathan M, Gan SH, Ezumi MFW, Faezahtul AH, Nurul AA. Phytochemical profiles and inhibitory effects of Tiger Milk mushroom (*Lignosus rhinocerus*) extract on ovalbumin-induced airway inflammation in a rodent model of asthma. *BMC Complement Altern Med*. 2016;16:167-.
15. Nallathamby N, Phan C-W, Seow SL-S, Baskaran A, Lakshmanan H, Abd Malek SN, et al. A Status Review of the Bioactive Activities of Tiger Milk Mushroom *Lignosus rhinocerotis* (Cooke) Ryvardeen. *Frontiers in pharmacology*. 2017;8:998.
16. Lau BF, Abdullah N, Aminudin N, Lee HB, Tan PJ. Ethnomedicinal uses, pharmacological activities, and cultivation of *Lignosus* spp.(tiger' s milk mushrooms) in Malaysia–A review. *Journal of ethnopharmacology*. 2015;169:441-58.
17. Jamil NAM, Rashid NMN, Hamid MHA, Rahmad N, Al-Obaidi JR. Comparative nutritional and mycochemical contents, biological activities and LC/MS screening of tuber from new recipe cultivation technique with wild type tuber of tiger's milk mushroom of species *Lignosus rhinocerus*. *World Journal of Microbiology and Biotechnology*. 2017;34(1):1.
18. Sillapachaiyaporn C, Chuchawankul S. HIV-1 protease and reverse transcriptase inhibition by tiger milk mushroom (*Lignosus rhinocerus*) sclerotium extracts: In vitro and in silico studies. *Journal of Traditional and Complementary Medicine*. 2020;10(4):396-404.

19. Noh HS, Hah YS, Nilufar R, Han J, Bong JH, Kang SS, et al. Acetoacetate protects neuronal cells from oxidative glutamate toxicity. *Journal of neuroscience research*. 2006;83(4):702-9.
20. Hunt PR. The *C. elegans* model in toxicity testing. *J Appl Toxicol*. 2017;37(1):50-9.
21. Ayuda-Durán B, González-Manzano S, González-Paramás AM, Santos-Buelga C. *Caenorhabditis elegans* as a Model Organism to Evaluate the Antioxidant Effects of Phytochemicals. *Molecules*. 2020;25(14):3194.
22. Brenner S. The genetics of *Caenorhabditis elegans*. *Genetics*. 1974;77(1):71-94.
23. Keum Y-S. Regulation of Nrf2-Mediated Phase II Detoxification and Anti-oxidant Genes. *Biomolecules & Therapeutics*. 2012;20(2):144-51.
24. Guha S, Cao M, Kane RM, Savino AM, Zou S, Dong Y. The longevity effect of cranberry extract in *Caenorhabditis elegans* is modulated by *daf-16* and *osr-1*. *Age (Dordr)*. 2013;35(5):1559-74.
25. Abbas S, Wink M. Green Tea Extract Induces the Resistance of *Caenorhabditis elegans* against Oxidative Stress. *Antioxidants*. 2014;3(1):129-43.
26. Wang X, Zhang J, Lu L, Zhou L. The longevity effect of echinacoside in *Caenorhabditis elegans* mediated through *daf-16*. *Bioscience, biotechnology, and biochemistry*. 2015;79(10):1676-83.
27. Duangjan C, Rangsinth P, Gu X, Wink M, Tencomnao T. Lifespan Extending and Oxidative Stress Resistance Properties of a Leaf Extracts from *Anacardium occidentale* L. in *Caenorhabditis elegans*. *Oxid Med Cell Longev*. 2019;2019:9012396-.
28. Duangjan C, Rangsinth P, Gu X, Zhang S, Wink M, Tencomnao T. *Glochidion zeylanicum* leaf extracts exhibit lifespan extending and oxidative stress resistance properties in *Caenorhabditis elegans* via DAF-16/FoxO and SKN-1/Nrf-2 signaling pathways. *Phytomedicine : international journal of phytotherapy and phytopharmacology*. 2019;64:153061.

29. Poljsak B, Milisav I. Aging, oxidative stress and antioxidants. *Oxidative Stress and Chronic Degenerative Diseases-A Role for Antioxidants: InTech*; 2013.
30. Evans MD, Dizdaroglu M, Cooke MS. Oxidative DNA damage and disease: induction, repair and significance. *Mutation Research/Reviews in Mutation Research*. 2004;567(1):1-61.
31. Mariani E, Polidori MC, Cherubini A, Mecocci P. Oxidative stress in brain aging, neurodegenerative and vascular diseases: An overview. *Journal of Chromatography B*. 2005;827(1):65-75.
32. Kim GH, Kim JE, Rhie SJ, Yoon S. The Role of Oxidative Stress in Neurodegenerative Diseases. *Experimental Neurobiology*. 2015;24(4):325-40.
33. Varadarajan S, Yatin S, Aksenova M, Butterfield DA. Review: Alzheimer's Amyloid  $\beta$ -Peptide-Associated Free Radical Oxidative Stress and Neurotoxicity. *Journal of Structural Biology*. 2000;130(2):184-208.
34. Peng C, Wang X, Chen J, Jiao R, Wang L, Li YM, et al. Biology of ageing and role of dietary antioxidants. *BioMed research international*. 2014;2014.
35. Shull S, Heintz N, Periasamy M, Manohar M, Janssen Y, Marsh J, et al. Differential regulation of antioxidant enzymes in response to oxidants. *Journal of Biological Chemistry*. 1991;266(36):24398-403.
36. Weinberg RB, VanderWerken BS, Anderson RA, Stegner JE, Thomas MJ. Pro-oxidant effect of vitamin E in cigarette smokers consuming a high polyunsaturated fat diet. *Arteriosclerosis, thrombosis, and vascular biology*. 2001;21(6):1029-33.
37. Balsano C, Alisi A. Antioxidant effects of natural bioactive compounds. *Current pharmaceutical design*. 2009;15(26):3063-73.
38. Basli A, Soulet S, Chaheer N, Méridon J-M, Chibane M, Monti J-P, et al. Wine polyphenols: potential agents in neuroprotection. *Oxid Med Cell Longev*. 2012;2012.
39. Ma Q. Role of Nrf2 in Oxidative Stress and Toxicity. *Annual review of pharmacology and toxicology*. 2013;53:401-26.

40. Yap YH, Tan N, Fung S, Aziz AA, Tan C, Ng S. Nutrient composition, antioxidant properties, and anti-proliferative activity of *Lignosus rhinocerus* Cooke sclerotium. *Journal of the Science of Food and Agriculture*. 2013;93(12):2945-52.
41. Yap H-YY, Chooi Y-H, Firdaus-Raih M, Fung S-Y, Ng S-T, Tan C-S, et al. The genome of the Tiger Milk mushroom, *Lignosus rhinocerotis*, provides insights into the genetic basis of its medicinal properties. *BMC genomics*. 2014;15(1):635.
42. CFR Ferreira I, A Vaz J, Vasconcelos MH, Martins A. Compounds from wild mushrooms with antitumor potential. *Anti-Cancer Agents in Medicinal Chemistry (Formerly Current Medicinal Chemistry-Anti-Cancer Agents)*. 2010;10(5):424-36.
43. Johnathan M, Aa N, Mohd Fuad WE, Gan S. Gas chromatography mass spectrometry analysis of volatile compounds from *Lignosus rhinocerus* (Tiger milk mushroom). *Research Journal of Pharmaceutical, Biological and Chemical Sciences*. 2016;7:5-16.
44. Johnathan M, Gan S, Ezumi MW, Faezahtul A, Nurul A. Phytochemical profiles and inhibitory effects of Tiger Milk mushroom (*Lignosus rhinocerus*) extract on ovalbumin-induced airway inflammation in a rodent model of asthma. *BMC Complement Altern Med*. 2016;16(1):167.
45. Kho TT. Fibrinolytic activities of a medicinal mushroom: *Lignosus rhinocerotis* (Cooke) ryvardeen/Kho Tieng Tieng: University of Malaya; 2014.
46. Lee SS, Tan NH, Fung SY, Sim SM, Tan CS, Ng ST. Anti-inflammatory effect of the sclerotium of *Lignosus rhinocerotis* (Cooke) Ryvardeen, the Tiger Milk mushroom. *BMC Complement Altern Med*. 2014;14(1):359.
47. Lee M, Tan N, Fung S, Tan C, Ng S. The antiproliferative activity of sclerotia of *Lignosus rhinocerus* (Tiger Milk Mushroom). *Evidence-based complementary and alternative medicine*. 2012;2012.

48. Baskaran A. Suppression of lipopolysaccharide and hydrogen peroxide-induced inflammatory responses in raw 264.7 macrophage by *pleurotus giganteus* and *lignosus rhinocerotis*/Asweni a/p Baskaran: University of Malaya; 2015.
49. Mohanarji S, Dharmalingam S, Kalusalingam A. Screening of *Lignosus rhinocerus* extracts as antimicrobial agents against selected human pathogens. *J Pharm Biomed Sci.* 2012;18(11):1-4.
50. Hoe T-L. *Lignosus rhinocerus* attenuated high fat diet induced non-alcoholic fatty liver. 2014.
51. Nallathamby N, Serm LG, Raman J, Abd Malek N, Vidyadaran S, Naidu M, et al. Identification and in vitro Evaluation of Lipids from Sclerotia of *Lignosus rhinocerotis* for Antioxidant and Anti-neuroinflammatory Activities. *NATURAL PRODUCT COMMUNICATIONS.* 2016;11(10):1485-90.
52. Khan A, Adil G, Masoodi F, Shaheen K, Mudasir A, editors. Antioxidant and functional properties of  $\beta$ -glucan extracted from edible mushrooms *Agaricus bisporus*, *Pleurotus ostreatus* and *Coprinus atramentarius*. Proceedings of 8th International Conference on Mushroom Biology and Mushroom Products (ICMBMP8), New Delhi, India, 19-22 November 2014 Volume I & II; 2014: ICAR-Directorate of Mushroom Research. จุฬาลงกรณ์มหาวิทยาลัย
53. Suziana Zaila C, Farida Zuraina M, Norfazlina M, Lek Mun L, Nurshahirah N, Florinsiah L, et al., editors. Antiproliferative effect of *Lignosus rhinocerotis*, the Tiger Milk Mushroom on HCT 116 human colorectal cancer cells. *The Open Conference Proceedings Journal*; 2013. CHULALONGKORN UNIVERSITY
54. Lai CK, Wong K-H, Cheung PCK. Antiproliferative effects of sclerotial polysaccharides from *Polyporus rhinocerus* Cooke (Aphyllphoromycetidae) on different kinds of leukemic cells. *International Journal of Medicinal Mushrooms.* 2008;10(3).

55. Lau BF, Abdullah N, Aminudin N, Lee HB. Chemical composition and cellular toxicity of ethnobotanical-based hot and cold aqueous preparations of the tiger's milk mushroom (*Lignosus rhinocerotis*). *Journal of ethnopharmacology*. 2013;150(1):252-62.
56. Kavithambigai E, Vikineswary S, Thayan R, editors. Antiviral activity and mode of action of mushroom extracts against dengue virus type-2. 3rd international conference on dengue and dengue haemorrhagic fever, Bangkok, Thailand; 2013.
57. Eik L-F, Naidu M, David P, Wong K-H, Tan Y-S, Sabaratnam V. *Lignosus rhinocerus* (Cooke) Ryarden: A medicinal mushroom that stimulates neurite outgrowth in PC-12 cells. *Evidence-Based Complementary and Alternative Medicine*. 2012;2012.
58. Phan C-W, David P, Naidu M, Wong K-H, Sabaratnam V. Neurite outgrowth stimulatory effects of culinary-medicinal mushrooms and their toxicity assessment using differentiating Neuro-2a and embryonic fibroblast BALB/3T3. *BMC Complement Altern Med*. 2013;13(1):261.
59. Dong Q, Wang Y, Shi L, Yao J, Li J, Ma F, et al. A novel water-soluble  $\beta$ -D-glucan isolated from the spores of *Ganoderma lucidum*. *Carbohydrate research*. 2012;353:100-5.
60. Du B, Bian Z, Xu B. Skin health promotion effects of natural beta-glucan derived from cereals and microorganisms: a review. *Phytotherapy research : PTR*. 2014;28(2):159-66.
61. Kopiasz Ł, Dziendzikowska K, Gajewska M, Wilczak J, Harasym J, Żyła E, et al. Time-Dependent Indirect Antioxidative Effects of Oat Beta-Glucans on Peripheral Blood Parameters in the Animal Model of Colon Inflammation. *Antioxidants*. 2020;9(5):375.
62. Murphy EA, Davis JM, Carmichael MD. Immune modulating effects of  $\beta$ -glucan. *Current opinion in clinical nutrition and metabolic care*. 2010;13(6):656-61.

63. Wong K-H, Lai C, Cheung P. Immunomodulatory activities of mushroom sclerotial polysaccharides. *Food hydrocolloids*. 2011;25(2):150-8.
64. Zhu F, Du B, Bian Z, Xu B. Beta-glucans from edible and medicinal mushrooms: Characteristics, physicochemical and biological activities. *Journal of Food Composition and Analysis*. 2015;41:165-73.
65. Meldrum BS. Glutamate as a neurotransmitter in the brain: review of physiology and pathology. *The Journal of nutrition*. 2000;130(4S Suppl):1007s-15s.
66. Choi DW. Glutamate neurotoxicity and diseases of the nervous system. *Neuron*. 1988;1(8):623-34.
67. Tan S, Sagara Y, Liu Y, Maher P, Schubert D. The regulation of reactive oxygen species production during programmed cell death. *The Journal of cell biology*. 1998;141(6):1423-32.
68. Wang Y, Qin ZH. Molecular and cellular mechanisms of excitotoxic neuronal death. *Apoptosis : an international journal on programmed cell death*. 2010;15(11):1382-402.
69. Schubert D, Kimura H, Maher P. Growth factors and vitamin E modify neuronal glutamate toxicity. *Proceedings of the National Academy of Sciences*. 1992;89(17):8264-7.
70. Nicholls DG, Budd SL. Neuronal excitotoxicity: the role of mitochondria. *Biofactors*. 1998;8(3-4):287-99.
71. Fukui M, Song JH, Choi J, Choi HJ, Zhu BT. Mechanism of glutamate-induced neurotoxicity in HT22 mouse hippocampal cells. *Eur J Pharmacol*. 2009;617(1-3):1-11.
72. Kritis AA, Stamoula EG, Paniskaki KA, Vavilis TD. Researching glutamate-induced cytotoxicity in different cell lines: a comparative/collective analysis/study. *Frontiers in cellular neuroscience*. 2015;9:91.
73. Zhang Y, Bhavnani BR. Glutamate-induced apoptosis in neuronal cells is mediated via caspase-dependent and independent mechanisms involving calpain and caspase-

- 3 proteases as well as apoptosis inducing factor (AIF) and this process is inhibited by equine estrogens. *BMC neuroscience*. 2006;7(1):49.
74. Tobaben S, Grohm J, Seiler A, Conrad M, Plesnila N, Culmsee C. Bid-mediated mitochondrial damage is a key mechanism in glutamate-induced oxidative stress and AIF-dependent cell death in immortalized HT-22 hippocampal neurons. *Cell death and differentiation*. 2011;18(2):282.
75. Prasansuklab A, Brimson JM, Tencomnao T. Potential Thai medicinal plants for neurodegenerative diseases: A review focusing on the anti-glutamate toxicity effect. *Journal of Traditional and Complementary Medicine*. 2020;10(3):301-8.
76. Braeckman BP, Houthoofd K, Vanfleteren JR. Insulin-like signaling, metabolism, stress resistance and aging in *Caenorhabditis elegans*. *Mech Ageing Dev*. 2001;122(7):673-93.
77. Herndon LA. INTRODUCTION TO *C. elegans* ANATOMY 2012 [updated April 24, 2012. Available from:  
<http://www.wormatlas.org/hermaphrodite/introduction/mainframe.htm>.
78. Tatar M, Bartke A, Antebi A. The endocrine regulation of aging by insulin-like signals. *Science*. 2003;299(5611):1346-51.
79. Larsen PL. Aging and resistance to oxidative damage in *Caenorhabditis elegans*. *Proceedings of the National Academy of Sciences of the United States of America*. 1993;90(19):8905-9.
80. Scott BA, Avidan MS, Crowder CM. Regulation of hypoxic death in *C. elegans* by the insulin/IGF receptor homolog DAF-2. *Science (New York, NY)*. 2002;296(5577):2388-91.
81. Lithgow GJ, White TM, Hinerfeld DA, Johnson TE. Thermotolerance of a long-lived mutant of *Caenorhabditis elegans*. *Journal of gerontology*. 1994;49(6):B270-6.
82. Murakami S, Johnson TE. A genetic pathway conferring life extension and resistance to UV stress in *Caenorhabditis elegans*. *Genetics*. 1996;143(3):1207-18.



83. Baryte D, Lovejoy DA, Lithgow GJ. Longevity and heavy metal resistance in daf-2 and age-1 long-lived mutants of *Caenorhabditis elegans*. *FASEB journal : official publication of the Federation of American Societies for Experimental Biology*. 2001;15(3):627-34.
84. Murphy CT, McCarroll SA, Bargmann CI, Fraser A, Kamath RS, Ahringer J, et al. Genes that act downstream of DAF-16 to influence the lifespan of *Caenorhabditis elegans*. *Nature*. 2003;424(6946):277-83.
85. Koch K, Havermann S, Büchter C, Wätjen W. *Caenorhabditis elegans* as Model System in Pharmacology and Toxicology: Effects of Flavonoids on Redox-Sensitive Signalling Pathways and Ageing. *TheScientificWorldJournal*. 2014;2014:920398.
86. Hodgkin J Introduction to genetics and genomics (September 6, 2005), WormBook, ed. The *C. elegans* Research Community, WormBook, doi/10.1895/wormbook.1.17.1, <http://www.wormbook.org>
87. Landis JN, Murphy CT. Integration of diverse inputs in the regulation of *C. elegans* DAF-16/FOXO. *Developmental dynamics : an official publication of the American Association of Anatomists*. 2010;239(5):10.1002/dvdy.22244.
88. Baumeister R, Schaffitzel E, Hertweck M. Endocrine signaling in *Caenorhabditis elegans* controls stress response and longevity. *The Journal of endocrinology*. 2006;190(2):191-202.
89. An JH, Blackwell TK. SKN-1 links *C. elegans* mesendodermal specification to a conserved oxidative stress response. *Genes & development*. 2003;17(15):1882-93.
90. Blackwell TK, Steinbaugh MJ, Hourihan JM, Ewald CY, Isik M. SKN-1/Nrf, stress responses, and aging in *Caenorhabditis elegans*. *Free radical biology & medicine*. 2015;88(Pt B):290-301.
91. Son HG, Altintas O, Kim EJE, Kwon S, Lee S-JV. Age-dependent changes and biomarkers of aging in *Caenorhabditis elegans*. *Aging Cell*. 2019;18(2):e12853-e.

92. Papaevgeniou N, Hoehn A, Grune T, Chondrogianni N. P 090 - Lipofuscin effects in *Caenorhabditis elegans* ageing model. *Free Radical Biology and Medicine*. 2017;108:S48.
93. Huang C, Xiong C, Kornfeld K. Measurements of age-related changes of physiological processes that predict lifespan of *Caenorhabditis elegans*. *Proc Natl Acad Sci U S A*. 2004;101(21):8084-9.
94. Avila D, Helmcke K, Aschner M. The *Caenorhabditis elegans* model as a reliable tool in neurotoxicology. *Hum Exp Toxicol*. 2012;31(3):236-43.
95. Chen BL, Hall DH, Chklovskii DB. Wiring optimization can relate neuronal structure and function. *Proceedings of the National Academy of Sciences*. 2006;103(12):4723-8.
96. Cole RD, Anderson GL, Williams PL. The nematode *Caenorhabditis elegans* as a model of organophosphate-induced mammalian neurotoxicity. *Toxicology and Applied Pharmacology*. 2004;194(3):248-56.
97. McVey K, Mink J, Snapp I, Timberlake W, Todt C, Negga R, et al. *Caenorhabditis elegans*: an emerging model system for pesticide neurotoxicity. *J Environment Analytic Toxicol S*. 2012;4:2161-0525.
98. Leung MC, Williams PL, Benedetto A, Au C, Helmcke KJ, Aschner M, et al. *Caenorhabditis elegans*: an emerging model in biomedical and environmental toxicology. *Toxicological sciences*. 2008;106(1):5-28.
99. Harlow PH, Perry SJ, Widdison S, Daniels S, Bondo E, Lamberth C, et al. The nematode *Caenorhabditis elegans* as a tool to predict chemical activity on mammalian development and identify mechanisms influencing toxicological outcome. *Scientific reports*. 2016;6:22965.
100. Sekirov I, Russell SL, Antunes LC, Finlay BB. Gut microbiota in health and disease. *Physiological reviews*. 2010;90(3):859-904.
101. Shapira M. Host-microbiota interactions in *Caenorhabditis elegans* and their significance. *Current Opinion in Microbiology*. 2017;38:142-7.

102. Douglas AE. Simple animal models for microbiome research. *Nature reviews Microbiology*. 2019;17(12):764-75.
103. Zhang F, Berg M, Dierking K, Félix M-A, Shapira M, Samuel BS, et al. *Caenorhabditis elegans* as a Model for Microbiome Research. *Front Microbiol*. 2017;8:485-.
104. Dirksen P, Assié A, Zimmermann J, Zhang F, Tietje A-M, Marsh SA, et al. CeMbio - The <em>C. elegans</em> microbiome resource. *bioRxiv*. 2020:2020.04.22.055426.
105. Montalvo-Katz S, Huang H, Appel MD, Berg M, Shapira M. Association with soil bacteria enhances p38-dependent infection resistance in *Caenorhabditis elegans*. *Infection and immunity*. 2013;81(2):514-20.
106. Dirksen P, Marsh SA, Braker I, Heitland N, Wagner S, Nakad R, et al. The native microbiome of the nematode *Caenorhabditis elegans*: gateway to a new host-microbiome model. *BMC biology*. 2016;14(1):38.
107. Govindan JA, Jayamani E, Zhang X, Mylonakis E, Ruvkun G. Dialogue between *E. coli* free radical pathways and the mitochondria of *C. elegans*. *Proc Natl Acad Sci U S A*. 2015;112(40):12456-61.
108. Gusarov I, Gautier L, Smolentseva O, Shamovsky I, Eremina S, Mironov A, et al. Bacterial nitric oxide extends the lifespan of *C. elegans*. *Cell*. 2013;152(4):818-30.
109. Gerbaba TK, Green-Harrison L, Buret AG. Modeling Host-Microbiome Interactions in *Caenorhabditis elegans*. *J Nematol*. 2017;49(4):348-56.
110. Zhang J, Holdorf AD, Walhout AJ. *C. elegans* and its bacterial diet as a model for systems-level understanding of host-microbiota interactions. *Curr Opin Biotechnol*. 2017;46:74-80.
111. Prior RL, Wu X, Schaich K. Standardized methods for the determination of antioxidant capacity and phenolics in foods and dietary supplements. *Journal of agricultural and food chemistry*. 2005;53(10):4290-302.

112. Boligon AA, Machado MM, Athayde ML. Technical evaluation of antioxidant activity. *Med chem.* 2014;4(7):517-22.
113. Amorim E, Nascimento J, Monteiro J, Sobrinho T, Araujo T, Albuquerque U. A Simple and Accurate Procedure for the Determination of Tannin and Flavonoid Levels and Some Applications in Ethnobotany and Ethnopharmacology. *Functional Ecosystems and Communities.* 2008;2:88-94.
114. Sukprasansap M, Chanvorachote P, Tencomnao T. Cyanidin-3-glucoside activates Nrf2-antioxidant response element and protects against glutamate-induced oxidative and endoplasmic reticulum stress in HT22 hippocampal neuronal cells. *BMC Complement Med Ther.* 2020;20(1):46-.
115. Wu Y, Wu Z, Butko P, Christen Y, Lambert MP, Klein WL, et al. Amyloid-beta-induced pathological behaviors are suppressed by Ginkgo biloba extract EGb 761 and ginkgolides in transgenic *Caenorhabditis elegans*. *The Journal of neuroscience : the official journal of the Society for Neuroscience.* 2006;26(50):13102-13.
116. Choi D, Kang W, Park T. Anti-Allergic and Anti-Inflammatory Effects of Undecane on Mast Cells and Keratinocytes. *Molecules.* 2020;25(7).
117. Souza CF, Baldissera MD, Silva LdL, Geihs MA, Baldisserotto B. Is monoterpene terpinen-4-ol the compound responsible for the anesthetic and antioxidant activity of *Melaleuca alternifolia* essential oil (tea tree oil) in silver catfish? *Aquaculture.* 2018;486:217-23.
118. Foti MC. Antioxidant properties of phenols. *The Journal of pharmacy and pharmacology.* 2007;59(12):1673-85.
119. Zheng J-R, Ren S-X, Ren N, Zhang J-J, Zhang D-H, Wang S-P. Synthesis, thermodynamic properties and antibacterial activities of lanthanide complexes with 3,5-dimethoxybenzoic acid and 1,10-phenanthroline. *Thermochimica Acta.* 2013;572:101-6.

120. Farag AK, Hassan AHE, Ahn BS, Park KD, Roh EJ. Reprofile of pyrimidine-based DAPK1/CSF1R dual inhibitors: identification of 2,5-diamino-4-pyrimidinol derivatives as novel potential anticancer lead compounds. *Journal of enzyme inhibition and medicinal chemistry*. 2020;35(1):311-24.
121. Agoramoorthy G, Chandrasekaran M, Venkatesalu V, Hsu M. Antibacterial and antifungal activities of fatty acid methyl esters of the blind-your-eye mangrove from India. *Brazilian Journal of Microbiology*. 2007;38:739-42.
122. Kim BR, Kim HM, Jin CH, Kang SY, Kim JB, Jeon YG, et al. Composition and Antioxidant Activities of Volatile Organic Compounds in Radiation-Bred *Coreopsis* Cultivars. *Plants (Basel, Switzerland)*. 2020;9(6).
123. Wei CC, Yen PL, Chang ST, Cheng PL, Lo YC, Liao VH. Antioxidative Activities of Both Oleic Acid and *Camellia tenuifolia* Seed Oil Are Regulated by the Transcription Factor DAF-16/FOXO in *Caenorhabditis elegans*. *PloS one*. 2016;11(6):e0157195.
124. Pinto MEA, Araújo SG, Morais MI, Sá NP, Lima CM, Rosa CA, et al. Antifungal and antioxidant activity of fatty acid methyl esters from vegetable oils. *An Acad Bras Cienc*. 2017;89(3):1671-81.
125. Kalpana D, R S, Mohan V. GC-MS analysis of ethanol extract of *Entada pursaetha* DC seed. *Bioscience Discovery*. 2012;3:30-3.
126. Elagbar ZA, Naik RR, Shakya AK, Bardaweel SK. Fatty Acids Analysis, Antioxidant and Biological Activity of Fixed Oil of *Annona muricata* L. Seeds. *Journal of Chemistry*. 2016;2016:6948098.
127. Rahman MM, Ahmad SH, Mohamed MTM, Ab Rahman MZ. Antimicrobial Compounds from Leaf Extracts of *Jatropha curcas*, *Psidium guajava*, and *Andrographis paniculata*. *The Scientific World Journal*. 2014;2014:635240.
128. mensah-agyei G, Kolawole I, Cajethan. GC-MS analysis of bioactive compounds and evaluation of antimicrobial activity of the extracts of *Daedalea elegans*: A Nigerian mushroom. *African Journal of Microbiology Research*. 2020;14:204-10.

129. Alcazar-Fuoli L, Mellado E. Ergosterol biosynthesis in *Aspergillus fumigatus*: its relevance as an antifungal target and role in antifungal drug resistance. *Front Microbiol.* 2013;3(439).
130. Rodrigues ML. The Multifunctional Fungal Ergosterol. *mBio.* 2018;9(5):e01755-18.
131. Jodeiri Farshbaf M, Ghaedi K. Huntington's Disease and Mitochondria. *Neurotoxicity research.* 2017;32(3):518-29.
132. Liu Z, Ren Z, Zhang J, Chuang CC, Kandaswamy E, Zhou T, et al. Role of ROS and Nutritional Antioxidants in Human Diseases. *Frontiers in physiology.* 2018;9:477.
133. Rao PV, Sujana P, Vijayakanth T, Naidu MD. *Rhinacanthus nasutus* – Its protective role in oxidative stress and antioxidant status in streptozotocin induced diabetic rats. *Asian Pacific Journal of Tropical Disease.* 2012;2(4):327-30.
134. Desjardins D, Cacho-Valadez B, Liu J-L, Wang Y, Yee C, Bernard K, et al. Antioxidants reveal an inverted U-shaped dose-response relationship between reactive oxygen species levels and the rate of aging in *Caenorhabditis elegans*. *Aging Cell.* 2017;16(1):104-12.
135. Han Y, Song S, Wu H, Zhang J, Ma E. Antioxidant enzymes and their role in phoxim and carbaryl stress in *Caenorhabditis elegans*. *Pesticide biochemistry and physiology.* 2017;138:43-50.
136. Xu DP, Li Y, Meng X, Zhou T, Zhou Y, Zheng J, et al. Natural Antioxidants in Foods and Medicinal Plants: Extraction, Assessment and Resources. *Int J Mol Sci.* 2017;18(1).
137. Prasansuklab A, Meemon K, Sobhon P, Tencomnao T. Ethanolic extract of *Streblus asper* leaves protects against glutamate-induced toxicity in HT22 hippocampal neuronal cells and extends lifespan of *Caenorhabditis elegans*. *BMC Complement Altern Med.* 2017;17(1):551.

138. Crowley LC, Marfell BJ, Scott AP, Waterhouse NJ. Quantitation of Apoptosis and Necrosis by Annexin V Binding, Propidium Iodide Uptake, and Flow Cytometry. *Cold Spring Harbor protocols*. 2016;2016(11).
139. Lau BF, Abdullah N, Aminudin N, Lee HB, Yap KC, Sabaratnam V. The potential of mycelium and culture broth of *Lignosus rhinocerotis* as substitutes for the naturally occurring sclerotium with regard to antioxidant capacity, cytotoxic effect, and low-molecular-weight chemical constituents. *PLoS one*. 2014;9(7):e102509.
140. Kofuji K, Aoki A, Tsubaki K, Konishi M, Isobe T, Murata Y. Antioxidant Activity of  $\beta$ -Glucan. *ISRN pharmaceuticals*. 2012;2012:125864.
141. Baxter PS, Bell KFS, Hasel P, Kaindl AM, Fricker M, Thomson D, et al. Synaptic NMDA receptor activity is coupled to the transcriptional control of the glutathione system. *Nature Communications*. 2015;6(1):6761.
142. Lee KH, Cha M, Lee BH. Neuroprotective Effect of Antioxidants in the Brain. *Int J Mol Sci*. 2020;21(19).
143. Gems D, Doonan R. Antioxidant defense and aging in *C. elegans*: is the oxidative damage theory of aging wrong? *Cell cycle (Georgetown, Tex)*. 2009;8(11):1681-7.
144. Inbaraj JJ, Chignell CF. Cytotoxic action of juglone and plumbagin: a mechanistic study using HaCaT keratinocytes. *Chemical research in toxicology*. 2004;17(1):55-62.
145. Strayer A, Wu Z, Christen Y, Link CD, Luo Y. Expression of the small heat-shock protein Hsp16-2 in *Caenorhabditis elegans* is suppressed by *Ginkgo biloba* extract EGb 761. *FASEB journal : official publication of the Federation of American Societies for Experimental Biology*. 2003;17(15):2305-7.
146. Swindell WR. Heat shock proteins in long-lived worms and mice with insulin/insulin-like signaling mutations. *Aging (Albany NY)*. 2009;1(6):573-7.
147. Kim DH, Ewbank JJ. Signaling in the innate immune response (August 14, 2018), *WormBook*, ed. The *C. elegans* Research Community, *WormBook*, doi/10.1895/wormbook.1.83.2, <http://www.wormbook.org>

148. Landis JN, Murphy CT. Integration of diverse inputs in the regulation of *Caenorhabditis elegans* DAF-16/FOXO. *Developmental dynamics : an official publication of the American Association of Anatomists.* 2010;239(5):1405-12.
149. Denzel MS, Lapierre LR, Mack HD. Emerging topics in *C. elegans* aging research: Transcriptional regulation, stress response and epigenetics. *Mech Ageing Dev.* 2019;177:4-21.
150. Abbas S, Wink M. Epigallocatechin gallate from green tea (*Camellia sinensis*) increases lifespan and stress resistance in *Caenorhabditis elegans*. *Planta medica.* 2009;75(3):216-21.
151. Chen W, Müller D, Richling E, Wink M. Anthocyanin-rich Purple Wheat Prolongs the Life Span of *Caenorhabditis elegans* Probably by Activating the DAF-16/FOXO Transcription Factor. *Journal of Agricultural and Food Chemistry.* 2013;61(12):3047-53.
152. Rangsinth P, Prasansuklab A, Duangjan C, Gu X, Meemon K, Wink M, et al. Leaf extract of *Caesalpinia mimosoides* enhances oxidative stress resistance and prolongs lifespan in *Caenorhabditis elegans*. *BMC Complement Altern Med.* 2019;19(1):164.
153. Shashikumar S, Pradeep H, Chinnu S, Rajini PS, Rajanikant GK. Alpha-linolenic acid suppresses dopaminergic neurodegeneration induced by 6-OHDA in *C. elegans*. *Physiology & Behavior.* 2015;151:563-9.
154. Lin C, Zhang X, Su Z, Xiao J, Lv M, Cao Y, et al. Carnosol Improved Lifespan and Healthspan by Promoting Antioxidant Capacity in *Caenorhabditis elegans*. *Oxid Med Cell Longev.* 2019;2019:5958043-.
155. Pincus Z, Slack FJ. Developmental biomarkers of aging in *Caenorhabditis elegans*. *Developmental dynamics : an official publication of the American Association of Anatomists.* 2010;239(5):1306-14.
156. Clokey GV, Jacobson LA. The autofluorescent "lipofuscin granules" in the intestinal cells of *Caenorhabditis elegans* are secondary lysosomes. *Mech Ageing Dev.* 1986;35(1):79-94.



157. Chow DK, Glenn CF, Johnston JL, Goldberg IG, Wolkow CA. Sarcopenia in the *Caenorhabditis elegans* pharynx correlates with muscle contraction rate over lifespan. *Experimental gerontology*. 2006;41(3):252-60.
158. Duangjan C, Rangsinth P, Gu X, Wink M, Tencomnao T. Lifespan Extending and Oxidative Stress Resistance Properties of a Leaf Extracts from *Anacardium occidentale* L. in *Caenorhabditis elegans*. *Oxid Med Cell Longev*. 2019;2019:9012396.
159. Chauhan AP, Chaubey MG, Patel SN, Madamwar D, Singh NK. Extension of life span and stress tolerance modulated by DAF-16 in *Caenorhabditis elegans* under the treatment of *Moringa oleifera* extract. *3 Biotech*. 2020;10(12):504.
160. Bloom GS. Amyloid- $\beta$  and tau: the trigger and bullet in Alzheimer disease pathogenesis. *JAMA neurology*. 2014;71(4):505-8.
161. Kotecha AM, Corrêa ADC, Fisher KM, Rushworth JV. Olfactory Dysfunction as a Global Biomarker for Sniffing out Alzheimer's Disease: A Meta-Analysis. *Biosensors (Basel)*. 2018;8(2):41.
162. Williams AJ, Paulson HL. Polyglutamine neurodegeneration: protein misfolding revisited. *Trends in neurosciences*. 2008;31(10):521-8.
163. Ross CA, Poirier MA. Protein aggregation and neurodegenerative disease. *Nature medicine*. 2004;10 Suppl:S10-7.
164. Lee GD, Wilson MA, Zhu M, Wolkow CA, de Cabo R, Ingram DK, et al. Dietary deprivation extends lifespan in *Caenorhabditis elegans*. *Aging Cell*. 2006;5(6):515-24.
165. Bae N, Chung S, Kim HJ, Cha JW, Oh H, Gu M-Y, et al. Neuroprotective effect of modified Chungsimyeolda-tang, a traditional Korean herbal formula, via autophagy induction in models of Parkinson's disease. *Journal of ethnopharmacology*. 2015;159:93-101.

166. Miyasaka T, Xie C, Yoshimura S, Shinzaki Y, Yoshina S, Kage-Nakadai E, et al. Curcumin improves tau-induced neuronal dysfunction of nematodes. *Neurobiol Aging*. 2016;39:69-81.
167. Abushouk AI, Negida A, Ahmed H, Abdel-Daim MM. Neuroprotective mechanisms of plant extracts against MPTP induced neurotoxicity: Future applications in Parkinson's disease. *Biomedicine & Pharmacotherapy*. 2017;85:635-45.
168. Hu X, Song Q, Li X, Li D, Zhang Q, Meng W, et al. Neuroprotective effects of kukoamine A on neurotoxin-induced parkinson's model through apoptosis inhibition and autophagy enhancement. *Neuropharmacology*. 2017;117:352-63.
169. Kou X, Chen N. Resveratrol as a Natural Autophagy Regulator for Prevention and Treatment of Alzheimer's Disease. *Nutrients*. 2017;9(9):927.
170. Thabit S, Handoussa H, Roxo M, El Sayed NS, Cestari de Azevedo B, Wink M. Evaluation of antioxidant and neuroprotective activities of *Cassia fistula* (L.) using the *Caenorhabditis elegans* model. *PeerJ*. 2018;6:e5159-e.
171. Zhang S, Duangjan C, Tencomnao T, Liu J, Lin J, Wink M. Neuroprotective effects of oolong tea extracts against glutamate-induced toxicity in cultured neuronal cells and  $\beta$ -amyloid-induced toxicity in *Caenorhabditis elegans*. *Food & function*. 2020;11(9):8179-92.
172. Gao C, King ML, Fitzpatrick ZL, Wei W, King JF, Wang M, et al. Prowashonupana barley dietary fibre reduces body fat and increases insulin sensitivity in *Caenorhabditis elegans* model. *J Funct Foods*. 2015;18(A):564-74.



จุฬาลงกรณ์มหาวิทยาลัย  
**CHULALONGKORN UNIVERSITY**

## VITA

NAME ภาวริณี กิตติมงคลสุข  
DATE OF BIRTH 6 พฤษภาคม 2530  
PLACE OF BIRTH กรุงเทพฯ  
INSTITUTIONS ATTENDED จุฬาลงกรณ์มหาวิทยาลัย  
HOME ADDRESS 124 ซ. ตากสิน 34 ดาวคะนอง ธนบุรี กทม. 10600



จุฬาลงกรณ์มหาวิทยาลัย  
CHULALONGKORN UNIVERSITY